Polyunsaturated fatty acid metabolism and effects on colon cancer cell biology *in vitro*

A thesis submitted in fulfilment of the requirements of the degree of

Master of Science in Biochemistry

of

Rhodes University

Candice Bulcao

January 2013

Abstract

Colon cancer is a leading cause of cancer related deaths worldwide. Lifestyle factors such as diet and exercise have been implicated as important agents in colon cancer development and progression. Epidemiological, *in vivo* and *in vitro* studies have found that n-3 polyunsaturated fatty acids (PUFAs) reduce colon carcinoma. The role of n-6 PUFAs remains a controversial topic, with studies indicating both promoting and preventing capabilities published. In order to better understand the effects of PUFAs on colon carcinoma, it is important to have an understanding of how they will be broken down in the body. During this study, *in silico* metabolism of eicosapentaenoic acid (EPA), docosahexaenoic acid (DHA) and arachidonic acid (AA) predicted the formation of hydroxy-, di-hydroxy- and epoxy-FAs. A gas chromatography-mass spectrometry method was developed and validated for the detection of these PUFAs and their cytochrome P450 (CYP) metabolites. A human liver microsomal system for the *in vitro* metabolism of EPA, DHA and AA was optimised in terms of microsomal and PUFA concentration. The system resulted in the metabolism of the positive control, lauric acid, to 12-hydroxy-lauric acid but was unable to metabolise the PUFAs of interest. EPA, DHA and AA reduced cell viability in the colon carcinoma cell lines SW480 and SW620 in the micromolar concentration range (25 – 200 µM). The CYP epoxidation metabolite of EPA, 17, 18-epoxyeicosatetraenoic acid (17, 18-EpETE) resulted in a significant reduction in SW480 cell viability relative to the parent compound at lower concentrations (25 and 50 µM). Annexin V apoptosis analysis revealed that EPA and 17, 18-EpETE did not result in apoptosis in SW480 cells at a concentration of 25 µM and over an incubation period of 24 hours. A significant reduction in reactive oxygen species production was seen in SW480 cells after incubation with 25 µM 17, 18-EpETE for 24 hours. EPA and 17, 18-EpETE were implicated in the reduction of colon cancer metastasis since they were able to reduce SW480 migration and anchorage independent cell growth. These results indicate that the dietary intake of EPA, DHA and AA may be beneficial to one's health due to the negative effects that these PUFAs had on colon carcinoma. Future studies are needed to confirm these benefits and compare the effects of the PUFAs to their CYP-metabolites.

Declaration

I hereby acknowledge that this is an original work completed by myself, the undersigned, and is submitted for the degree of Master of Science of Rhodes University. I declare that this work has never been presented to any other tertiary institution for any other qualification.

Candice Bulcao

January 2013

Acknowledgements

I would like to take this opportunity to sincerely thank my supervisor, Dr Brendan Wilhelmi. Without your guidance, support and encouragement this research would not have been possible. Thank you for always believing in me and inspiring me to be the best that I can be.

I would also like to thank my co-supervisor, Dr Adrienne Edkins. Your input went way beyond the definition of a co-supervisor and I am grateful for all the time and resources you dedicated to me and for the opportunity to have worked under your guidance.

Thank you to the members of both Lab 412 and BioBRU, especially Roxann Morrison, Jo-Anne de la Mare and Cindy Slater. I appreciate all the advice and helpful tips you have given me over the duration of this research project.

Thanks and acknowledgement are due to Dr Nicole Richoux and the Fatty Acid Facility at Rhodes University for utilisation of their facilities and guidance during gas chromatography analysis.

Finally, I would like to thank my parents for all their support throughout my studies.

The financial assistance from the NRF towards this research is hereby acknowledged. Opinions expressed and conclusions arrived at are those of the author and are not necessarily to be attributed to Rhodes University or the donor.

Table of Contents

List of Tables

List of Figures

List of Abbreviations

AA	Arachidonic acid
Bax	Bcl-2-associated X protein
Bcl-2	B-cell lymphoma 2
Bcl-xl	B-cell lymphoma-extra large
COX	Cyclo-oxygenase
CYP	Cytochrome P450
DHA	Docosahexaenoic acid
DHET	Dihydroxyeicosatrienoic acid
DHEQ	Dihydroxyeicosatetraenoic acid
DCFH-DA	2', 7'-dichloroflourescein diacetate
EDA	Eicosadienoic acid
EET	Epoxyeicosatrienoic acid
EPA	Eicosapentaenoic acid
EpDPE	Epoxydocosapentaenoic acid
EpETE	Epoxyeicosatetraenoic acid
FA	Fatty acid
FAME	Fatty acid methyl ester
G6P	Glucose-6-phosphate
G6PDH	Glucose-6-phosphate dehydrogenase
GC	Gas chromatography
FACS	Fluorescence-activated cell sorting
FID	Flame ionisation detector
FLIP	FLICE-like inhibitory protein
HDoHE	Hydroxydocosahexaenoic acid
HEPE	Hydroxyeicosapentaenoic acid

HETE	Hydroxyeicosatetraenoic acid
HPLC	High performance liquid chromatography
IS	Internal standard
LA	Lauric acid
LOD	Limit of detection
LOQ	Limit of quantification
LOX	Lipo-oxygenase
LNA	α-Linolenic acid
mEH	Microsomal epoxide hydrolase
MS	Mass spectrometry
PBS	Phosphate buffered saline
PUFA	Polyunsaturated fatty acid
ROS	Reactive oxygen species
sEH	Soluble epoxide hydrolase
TNF	Tumor necrosis factor
12-OH-LA	12-Hydroxy-lauric acid
XIAP	X-linked inhibitor of apoptosis protein

Chapter 1

Literature Review

1.1 Introduction

A link between diet and cancer has been proposed (Bartsch *et al*., 1999; Milner, 2004), with polyunsaturated fatty acids (PUFAs) being implicated as bioactive food components (Bartsch *et al*., 1999; Schley *et al*., 2005; Bougnoux *et al*., 2010). Optimizing the intake of specific foods and/or their bioactive components, such as PUFAs, may be a practical, noninvasive, and cost-effective strategy for reducing the incidence of cancer (Milner, 2004). However, this solution is not a simple one since the complexity of the diet and the heterogeneity of carcinogenesis make it difficult to establish true interrelationships (Milner, 2004). The response to bioactive food components is highly dependent on a number of cellular events and regulatory processes, including metabolism (Milner, 2004). Hence it is important to understand how PUFAs are broken down in the body and how this metabolism will impact their effectiveness. Whilst epidemiological studies are helpful in identifying food components that may reduce the incidence of cancer, their results are often highly variable due to the considerable variation in the concentration of bioactive components that occur in a particular food (Milner, 2004). For this reason, *in vitro* studies are a helpful tool for identifying the effects of bioactive food components on carcinogenesis and the level of exposure required in order for these effects to be beneficial.

1.2 Cancer

1.2.1 Cancer overview

Cancer is a major health problem in many parts of the world (Jemal *et al*., 2010). The National Cancer Registry (NCR) reported 27 392 new cases of cancer in males and 28 161 new cases of cancer in females in South Africa in 2004. Over 100 types of cancer have been identified, each one having different causes and symptoms (Almeida and Barry, 2010). Cancer is divided into four major types: carcinomas, sarcomas, leukemias, and lymphomas (Almeida and Barry, 2010). Carcinomas account for about 90% of human cancers, and they arise from the epithelium of internal organs, glands and body cavities (Almeida and Barry,

2010). Breast, colorectal, lung, prostate, and skin tissues often give rise to carcinomas (Almeida and Barry, 2010). Sarcomas are less common than carcinomas, and they are formed in connective tissue such as cartilage and bone (Almeida and Barry, 2010). Lymphomas and leukemias do not form solid tumors (Almeida and Barry, 2010). Lymphomas are cancers of the lymphatic system whilst leukemias are cancers of the bone marrow which lead to overproduction and early release of immature leukocytes (Almeida and Barry, 2010; Kim *et al*., 2010).

1.2.2 Cancer cell physiology

A balance between cell proliferation and cell death exists in the human body such that the total number of cells remains relatively constant (Bertram, 2001). Factors altering this balance may potentially alter the total number of cells in a particular organ or tissue (Bertram, 2001). The abnormal proliferation of cells over many cell generations is clinically detectable as a neoplasm, which may be benign, pre-malignant, or malignant (Terpstra *et al*., 1987; Risio *et al*., 1993; Sandler *et al*., 2000). Genes that alter the production rate or death rate of individual cells have been implicated as causative in the carcinogenic process, with the origin of cancer being the accumulation of multiple random mutations within a cell (Loeb and Loeb, 2000; Campbell Marotta and Polyak, 2009). Very few mutations that give rise to cancer are inherited; most occur spontaneously due to DNA damage that results in the function of crucial genes being altered (Loeb and Loeb, 2000; Dove-Edwin and Thomas, 2001; Matsuura *et al*., 2006). DNA damage may occur spontaneously either directly as a result of errors in replication, or indirectly due to damage to DNA caused by endogenous chemicals which leads to errors in the correct reading of the damaged DNA by DNA polymerase during replication (Jackson and Loeb, 2001). DNA may also be damaged by exogenous chemical and physical agents, which are known as environmental carcinogens (Multani *et al*., 2000). An example of a chemical carcinogen is 2-naphthylamine, used in rubber and chemical industries, which has been implicated as a bladder carcinogen (Bertram, 2001). Ionizing radiation and ultraviolet radiation are both examples of physical carcinogens (Ananthaswamy and Pierceall, 1990; Sachs and Brenner, 2005). Microbial carcinogens have also been implicated as a source of genetic change that gives rise to

cancer (van Poppel and van den Berg, 1997). Mutation rates and hence the rate of neoplastic progression are increased by defects in DNA repair mechanisms (Eshleman *et al*., 1995; Ciotta *et al*., 1998). Several inherited diseases (for example the UV sensitivity disease xeroderma pigmentosum) which lead to cancer are caused by defects in DNA repair mechanisms (Bertram, 2001).

Through the process of micro-evolution, cancer cells have acquired alterations in cell physiology that collectively result in malignant growth (Hanahan and Weinberg, 2011) (Figure 1.1). These alterations are as follows. Cancer cells are not under the control of external growth signals (both stimulatory and inhibitory) that regulate normal cell proliferation (Hornberg *et al*., 2006; Campbell Marotta and Polyak, 2009; Hanahan and Weinberg, 2011). They are able to evade apoptosis (i.e. programmed cell death) (Bertram, 2001; Hornberg *et al*., 2006; Wicha *et al*., 2006; Campbell Marotta and Polyak, 2009; Hanahan and Weinberg, 2011). Cancer cells are able to avoid replicative senescence (through the reactivation of telomerase) and are therefore immortal and capable of infinite proliferation (Wicha *et al*., 2006; Hanahan and Weinberg, 2011). They have the potential to stimulate angiogenesis (the formation of new blood vessels and capillaries) thus ensuring an adequate supply of nutrients for growth and the elimination of metabolic waste products (Hornberg *et al*., 2006; Hanahan and Weinberg, 2011; Xu *et al.,* 2011). They are genetically unstable (Bertram, 2001). Cancer cells are unable to communicate with neighbouring cells through gap junctions and are able to escape interactions with host cells (e.g. cells of the immune system) (Bertram, 2001). They are capable of metastasis, a multistep process that involves the dissociation of cancer cells from primary sites, survival in the vascular system, and proliferation in distant target organs (Hornberg *et al*., 2006; Wicha *et al*., 2006; Guadamillas *et al*., 2011; Hanahan and Weinberg, 2011; Kim *et al*., 2012). Cancer cells are therefore able to invade healthy tissues. Uncontrolled tumor growth and metastasis are the main origins of the pathological consequences of cancer, and both result from abnormal tumor cell proliferation, adhesion, invasion, and migration (Xu *et al.,* 2011).

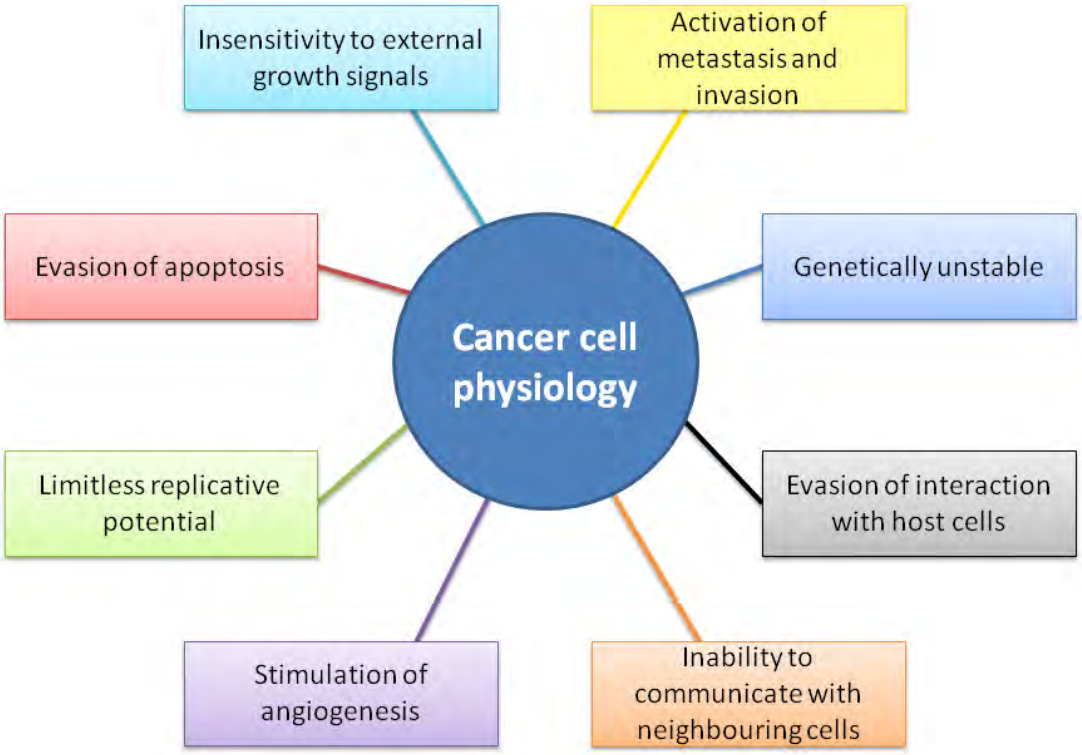

Figure 1.1: Acquired physiology of cancer cells.
An overview of the physiological traits acquired by cancer cells, through micro-evolution, that lead to malignant cell growth. (Adapted from Hanahan and Weinberg, 2011).

1.2.3 Programmed cell death and carcinogenesis

Apoptosis is an evolutionally conserved protective process that eliminates irreversibly damaged or potentially harmful cells from the body (Hur *et al*., 2008). It is the preferred method of managing cancer, and many chemopreventive and/or chemotherapeutic agents can cause tumor cell death via the induction of apoptosis (Kim *et al.,* 2010). Caspases are a family of proteases that participate in apoptosis (Nelson and Cox, 2005). Apoptosis can be initiated in two ways; by an extrinsic pathway, or by an intrinsic pathway (Hur *et al*., 2008; Kim *et al*., 2010; Fauser *et al*., 2011). In the extrinsic pathway, plasma membrane death receptors are involved and the apoptosis signal is provided by the interaction between a death ligand (such as tumor necrosis factor (TNF)) and the death receptor, which then activates the initiator caspase-8 (Hur *et al*., 2008; Kim *et al*., 2010; Fauser *et al*., 2011). Caspase-8 activates the effector caspase-3 which cleaves several substrates, resulting in apoptotic cell death (Hur *et al*., 2008; Kim *et al*., 2010; Fauser *et al*., 2011). The intrinsic

pathway is activated by stimuli from within the cell (e.g. DNA damage) which lead to a change in the permeability of the mitochondrial outer membrane, which in turn results in the release of cytochrome *c* into the cytosol (Hur *et al*., 2008; Kim *et al*., 2010). It is thought that the release of cytochrome *c* from the mitochondria into the cytosol is a key event in the intrinsic pathway (Kim *et al*., 2010). Once in the cytosol, cytochrome *c* binds to the Apaf-1 complex thereby activating the effector, caspase-9, which in turn cleaves and activates caspase-3 (Hur *et al*., 2008; Kim *et al*., 2010; Fauser *et al*., 2011). Caspase-3 then cleaves several specific substrates, including poly (ADP-ribose) polymerase (PARP), which leads to apoptosis (Kim *et al*., 2010). Caspase activated cell death is regulated by genes including the pro- and anti-apoptosis genes, B-cell lymphoma 2 (Bcl-2) and Bcl-2-associated X protein (Bax), respectively, which induce apoptosis, either synergistically, or in opposition to one another (Fauser *et al*., 2011).

Anoikis (or cell-detachment-induced apoptosis) is a form of caspase-mediated programmed cell death that results from a loss of contact with the extracellular matrix or neighbouring cells (Kim *et al*., 2012). It is a self-defence strategy that organisms use to eliminate 'misplaced' cells, i.e. cells that are in an inappropriate location, and therefore prevent dysplastic growth (Guadamillas *et al*., 2011). Cancer cells use a variety of strategies to evade anoikis and thus escape the requirement for integrin-extracellular matrix interactions for cell proliferation (Guadamillas *et al*., 2011). The resulting anchorage-independent growth is a crucial step in the acquisition of malignancy (Guadamillas *et al*., 2011). Anoikis resistance and anchorage-independency allow tumor cells to expand and invade adjacent tissues, and to disseminate through the body, giving rise to metastases (Guadamillas *et al*., 2011; Kim *et al*., 2012).

1.2.4 Carcinogenesis models

There are two main types of carcinogenesis models, the stochastic model and the cancer stem cell model (Wicha *et al*., 2006). In the stochastic model, any cell can be the target of carcinogenesis, and the model proposes that transformation is caused by random mutation

followed by clonal selection (Wicha *et al*., 2006). The stem cell model proposes the existence of cancer stem cells which are defined as a subset of cancer cells that have the stem-cell-like ability to produce all cancer cell types present in a tumour, which may comprise cells with more differentiated features (Hamburger and Salmon, 1977; Campbell Marotta and Polyak, 2009). Cancer stem cells also serve as the seeds of metastatic spread of cancer (Hamburger and Salmon, 1977; Liu *et al*., 2011). They are likely to be derived from normal stem cells since these cells are present in almost all bodily tissues, are long-lived and therefore more likely than other cells to accumulate the multiple mutations required for carcinogenesis (Wicha *et al*., 2006; Campbell Marotta and Polyak, 2009). However, it has also been proposed that they may be derived from differentiated cells that have accumulated mutations and have de-differentiated back to the stem cell state (Campbell Marotta and Polyak, 2009). The extent to which cancer stem cells have normal stem cell properties is not clear (Campbell Marotta and Polyak, 2009). Previous studies indicate that most, if not all, malignancies are cancer stem cell driven and that these cells may be resistant to current therapeutic agents (Wicha *et al*., 2006). Cancer stem cells are thought to be involved in oncogenesis, tumor growth, metastasis, and cancer recurrence (Campbell Marotta and Polyak, 2009).

1.2.5 Colon cancer and diet

Colon cancer is one of the most frequent causes of cancer mortality in the world (Sack *et al*., 2011). It is the third most common cancer worldwide and has the fourth highest mortality rate, accounting for 7.6% of cancer-related deaths (W.H.O., 2008). In South Africa, it is one of the leading cancers, accounting for 4.43% and 3.59% of new cases in 2004 in males and females respectively (The 2004 National Cancer Registry report). The reason for poor survival rates is because colon cancer is highly metastatic (Sack *et al*., 2011) and most cases are diagnosed at an advanced stage (Dove-Edwin and Thomas, 2001). Patients with nonmetastatic, local stage 1 tumors have a 5-year survival rate of 90% (Sack *et al*., 2011). However, this rate drastically drops to approximately 10% when distant metastases have formed at the time of diagnosis (Sack *et al*., 2011).

Evidence has been found to support the idea that dietary habits are a significant environmental factor in the overall cancer process (Bougnoux, 1999; Milner, 2004). Colon cancer occurs through the accumulation of multiple genetic mutations over a period of about 10-20 years in somatic cells; resulting in the progression of normal colonic mucosa to adenoma and finally to carcinoma (Dove-Edwin and Thomas, 2001). This process may be influenced by several lifestyle factors such as diet, exercise and other environmental factors (Dove-Edwin and Thomas, 2001; Matsuura *et al*., 2006). Most incidences of colorectal cancer have been found to be initiated by non-inherited, lifestyle factors (Dove-Edwin and Thomas, 2001; Matsuura *et al*., 2006). This suggests that colon cancer can be prevented to some degree by lifestyle alterations (Matsuura *et al*., 2006). Dietary prevention, chemoprevention and endoscopic intervention are current strategies employed in colorectal cancer prevention (Dove-Edwin and Thomas, 2001). Polyunsaturated fatty acids (PUFAs) have been implicated as important bioactive food components and a link between dietary intake of PUFAs and carcinogenesis has been proposed (Schloss *et al*., 1997; Bartsch *et al*., 1999; Schley *et al*., 2005; Bougnoux *et al*., 2010; Lu *et al*., 2010).

1.3 **Polyunsaturated fatty acids**

1.3.1 Polyunsaturated fatty acids overview

PUFAs are classified into two groups, omega-6 (n-6) and omega-3 (n-3) (Schmitz and Ecker, 2008; Bougnoux *et al*., 2010). This classification is based on the position of the last double bond relative to the terminal methyl end of the molecule (Schmitz and Ecker, 2008). Both types of PUFA are termed essential since they are important for human health but cannot be synthesized *de novo* and must therefore be obtained through the diet (Bartsch *et al*., 1999; Yao *et al*., 2006; Schmitz and Ecker, 2008; Arnold *et al.*, 2010; Konkel and Schunck, 2011). Since mammals (unlike plants, phytoplankton, or nematodes) lack the desaturases needed to introduce a double bond at the ω-6 or ω-3 position, they are unable to produce and interconvert n-6 and n-3 PUFAs (Konkel and Schunck, 2011). Linoleic acid (*cis*, *cis*-C18:2 n-6) and α-linolenic acid (LNA, C18:3 n-3) are precursors in the n-6 and n-3 series respectively (Bougnoux *et al*., 2010). Linoleic acid is the predominant PUFA in the westernized human diet and is abundant in vegetable oils (such as those from soybeans,

corn and sunflowers) and food of animal origin (Bartsch *et al*., 1999; Schmitz and Ecker, 2008; Bougnoux *et al*., 2010). LNA is found in dark green vegetables and in several vegetable oils, mainly linseed (50%), rapeseed (12%), soybean (7%), as well as in the fats of walnuts (6.8%) and other edible nuts (Bartsch *et al*., 1999; Crawford *et al*., 2000; Bougnoux *et al*., 2010; Konkel and Schunck, 2011). In animals and humans, linoleic acid and LNA are metabolised to longer and more unsaturated n-6 and n-3 FAs respectively through desaturation and elongation pathways, with the desaturations being the rate limiting reactions (Crawford *et al*., 2000; Yao *et al*., 2006; Schmitz and Ecker, 2008) (Figure 1.2). Linoleic acid is converted to γ-linolenic acid (C18:3 n-6), and dihomo-γ-linolenic acid (C20:3 n-6) to form the significant intermediate arachidonic acid (AA) (Schmitz and Ecker, 2008). AA is required as a constituent of membrane phospholipids (Konkel and Schunck, 2011). It may also be obtained directly from the diet through meat and dairy products (Konkel and Schunck, 2011) and is further metabolised to docosapentaenoic acid (C22:5 n-6) or eicosanoids by cyclo-oxygenase (COX), lipo-oxygenase (LOX) and cytochrome P450 (CYP) enzymes (Schmitz and Ecker, 2008; Arnold *et al*., 2010). The n-3 PUFA LNA is converted to stearidonic acid (C18:4 n-3) and eicosatetraenoic acid (C20:4 n-3), which is further metabolised to eicosapentaenoic acid (EPA) using the same series of enzymes used to synthesise AA (Schmitz and Ecker, 2008). EPA differs from AA solely by the presence of one additional double bond located between C17 and C18, and both EPA and AA are mainly incorporated into the *sn*-2 position of membrane phospholipids (Konkel and Schunck, 2011). EPA is further metabolised to docosahexaenoic acid (DHA) or eicosanoids (Schmitz and Ecker, 2008). DHA, the longest and most unsaturated n-3 PUFA, is the precursor of signalling molecules termed docosanoids, and is a crucial constituent of cell membranes particularly in the brain, retina and heart (Konkel and Schunck, 2011). It is important to note that the conversion of LNA to EPA and DHA is very limited in humans (Larsson *et al*., 2004; Konkel and Schunck, 2011). Furthermore, the desaturase and elongase genes controlling this metabolic pathway are highly polymorphic and are regulated by sex hormones, which leads to large interindividual differences in the efficiencies to convert LNA to EPA and DHA (Konkel and Schunck, 2011). Since n-3 and n-6 PUFA metabolism involves the same enzymatic system, competition exists between these FAs such that an excess of one causes a significant decrease in the conversion of the other (Crawford *et al*., 2000; Schmitz and Ecker, 2008; Konkel and Schunck, 2011). For these reasons, EPA and DHA need to be

obtained through the diet in order to meet the body's requirements for these PUFAs (Konkel and Schunck, 2011). Deep cold-water fatty fish (e.g., mackerel, salmon and herring), fish oil and other sea food are a rich source of EPA and DHA since the marine food chain begins with EPA and DHA producing phytoplankton (Bartsch *et al.*, 1999; Konkel and Schunck, 2011).

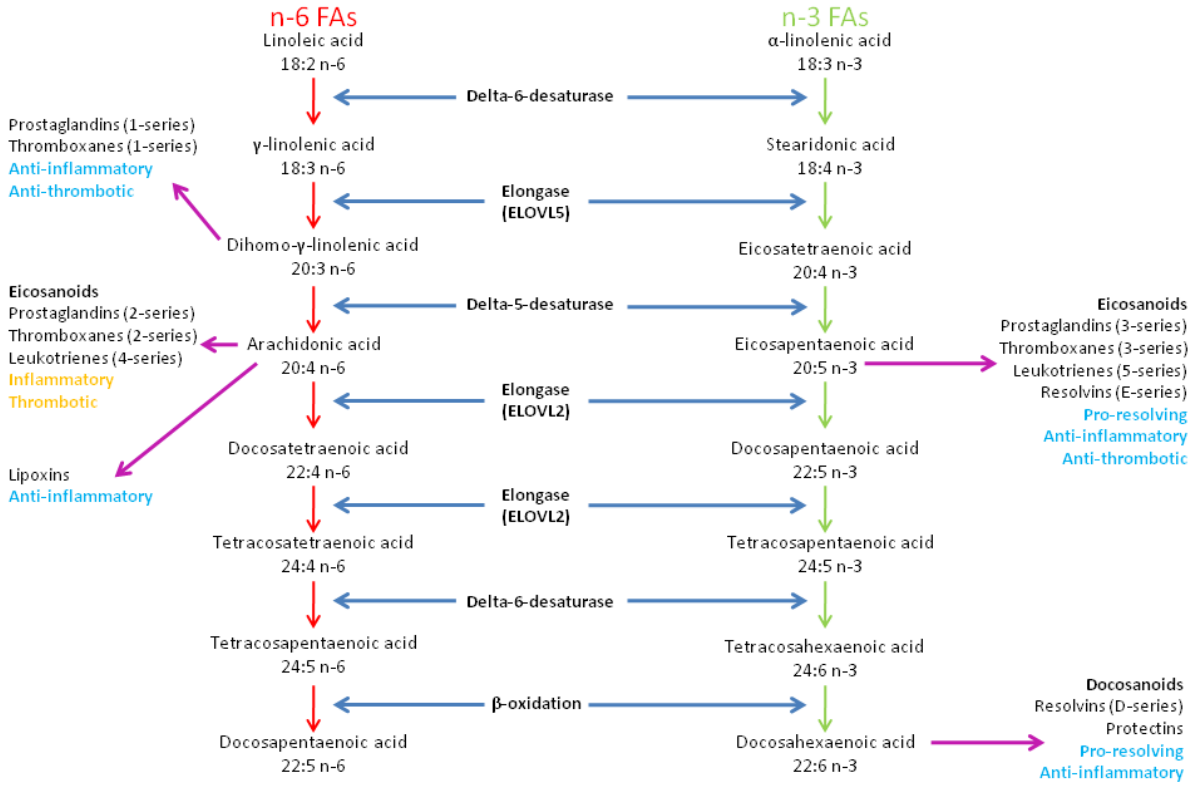

Figure 1.2: Omega-6 and omega-3 polyunsaturated fatty acid metabolism.
Compounds formed from n-3 and n-6 PUFA metabolism indicating general biological effects and enzymes involved. (Adapted from Schmitz and Ecker 2008; Gleissman *et al.*, 2010).

The ratio of n-6:n-3 PUFAs in the diet has been shown to be an important factor, however an optimal ratio has not been conclusively established (Bartsch *et al.*, 1999; Rose and Connolly, 1999; Arnold *et al.*, 2010). The ratio seems to be increasing over time, while the diet of Mesolithic man had a ratio of 1-4:1, European and Western diets now contain a ratio of 10-15:1 (Bartsch *et al.*, 1999; Arnold *et al.*, 2010). One of the highest ratios in the world is in Israel, 22-26:1 (Bartsch *et al.*, 1999). A diet high in n-6 PUFAs was at one stage extensively recommended, however, it has recently been demonstrated that an excess intake of n-6

PUFAs may have long-term side-effects, including tumourigenesis, cardiovascular disease, hyperinsulinaemia and atherosclerosis (Bartsch *et al*., 1999; Arnold *et al*., 2010).

FAs are incorporated into membrane phospholipids and thereby play an important role in membrane structure and function (Obermeier *et al*., 1995; Yao *et al*., 2006; Martins De Lima *et al*., 2007; Schmitz and Ecker, 2008). They strongly influence the fluidity of biological membranes, with an increase in unsaturated FAs resulting in an increase in membrane fluidity since PUFA acyl chains are flexible and can rapidly change conformational states (Schmitz and Ecker, 2008). By modulating membrane fluidity, FAs modify signal transduction across the cell membrane and thereby indirectly modulate intracellular signalling pathways (Obermeier *et al*., 1995; Martins De Lima *et al*., 2007). They can also act directly on cell membrane receptors (such as toll-like receptors, TLRs) or nuclear receptors (such as peroxisome-proliferator-activated receptors, PPARs) (Martins De Lima *et al*., 2007). Since the flexibility of acyl chains also differs significantly between n-3 and n-6 PUFAs, and the number of double bonds alters membrane fluidity, the n-3 and n-6 PUFAs composition of biological membranes significantly influences their physical properties, thereby altering protein function and trafficking, and vesicle budding and fusion (Schmitz and Ecker, 2008). FAs are also able to regulate key immune responses through the generation of biologically active metabolites (Martins De Lima *et al*., 2007). In general, the cellular free PUFA levels in normal tissues are low and almost undetectable (Yao *et al*., 2006). During inflammation, PUFAs are released from the membrane by phospholipase A2 and are oxidised by COX, LOX, and CYP enzymes to form physiologically important eicosanoid families, such as prostaglandins, thromboxanes, and leukotrines (Yao *et al*., 2006; Schmitz and Ecker, 2008) (Figure 1.2). In general, metabolites formed from AA are pro-inflammatory and thrombotic whilst those formed from EPA and DHA are anti-inflammatory, anti-thrombotic and pro-resolving (Schmitz and Ecker, 2008; Gleissman *et al*., 2010).

1.3.2 Polyunsaturated fatty acids and cancer

Epidemiological studies have revealed a link between high *per capita* fish consumption and lower incidence of cancer in the population. Eskimos, whose diet consists of fish and meat from marine mammals rich in n-3 FAs, and Japanese fishermen, who have the highest *per capita* fish consumption in the world, have high blood levels of long chain n-3 PUFAs, such as EPA, and low rates of cancers of the breast and colon, despite their overall high fat consumption (Bartsch *et al*., 1999). In South Africa, the incidence of colorectal cancer in the Cape Town urban population was 6.8 times greater than in the West Coast fisherman population during a study conducted over a period of 5 years (Schloss *et al*., 1997). This lower incidence of colorectal cancer in the fishermen was associated with a higher intake of fish by the fishermen (110 versus 30 g/day, $P < 0.001$). The study revealed that the daily intake of n-3 PUFAs, DHA and EPA, in the West Coast population was considerably higher than in the urban population due to their higher fish intake (Schloss *et al*., 1997). This led to higher levels of circulating DHA and EPA and lower levels of n-6 PUFAs in the fishermen's plasma in comparison to the urban group (Schloss *et al*., 1997). A study conducted by Lands *et al*. (1990) showed that an increase in saturated FA intake in the Japanese diet from 1960 to 1985, together with a decrease in PUFA intake and a decrease in the n-3 to n-6 FA ratio has been linked to an increased incidence of colon and breast cancer in this society.

In vitro and *in vivo* studies support the findings of epidemiological studies and have shown a correlation between PUFAs and cancer. Most studies have demonstrated that n-6 PUFAs, particularly AA, promote cancer (Schley *et al*., 2005; Ligo *et al*., 1997) or have no impact on cancer cell growth (Lu *et al*., 2010) whilst n-3 PUFAs, in particular EPA and DHA, have inhibitory effects on carcinogenesis (Ligo *et al*., 1997; Chamras *et al*., 2002; Schley *et al*., 2005; Bougnoux *et al*., 2010; Lu *et al*., 2010). n-3 PUFAs, such as DHA or EPA, have also been found to improve cytotoxic effects of several anti-cancer drugs such as doxorubicin and paclitaxel, toward various human cancer cell lines, including those of breast, colon, bladder, neuroblastoma, and glioblastoma (Bougnoux *et al*., 2010). Dietary supplementation with DHA (0.7 g/day) has been found to increase the sensitivity of resistant tumors to chemo- and radiation therapy in animal models of breast cancer, with no additional toxicity to non-

tumor tissues (Bougnoux *et al*., 2010). The addition of antioxidants abolished this sensitizing effect in a dose-dependent manner, suggesting that peroxidation of DHA is an important factor in this response (Bougnoux *et al*., 2010).

The metastasis, to the lung, of the highly metastatic colon carcinoma Co 26Lu implanted subcutaneously on the right thighs of mice, or injected into the tail vein, was significantly reduced by EPA and DHA when administered at 0.2 ml per day (98% purity) (Ligo *et al*., 1997). EPA and DHA were also found to result in a significant decrease in tumor growth of subcutaneous implanted Co 26Lu (Ligo *et al*., 1997). An *in vitro* study found EPA and DHA to be cytotoxic to Co 26Lu cells, having IC_{50} values of approximately 50 µM (Ligo *et al*., 1997). It was also found that the n-6 PUFA LA promoted Co 26Lu metastasis to the lungs when administered at 0.2 ml per mouse per day (98% purity) (Ligo *et al*., 1997).

A study performed on Sprague-Dawley rats that were fed high fat diets (45% of total calories from fat) showed that a high intake of corn oil, a rich source of LA, stimulated colon cell proliferation (used as an intermediate biomarker for colon carcinogenesis); whilst a high intake of fish oil, a rich source of EPA and DHA, had a protective affect on colon cell proliferation (Kim *et al*., 1998).

The molecular mechanism by which PUFAs affect carcinogenesis is not fully understood and several mechanisms have been proposed. One proposed mechanism is that n-3 PUFAs alter estrogen metabolism and therefore cause a reduction in estrogen-stimulated cell growth (Larsson *et al*., 2004). Approximately two thirds of breast cancers in women are hormone-dependent and require estrogen for growth (Lu *et al*., 2010), and some other cancers, such as prostate cancer, have been found to be hormone-dependant (Huggins 1963; Etsuro, 2000). Estrogen receptor α (ERα) and ERβ, members of the steroid/nuclear hormone receptor superfamily, are the two main estrogen receptors that mediate the actions of estrogen (Lu *et al*., 2010). ERα promotes estrogen-stimulated breast cancer cell proliferation, whilst ERβ inhibits it (Lu *et al*., 2010). Lu *et al*. (2010) found that

supplementation with 10 and 60 μM DHA inhibits MCF-7 cell proliferation by proteasome-dependent degradation of ERα and reduced cyclin D1 expression and mitogen-activated protein kinase (MAPK) signalling. EPA has also been implicated in this mechanism. Prostaglandin-2 is derived from AA and has been shown to stimulate the activity of aromatase P450, which converts 19-carbon steroids to estrogen (Larsson *et al*., 2004). In contrast, prostaglandin-3, which is derived from EPA, does not activate aromatase P450 (Larsson *et al*., 2004). Therefore, a decrease in estrogen production and reduced estrogen-stimulated cell growth is associated with an increased intake of EPA (Larsson *et al*., 2004).

Another mechanism proposes that n-3 PUFAs influence transcription factor activity, gene expression, and signal transduction, leading to changes in metabolism, cell growth, differentiation, apoptosis, angiogenesis, and metastasis (Larsson *et al*., 2004). Schley *et al*. (2005) proposed that the decreased MDA-MB-231 cell proliferation and increased apoptosis observed during their study with EPA and DHA was caused by altered signalling through the Akt/NFκB (nuclear factor-kappaB) cell survival signalling pathway. Akt is a serine/threonine kinase that is activated in response to cytokines and growth factors (Schley *et al*., 2005). It is activated by translocation to the plasma membrane and phosphorylation at two key residues, namely Thr308 and Ser437 (Schley *et al*., 2005). Akt promotes cell survival and protects cells from apoptotic cell death by phosphorylating and inactivating components of the cell death machinery (Schley *et al*., 2005). Akt can also promote cell survival indirectly by activating prosurvival transcription factors such as NFκB (Schley *et al*., 2005). NFκB is a pro-inflammatory transcription factor (Arnold *et al*., 2010). It protects cells from apoptosis and promotes cell growth by inducing the transcription of prosurvival and anti-apoptotic genes (Schley *et al*., 2005). Both Akt and NFκB have been found to be active in many human cancers (Schley *et al*., 2005). During their study, Schley *et al*. (2005) found that EPA and DHA decreased the phosphorylation of Akt (at Ser473) and significantly decreased the DNA binding activity of NFκB.

The suppression of the biosynthesis of AA-derived eicosanoids has also been proposed as a mechanism by which n-3 PUFAs exert their anti-cancer activity (Larsson *et al*., 2004).

Inflammation has recently been shown to play a pivotal role in cancer (Serhan *et al*., 2004). Effectors and mediators of inflammation such as cytokines, chemokines, and eicosanoids form significant components of the tumor microenvironment (Gleissman *et al*., 2010). They have been found to support the growth and survival of malignant cells, promote angiogenesis and metastasis, affect adaptive immune responses, and alter the effect of hormones and chemotherapeutic drugs (Gleissman *et al*., 2010). EPA and DHA metabolites, eicosanoids and docosanoids, have potent anti-inflammatory and pro-resolution properties (Arnold *et al*., 2010; Gleissman *et al*., 2010). They are therefore able to dampen the stimuli of these effectors and mediators, making the microenvironment less suited to tumor growth, which may lead to decreased cancer cell proliferation, metastasis, and angiogenesis; and increased apoptosis (Gleissman *et al*., 2010). A diet high in n-3 PUFAs reduces the production of AA-derived eicosanoids through several means. Firstly, since n-3 PUFAs compete with n-6 PUFAs for desaturases and elongases, and n-3 PUFAs have greater affinities for the enzymes than n-6 PUFAs, a higher intake of n-3 PUFAs reduces the conversion of LA to AA and thus the production of AA-derived eicosanoids is decreased (Larsson *et al*., 2004; Arnold *et al*., 2010). Secondly, n-3 PUFAs suppress COX-2 and compete with AA for COX and LOX enzymes, thereby modulating the production and bioactivity of prostanoids and leukotrienes (Larsson *et al*., 2004; Arnold *et al*., 2010). Consequently, a higher intake of n-3 PUFAs results in a decrease in n-6 eicosanoid production (Larsson *et al*., 2004). For example, AA is metabolised to leukotriene B_4 (LTB_4) by the enzyme 5-LOX (Arnold *et al*., 2010). LTB_4 is a powerful inducer of inflammation and acts as a chemoattractant of neutrophils (Arnold *et al*., 2010). In the presence of EPA, LTB_4 production is inhibited and LTB_5 (a metabolite approximately 30 times less potent than LTB_4) is metabolised from EPA (Arnold *et al*., 2010). Lastly, n-6 eicosanoid catabolism is enhanced by n-3 PUFAs through the induction of peroxisomal enzymes (Larsson *et al*., 2004). It is important to note that the potency of dietary EPA and DHA is approximately five times that of LNA for the suppression of AA-derived eicosanoids (Larsson *et al*., 2004). Gleissman *et al*. (2010) showed that neuroblastoma cells do not produce n-3 eicosanoids or docosanoids in the presence of EPA and DHA, despite the presence of the enzymes required for this conversion. This may be a survival strategy adopted by these cells (Gleissman *et al*., 2010).

Other proposed mechanisms for the effect on n-3 PUFAs on carcinogenesis include an increase in PUFA-derived reactive lipid compounds; an increase or decrease in the production of free radicals and reactive oxygen species (ROS); and mechanisms involving insulin sensitivity and membrane fluidity (Field and Schley, 2004; Larsson *et al*., 2004). PUFAs are the main intracellular substrates for lipid peroxidation; therefore PUFA-derived reactive lipid compounds could lead to necrosis through the damage of cell membranes (Field and Schley, 2004). The mechanism involving a decrease in free radicals and ROS has been linked to inflammation. It has been hypothesised that inflammation increases the production of free radicals and ROS, which leads to carcinogenesis (Larsson *et al*., 2004). ROS have been implicated as key second messengers during growth factor and cytokine stimulation to elicit prosurvival signals (Kim *et al*., 2012). n-6 PUFAs enhance these events through the production of AA-derived proinflammatory eicosanoids, whilst n-3 PUFAs suppress inflammation and thus the overproduction of free radicals and ROS, thereby suppressing carcinogenesis (Larsson *et al*., 2004). On the other hand, Gleissman *et al*. (2010) found that DHA induces cytotoxicity of neuroblastoma cells through the accumulation of ROS and mitochondrial-dependent apoptosis. In order to better understand the effects of PUFAs on carcinogenesis and the molecular mechanism by which they exert these effects it is important to have an understanding of how PUFAs are broken down in the body.

1.4 Metabolism

1.4.1 Cytochrome P450-mediated metabolism

The CYP family of enzymes is one of the major drug metabolising systems in man (Glue and Clement, 1999). These enzymes are involved in the metabolism of various exogenous compounds including drugs, environmental chemicals and pollutants, and natural plant products (Nebert and Russell, 2002). This enzyme system has also been shown to metabolise many endogenous substrates including saturated and unsaturated fatty acids, eicosanoids, sterols and steroids, prostaglandins, bile acids, vitamin D and retinoids (Nelson *et al*., 1993; Liska 1998; Adas *et al*., 1999; Yao *et al*., 2006). Although it was originally believed that these enzymes were predominantly present in the liver, they have been

shown to be expressed in almost all cell types in mammals; being found in the endoplasmic reticulum and mitochondria (Glue and Clement, 1999; Nebert and Dieter, 2000; Chen *et al*., 2001). CYP proteins are arranged into families and subfamilies according to amino acid sequence identity. Enzymes that share ≥ 40% identity are allocated to a particular family designated by an Arabic numeral, and those sharing ≥ 55% identity form part of a subfamily within that family, designated by a letter (Nelson *et al*., 1993). There is a highly conserved amino acid sequence found in some bacteria and nearly all eukaryotic cells (Glue and Clement, 1999). It is a 26-residue region found near the carboxy terminus of CYP proteins, the heme-binding domain (Glue and Clement, 1999). There are more than 270 different CYP gene families currently identified, with CYP2 being the largest P450 family in mammals (Nebert and Russell, 2002). In humans, there are 57 CYP genes and 33 pseudogenes arranged into 18 families and 42 subfamilies (Nebert and Russell, 2002).

Metabolism can be broken down into two groups, namely Phase 1 reactions and Phase 2 reactions (Glue and Clement, 1999). Phase 1 reactions involve the chemical alteration of a compounds structure (e.g., by oxidation), whilst Phase 2 reactions are conjugation reactions (e.g., glucuronidation) (Glue and Clement, 1999). CYP enzymes are the main enzymes involved in Phase I metabolism (Pearce *et al*., 1996; Yamazaki and Shimada, 1997; Liska, 1998; Yao *et al*., 2006). They are a superfamily of heme-containing monooxygenases (Adas *et al*., 1999; Domanski and Halpert, 2001) and represent the most abundant and extensively distributed group of eukaryotic monooxygenases (Chen *et al*., 2001). CYPs catalyze both oxidative and reductive reactions, with oxidative biotransformations being more frequent (Guengerich, 2001; Cruciani *et al*., 2005). These oxidative reactions include side chain and aromatic hydroxylation, N-, O-, S-dealkylation, N-oxidation, sulfoxidation, N-hydroxylation, deamination, dehalogenation, and desulfuration (Glue and Clement, 1999; Cruciani *et al*., 2005). Most of these reactions involve the formation of radical species, which is normally the rate-limiting step (Cruciani *et al*., 2005). CYPs contain a protoporphyrin group with a central iron atom that is hexacoordinated in ferric form (Cruciani *et al*., 2005). The substrate binds reversibly to the enzyme, and the complex undergoes reduction to the ferrous state (Cruciani *et al*., 2005) (Figure 1.3). The electrons come from a reduced cofactor (NADH or NADPH) (Glue and Clement, 1999; Guengerich, 2001). This cofactor passes electrons to the

CYPs heme prosthetic group through the intermediary enzyme cytochrome P450 reductase (Chapple, 1998). The reduction of the iron atom to the ferrous state allows molecular oxygen to bind the enzyme-substrate complex (Guengerich, 2001; Cruciani *et al*., 2005). The oxygen is converted to oxene, an electrophilic and reactive species, which typically draws a hydrogen radical away from the substrate and transfers a hydroxyl group back (Chapple, 1998; Cruciani *et al*., 2005; Gonzalez and Tukey, 2005). The CYP then releases the product and is ready for a new cycle (Cruciani *et al*., 2005). For most CYPs, the reaction is uncoupled, consuming more O_2 than substrate metabolised and therefore resulting in the formation of O_2^- which is usually converted to water by the enzyme superoxide dismutase (Gonzalez and Tukey, 2005). Phase I detoxification therefore involves the CYP-dependent hydroxylation or carboxylation of relatively insoluble (lipophilic) organic compounds, causing them to become more polar water-soluble compounds and thereby allowing them to be broken down further (through conjugation in Phase 2 metabolism) and/or excreted from the body (Lewis *et al*., 1998; Glue and Clement, 1999).

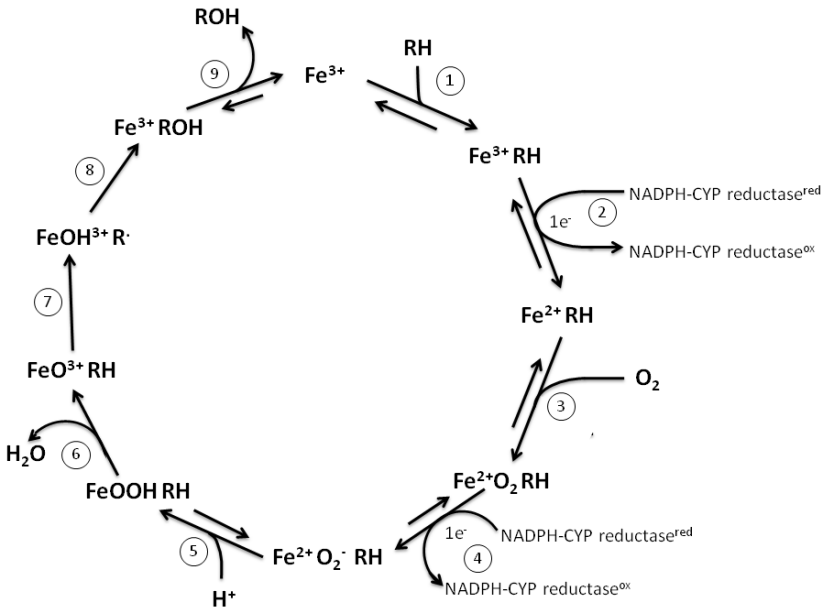

Figure 1.3: Cytochrome P450 catalytic cycle.
Fe = iron atom in CYP heme prosthetic group, RH = substrate, ROH = product, red and ox indicate the reduced and oxidised states of the intermediary enzyme CYP reductase 1) Substrate binds. 2) A single electron is transferred from NADPH to CYPs heme group through CYP reductase. 3) Oxygen is now able to bind. 4) A second electron is transferred 5) Cleavage of the oxygen bond. 6) Release of water and formation of ferryl intermediate. 7) Removal of hydrogen from substrate to form radical. 8) Radical captures hydroxyl from heme iron to form product. 9) Product released and CYP ready for another catalytic cycle. (Adapted from Guengerich, 2001).

During Phase II metabolism, enzymes (such as uridine diphosphate-glucuronosyltransferases, glutathione transferases, and sulfotransferases) conjugate the newly generated hydroxyl or carboxyl groups to polar substances such as glucuronic acid, glycine, sulphate, and acetate, which further increases the substrates aqueous solubility (Lewis *et al*., 1998; Liska, 1998; Nebert and Dieter, 2000). Phase II reactions therefore involve cofactors which have to be replenished through dietary sources (Liska, 1998). The combined result of Phase I and Phase II detoxification is the biotransformation of a lipophilic compound to a water-soluble compound that is able to be excreted through urine or bile (Liska 1998). Although CYP enzymes most likely evolved to detoxify and help eliminate harmful substances, in some cases they have been shown to convert relatively harmless compounds to toxic metabolites that contribute to increased risks of cancer initiation, promotion, and progression; birth defects; and other toxic effects (Nelson *et al*., 1993; Nebert and Russell, 2002; Guengerich, 2006). For example, environmental carcinogens have great chemical stability, but form highly reactive chemical species through a process of metabolic activation by the enzymes involved in the detoxification of xenobiotic compounds (Bertram, 2001). Having an understanding of CYP metabolism is important since it provides a basis for the explanation and prediction of certain compound interactions; offers guidelines for dose selection (or appropriate dietary concentrations in the case of PUFAs) in some patient groups; and may explain unexpected toxicity or lack of efficacy (Glue and Clement, 1999).

1.4.2 Cytochrome P450-mediated metabolism of polyunsaturated fatty acids

CYP-mediated metabolism of PUFAs generates hydroxy-fatty acids, di-hydroxy-fatty acids, and epoxy-fatty acids (Larsson *et al*., 2004; Fer *et al*., 2008a) (Figure 1.4). In terms of EPA, DHA, and AA; EPA is the preferred substrate for the majority of CYP isoforms, with DHA and AA having similar metabolism rates (Arnold *et al*., 2010). The CYP4 family, containing 5 subfamilies and 12 members, has been implicated in FA metabolism (Nebert and Russell, 2002). The CYP4A subfamily is a group of conserved, specialized FA hydroxylases that have been found to have little activity toward the majority of other characteristic CYP substrates (Domanski and Halpert, 2001). Konkel and Schunck (2011) showed that liver and renal

microsomal CYP enzymes metabolise EPA and DHA by epoxidation and hydroxylation. The n-3 double bond that distinguishes EPA and DHA from their n-6 counterparts is a predominant site of epoxidation for many CYP isoforms, including several members of the CYP4A subfamily (Arnold *et al.,* 2010; Konkel and Shunck, 2011). The main EPA metabolites produced by CYPs include ω/(ω-1)-hydroxyeicosapentaenoic acids (20- and 19-HEPE) and 5 regioisomeric epoxyeicosatetraenoic acids (EpETEs) (Arnold *et al*., 2010; Konkel and Schunck, 2011). DHA is metabolised by CYPs to ω/(ω-1)-hydroxydocosahexaenoic acids (22- and 21-HDoHE) and 6 regioisomeric epoxydocosapentaenoic acids (EpDPEs) (Arnold *et al*., 2010; Konkel and Schunck, 2011). Fer *et al*. (2008b) tested a range of human recombinant CYPs and found that CYP2C9/2C19 and 1A2 were the most efficient epoxygenases of EPA and DHA. They also found that in human liver microsomes, the hydroxylase activity was greater than the epoxygenase activity (Fer *et al*., 2008b). Adas *et al*. (1999) showed that fatty acid (ω-1)-hydroxylase activity is catalysed by CYP2E1 in the mammalian species, while the FA ω-hydroxylase activity may be catalysed by CYPs from the 4A family. Van Rollins *et al*. (1983) found that the main CYP metabolites of DHA produced in rat liver microsomes were 19, 20-; 16, 17-; 13, 14-; 10, 11-; and 7, 8- dihydroxydocosapentanoic acids and 22- and 21-hydroxydocosahexaenoic acids. These major products were a result of three classes of oxidation, namely, ω-hydroxylations, (ω-1)-hydroxylations and epoxidations (Van Rollins *et al*., 1983).

Arachidonic acid is metabolised by CYP epoxygenases to four regioisomers termed *cis*-epoxyeicosatrienoic acids (EETs) (Jiang *et al.*, 2007; Xu *et al.*, 2011), as well as other bioactive eicosanoids termed hydroxyeicosatetraenoic acids (HETEs) (Node *et al*., 1999). EETs are further metabolised to dihydroxyeicosatrienoic acids (DHETs) which are more stable and less biologically active than EETs (Xu *et al.*, 2011). CYP4A and CYP4F are AA ω/(ω-1)-hydroxylases, producing 20-hydroxyeicosatetraenoic acid (20-HETE) as their predominant product (Arnold *et al*., 2010). The CYP2 family of epoxygenases are the main enzymes involved in EET formation, with CYP2J2 being a predominant human AA epoxygenase that generates all four EETs, namely 5,6-; 8, 9-; 11,12-; and 14,15-EET, through the addition of an epoxide group to one of the four double bonds of AA (Jiang *et al.*, 2007; Xu *et al.*, 2011). CYP2J2 is mainly expressed in endothelium cells and myocardiocytes (Xu *et al.*, 2011). EETs

have been found to be antihypertensive and organ-protective, implicated in the mediation of anti-inflammatory and anti-apoptotic mechanisms that protect against cell and organ injury (Arnold *et al*., 2010).

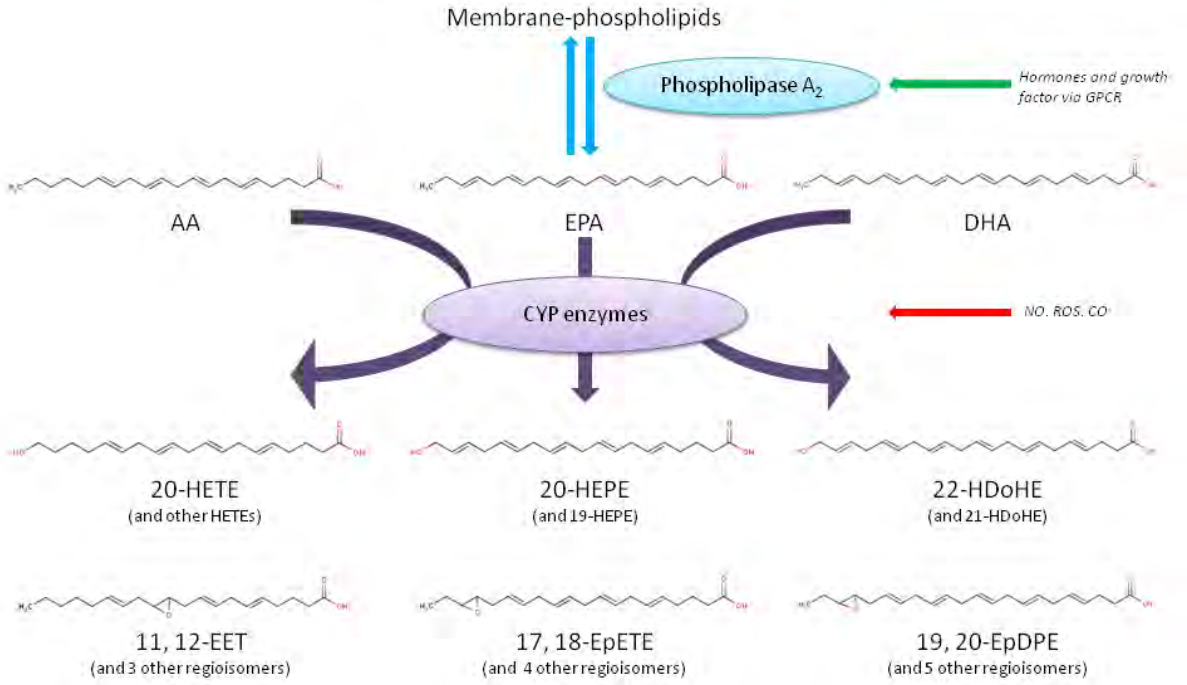

Figure 1.4: Cytochrome P450-dependent metabolism of AA, EPA and DHA.
Phospholipase A_2, activated by various hormones and growth factors via G-protein coupled receptors (GPCR), releases AA, EPA and DHA from membrane phospholipids. The free FAs compete for conversion by CYPs, with EPA being the preferred substrate for many CYP isoforms. CYP metabolism results in hydroxylation and epoxidation of the FAs. Nitric oxide (NO), carbon monoxide (CO) and reactive oxygen species (ROS), which are produced in variable amounts depending on inflammation and other disease states, inhibit CYPs. (Adapted from Arnold *et al*., 2010).

1.5 **Rationale and motivation**

The positive effects and dietary benefits of n-3 PUFAs on carcinogenesis have been previously reported. On the other hand, most studies report that n-6 PUFAs promote or have no impact on carcinogenesis. In order to have a better understanding of how these PUFAs influence carcinogenesis it is important to gain knowledge about their metabolism and comprehend how their effects will be altered upon transformation in the body. The effects of AA, EPA and DHA CYP metabolites on colon carcinoma have not previously been reported or compared to the effects of the parent compounds. This information is

important since it would determine whether the parent compound or its metabolite is having a greater effect.

1.6 **Hypothesis**

We hypothesised that EPA, DHA and AA would be metabolised by CYP enzymes within a human liver microsomal system *in vitro* and that the effects of the parent and metabolite on colon cancer cell biology would differ.

1.7 **Objectives**

The objectives of this research project were as follows:

1. Prediction of EPA, DHA and AA metabolites *in silico.*
2. Detection and *in vitro* metabolism of EPA, DHA and AA.
    I. Analytical method development and validation.
    II. Optimisation of a human liver microsomal system for *in vitro* metabolism of EPA, DHA and AA.
3. Assessment of the effect of EPA, DHA and AA on colon cancer cell viability.
4. Comparison of the effects of the parent compounds and their CYP metabolites on colon cancer cell biology.

Chapter Two

In Silico Metabolism of EPA, DHA and AA

2.1 Introduction

Determining the metabolic biotransformations a compound will undergo in the body is important since these transformations will directly affect the compounds bioavailability, activity, toxicity, distribution, and elimination from the body (Korolev *et al*., 2003). Determination of the site of metabolism is relevant because through the addition of stable groups or steric shields at the metabolically susceptible position, or the removal or replacement of metabolically susceptible groups, labile compounds can be stabilized (Cruciani *et al*., 2005). One important implication of this is that the formation of toxic metabolites can be prevented (Cruciani *et al*., 2005). Knowledge of the site of metabolism is also significant in cases where metabolism results in the compound becoming active, and in compounds which exhibit excessively long half lives (Cruciani *et al*., 2005). Information about where functional groups are metabolised can lead to improved pharmacokinetics, for example increased bioavailability and half-life, through the blockage of the major site of metabolism for the compound (Cruciani *et al*., 2005). *In silico* studies which use computational predictive methods to identify potential sites of metabolism are useful tools in early metabolism studies. Since the kinetic profile of a compound is highly dependent on the compounds biotransformation by CYP enzymes during phase 1 metabolism, prediction of the sites of metabolism during these reactions is usually the starting point in many *in silico* analyses (Cruciani *et al*., 2005; Rydberg *et al*., 2010). SMARTCyp and MetaSite are two predictive softwares that are available for such *in silico* predictions.

SMARTCyp is a rule-based web application for CYP-mediated site of metabolism predictions. SMARTCyp is able to use the 2D structure of a molecule and doesn't require the generation of 3D structures (Rydberg *et al*., 2010). The SMARTCyp algorithm involves two descriptors, namely a reactivity descriptor, E, and an accessibility descriptor, A (Rydberg *et al*., 2010). The reactivity descriptor is an estimation of the energy required for a CYP to react at a specific atom whilst the accessibility descriptor describes the position of the atom relative

to the 2D centre of the molecule (Rydberg *et al*., 2010). The score, S, for each atom is calculated according to the following equation:

$$S = E - 8A$$

with a lower score indicating a higher probability of being a site of metabolism (Rydberg *et al*., 2010). The constant 8 allows for slightly less reactive atoms, which have a significantly greater accessibility, to be ranked higher (Rydberg *et al*., 2010). Reactivity rules are based on reaction steps requiring the highest activation energy for the respective reactions (Rydberg *et al*., 2010). This reaction step is a hydrogen extraction from a carbon atom for hydroxylation and dealkylation reactions; and the attack of the oxygen on the respective atom for oxidation and epoxidation reactions (Rydberg *et al*., 2010).

MetaSite is a fully automated software program that is able to predict the site of metabolism, isoform selectivity, and ligand-cytochrome complementarity during CYP-mediated phase 1 metabolism in humans, and encompasses all the cytochromes for which 3D structure is known (Cruciani *et al*., 2005). This software also provides information about the predicted metabolites monoisotopic mass, partition coefficient (log *P*) and distribution coefficient (log *D*) which are important factors in the evaluation of the drug-likeness of a compound using the Rule of 5 (Ro5) (Lipinski *et al*., 2001). The advantage that MetaSite has over rule-based methods is that it is human-specific and therefore produces a relatively smaller number of possible final metabolites with a greater amount of accuracy (Cruciani *et al*., 2005). The program requires the user to input the substrate's structure in SMILES notation, 2D SDF format, or 3D coordinates. The computational method involves the calculation of two sets of descriptors, one for the CYP enzyme and one for the substrate of interest, which then represent the chemical fingerprint of the enzyme and the substrate respectively (Cruciani *et al*., 2005). The descriptors created for the enzyme are independent of the initial side chain position of the CYP 3D structure and are therefore able to simulate the adaptation of the enzyme to the substrate structure better (Cruciani *et al*., 2005). The fingerprint created for the potential substrate is composed of four descriptor sets, one set for each of the following atom categories: hydrophobic, hydrogen-bond acceptor, hydrogen-bond donor and charged (Cruciani *et al*., 2005). The descriptors are used to compare the

cytochrome fingerprint with that of the substrate (Cruciani *et al*., 2005). The sites of metabolism are then ranked based on a calculation of the approximate free energy required for the reaction to occur (Cruciani *et al*., 2005). This is calculated using the following equation:

$$P_{sm}(i) = E_i R_i$$

where $P_{sm}(i)$ represents the probability for the site of metabolism at atom *i* of the substrate. E_i represents a score proportional to the accessibility of atom *i* toward the reactive heme and is dependent on the 3D structure, conformation, and chirality of the substrate; and the 3D structure and side chain flexibility of the CYP enzyme. R_i represents a score proportional to the reactivity of atom *i* in a specific reaction mechanism (representing the activation energy required to produce the reactive intermediate) and is dependent on the 3D structure of the substrate and on the reaction mechanism. Therefore, an atom *i* needs to possess significant accessibility and reactivity components related to the heme in order to be classified as a site of metabolism (Cruciani *et al*., 2005).

In this chapter, MetaSite and SMARTCyp were used to predict the possible sites of metabolism for EPA, DHA and AA during the CYP-mediate reactions of phase 1 metabolism. MetaSite was also used to determine important Ro5 parameters.

2.2 Methods and Materials

SMARTCyp (www.farma.ku.dk/smartcyp) and MetaSite (Molecular Discovery Ltd., Middlesex, UK) were used for the *in silico* metabolism of EPA, DHA and AA. Both are fully automated computational procedures that predict and rank the possible sites of metabolism during the CYP-mediated reactions of phase-1 metabolism. MetaSite was also able to predict the possible metabolites that will be formed along with their monoisotopic masses, log *P* and log *D* values. The twelve most likely sites of metabolism as predicted by SMARTCyp and MetaSite are reported as well as the twelve most likely metabolites predicted by MetaSite along with their monoisotopic masses, log *P* and log *D* values.

2.3 Results

The three most likely sites of metabolism predicted by MetaSite for EPA were formed through aliphatic hydroxylation and occurred at C13, C16 and C19 (Table 2.1 and 2.2). C16 and C13 were also ranked in the top three sites of metabolism by SMARTCyp with C13 being ranked as the second site and having an equal probability with C7 (Table 2.1). These reactions were also predicted to be hydroxylation reactions by SMARTCyp. The n-3 double bond was ranked 8th and 9th by Metasite (olefinic epoxidation) and 5th and 6th by SMARTCyp (hydroxylation) (Table 2.1 and 2.2). The ω and ω-1 carbon atoms (C20 and C19) were ranked 6th and 3rd by Metasite, and 19th and 7th by SMARTCyp, with both programs predicting these to be hydroxylation reactions.

The three most likely sites of metabolism for DHA predicted by Metasite were C12 and C15 (with equal probability) and C18, with aliphatic hydroxylation being the proposed mechanism (Table 2.1 and 2.2). Both C15 and C18 were ranked within the three most likely sites of metabolism by SMARTCyp, with the ranking order being C18, C6 and C15 respectively and the predicted mechanism being hydroxylation (Table 2.1). The n-3 double bond was ranked 15th and 16th by Metasite (data not shown) and 6th and 7th by SMARTCyp (hydroxylation) (Table 2.1). The ω and ω-1 carbon atoms (C22 and C21) were ranked 9th and 4th by Metasite, and 21st and 8th by SMARTCyp, with both programs predicting these to be hydroxylation reactions (Table 2.1 and 2.2).

The three most likely sites of metabolism for AA according to Metasite were C19, C13 and C16, with the mechanism being that of aliphatic hydroxylation for C19 and C13, and dehydrogenation for C16 (Table 2.1 and 2.2). SMARTCyp predicted the three most likely sites of metabolism to be C7, C13 and C10, with the mechanism being hydroxylation (Table 2.1). The ω and ω-1 carbon atoms (C20 and C19) were ranked 7th and 1st by MetaSite, and 19th and 15th by SMARTCyp (Table 2.1 and 2.2).

Table 2.1: A comparison of the rank of metabolism sites predicted by MetaSite and SMARTCyp.

	MetaSite	SMARTCyp
EPA	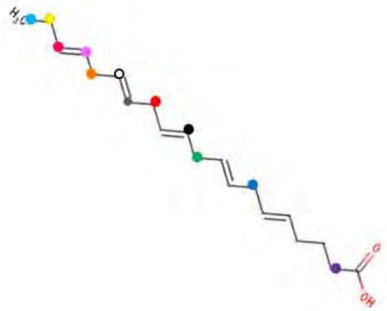 (C13, C16, C19, C10, C7, C20, C2, C18, C17, C14, C15, C11)	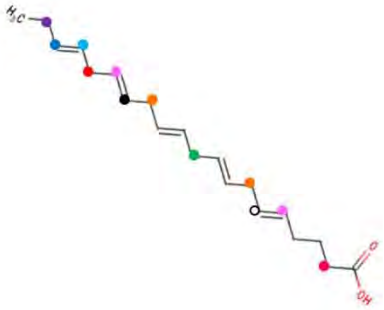 (C16, C13, C7, C10, C18, C17, C19, C2, C15, C5, C6, C14)
DHA	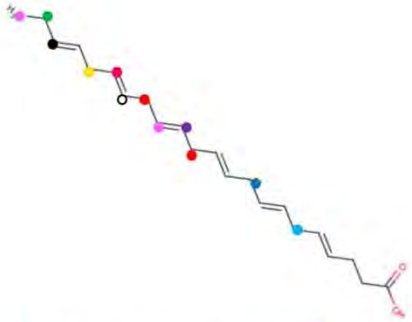 (C12, C15, C18, C21, C9, C6, C13, C17, C22, C14, C16, C3)	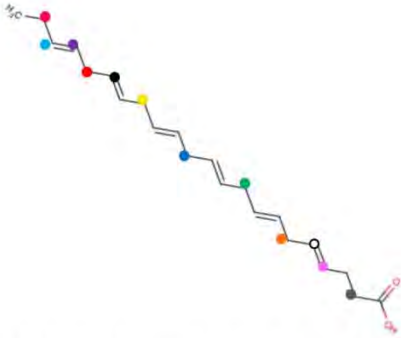 (C18, C6, C15, C9, C12, C20, C19, C21, C4, C2, C5, C17)
AA	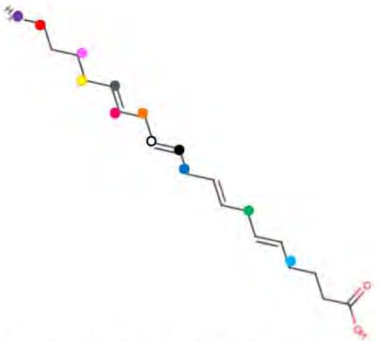 (C19, C13, C16, C7, C10, C4, C20, C14, C17, C15, C12, C11)	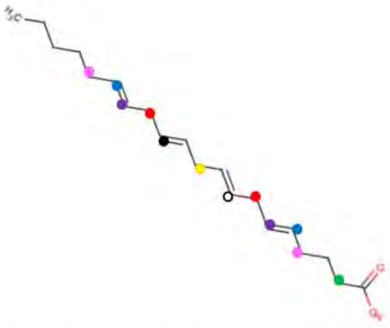 (C7, C13, C10, C2, C5, C15, C6, C14, C4, C16, C8, C12)
Ranking	1 2 3 4 5	6 7 8 9 10 11 12

The twelve most likely sites of metabolism are indicated on the relative structures using the colour coding illustrated at the bottom of the table. The sites of metabolism are also listed in rank order in parentheses, with carbon atoms having the same probability represented in colour. Carbon numbering from the carboxy terminal.

Table 2.2: Metasite metabolite predictions for EPA, DHA and AA.

	EPA	DHA	AA
Parent	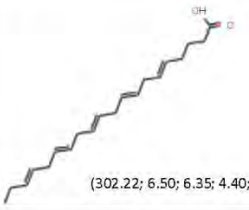 (302.22; 6.50; 6.35; 4.40; 3.22)	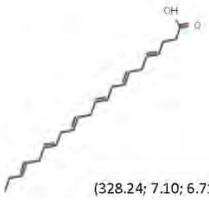 (328.24; 7.10; 6.71; 4.51; 3.77)	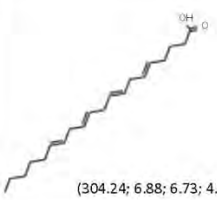 (304.24; 6.88; 6.73; 4.78; 3.60)
Metabolite 1	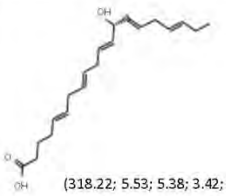 (318.22; 5.53; 5.38; 3.42; 2.12; AH)	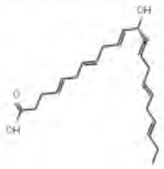 (344.24; 6.13; 5.73; 3.52; 2.66; AH)	 (320.24; 5.75; 5.60; 3.65; 2.47; AH)
Metabolite 2	 (318.22; 5.53; 5.38; 3.42; 2.12; AH)	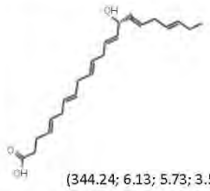 (344.24; 6.13; 5.73; 3.52; 2.66; AH)	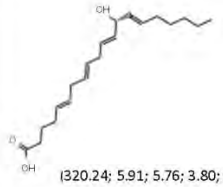 (320.24; 5.91; 5.76; 3.80; 2.50; AH)
Metabolite 3	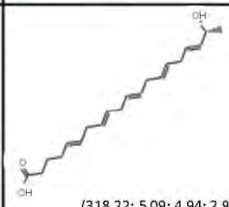 (318.22; 5.09; 4.94; 2.99; 1.81; AH)	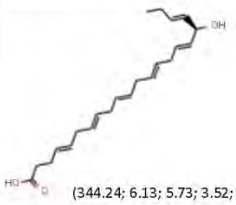 (344.24; 6.13; 5.73; 3.52; 2.66; AH)	 (302.22; 6.99; 6.84; 4.90; 3.71; D)
Metabolite 4	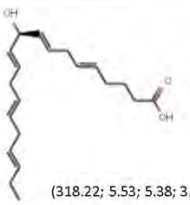 (318.22; 5.53; 5.38; 3.42; 2.12; AH)	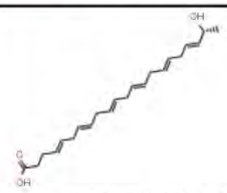 (344.24; 5.69; 5.29; 3.10; 2.36; AH)	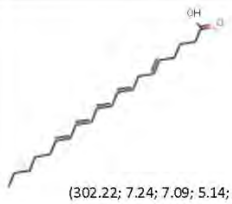 (302.22; 7.24; 7.09; 5.14; 3.96; D)
Metabolite 5	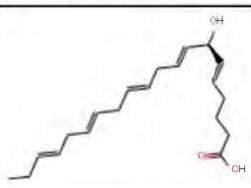 (318.22; 5.53; 5.38; 3.42; 2.12; AH)	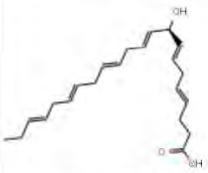 (344.24; 6.13; 5.73; 3.52; 2.66; AH)	 (318.22; 5.79; 5.64; 3.69; 2.39; AC)
Metabolite 6	 (318.22; 5.31; 5.16; 3.22; 2.03; AH)	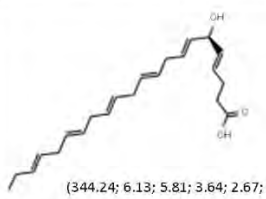 (344.24; 6.13; 5.81; 3.64; 2.67; AH)	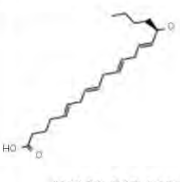 (320.24; 5.47; 5.32; 3.37; 2.19; AH)

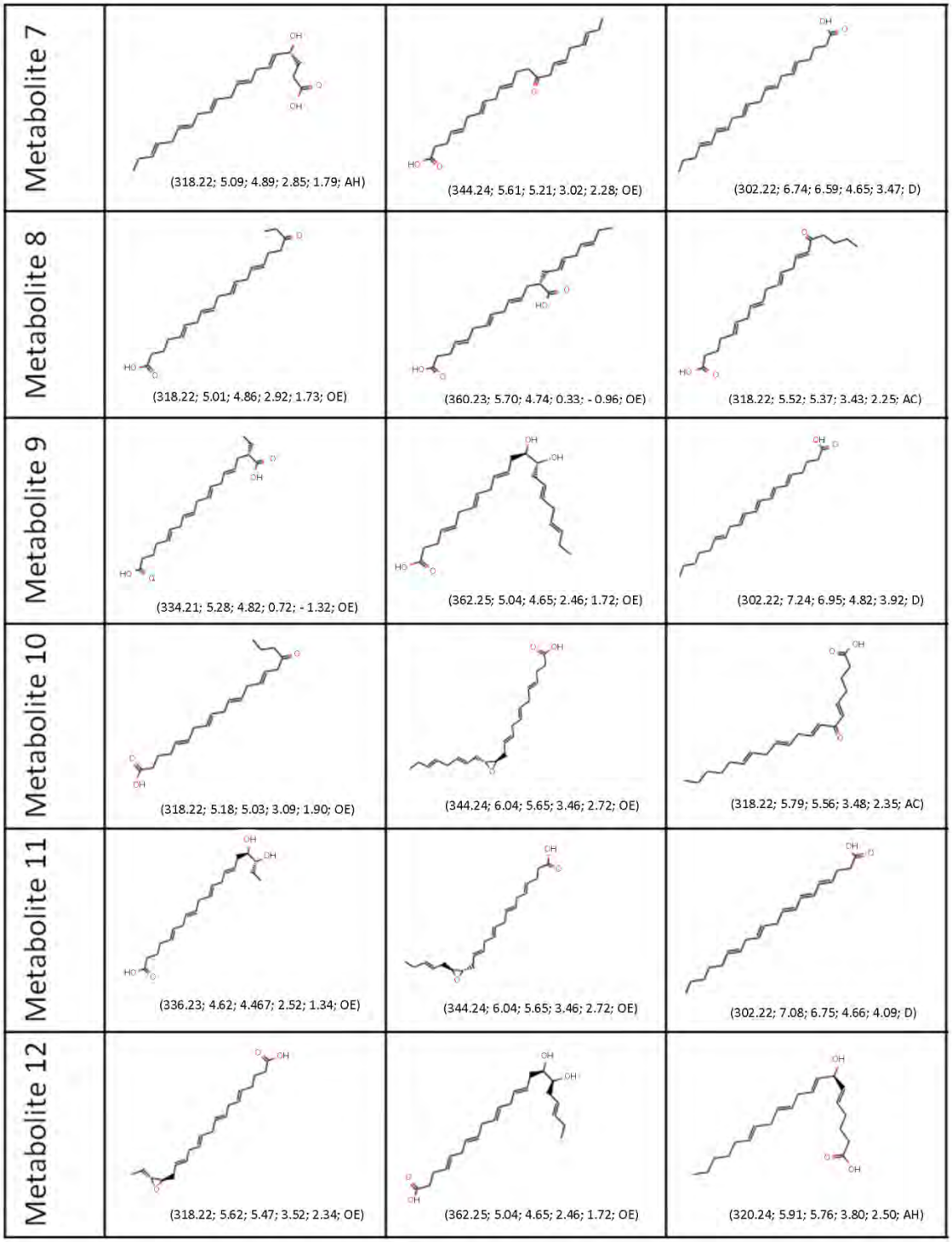

Summary of the 12 most likely CYP-mediated phase 1 metabolites of EPA, DHA and AA as predicted by MetaSite. Monoisotopic masses (MiM), log *P*, log D_4, log D_7, log D_9, and the proposed mechanism are indicated in parentheses in that order. Note that log *D* is a pH dependent version of the partition coefficient, log *P,* and the numerical subscripts represent the respective pH. Mechanism key: Aliphatic hydroxylation: AH; Olefinic Epoxidation OE; Dehydrogenation D; Aliphatic Carbonylation AC.

2.4 Discussion

CYP-mediated metabolism of PUFAs has been found to generate hydroxy-, di-hydroxy-, and epoxy-fatty acids (Larsson *et al*., 2004; Fer *et al*., 2008a). MetaSite predictions encompassed all three of these metabolite types, but SMARTCyp was limited in its predictions because it was only able to predict that the transformation that would occur during CYP metabolism of FAs would be a hydroxylation. This is a restrictive factor for SMARTCyp since it simply predicts that all transformations that occur at a carbon atom will be hydroxylation reactions. Another limiting factor of SMARTCyp is that it is bias towards the CYP3A4 isoform. The SMARTCyp method identifies the sites in a molecule that are most reactive with regard to CYP-mediated reactions (Rydberg *et al*., 2010). Since the 3A4 isoform has the largest active site and the most flexible structure, it is the most promiscuous isoform, with small restrictions on the size and shape of its substrates (Rydberg *et al*., 2010). Reactivity is therefore key in determining the site of metabolism for this isoform, and since SMARTCyp is foremost a reactivity model, it shows a preference for predicting sites that are metabolised by the CYP3A4 isoform (Rydberg *et al*., 2010).

The n-3 double bond of EPA and DHA has previously been found to be a major site of epoxidation for many CYP isoforms (Konkel and Shunck, 2011). It was therefore expected that this site would be ranked as a likely site of metabolism by Metasite and SMARTCyp, and that the predicted mechanism would be that of epoxidation. For both EPA and DHA, Metasite predicted that the transformation that would occur at this double bond would be an olefinic epoxidation. For EPA, this site was ranked 8^{th} through to 12^{th} and for DHA it was ranked 15^{th} and 16^{th}. SMARTCyp ranked this double bond 5^{th} and 6^{th} for EPA and 6^{th} and 7^{th} for DHA, however the predicted mechanism was not that of epoxidation, but rather hydroxylation due to SMARTCyp's limitations.

Previous studies have found that AA is metabolised by CYP epoxygenases to four regioisomers termed *cis*-epoxyeicosatrienoic acids (EET) (Jiang *et al.*, 2007). These metabolites were however not predicted by MetaSite or SMARTCyp. AA has also been found

to be metabolised to dihydroxyeicosatrienoic acids (DHETs) and hydroxyeicosatetraenoic acids (HETEs) (Node *et al*., 1999). MetaSite and SMARTCyp did not predict the formation of DHETs but were able to predict the formation of HETEs.

It was expected that the ω/(ω-1) position would be ranked as a likely site of hydroxylation for EPA, DHA and AA (Konkel and Schunck, 2011). Both programs predicted the transformation that would occur at these carbon atoms to be hydroxylation reactions. For EPA, the ω carbon was ranked 6th and 19th and the ω-1 carbon 3rd and 7th; for DHA, the ω carbon was ranked 9th and 21st and the ω-1 carbon 4th and 8th; for AA, the ω carbon was ranked 7th and 19th and the ω-1 carbon 1st and 15th by MetaSite and SMARTCyp respectively. Both programs therefore predicted the ω-1 carbon to be a greater site of metabolism than the ω carbon. SMARTCyp ranked the ω carbon as the second to last possible site of metabolism for all three FAs.

The Rule of 5 (Ro5) is used to evaluate drug-likeness of compounds, i.e. it gives an indication of whether a chemical compound has pharmacokinetic properties that would make it a suitable orally administered therapeutic agent (Bhal *et al*., 2007). The Ro5 states that in order for a compound to be considered drug-like it must have a molecular weight less than 500; a partition coefficient (log *P*) less than 5; less than 5 hydrogen bond donor atoms; and less than 10 nitrogen and oxygen atoms combined (Lipinski *et al*., 2001; Bhal *et al*., 2007). Compounds that violate these rules show poor pharmacokinetic properties for oral administration (Bhal *et al*., 2007). Log *P* (the partition coefficient) is a measure of lipophilicity that describes the differential partitioning of a neutral compound between two immiscible solvents, most commonly octan-1-ol and water (Bhal *et al*., 2007). The MetaSite predicted metabolites of EPA, DHA and AA all have log *P* values greater than 5. When considering log *P* values only, these compounds will be strongly lipophilic, which is expected since they are derived from fatty acids. The problem with highly lipophilic compounds is that they are likely to be rapidly metabolised and bioaccumulated, have low aqueous solubility and poor absorption properties (Bhal *et al*., 2007). However, log *D* values also need to be taken into account, which need to be equal to or less than 5 in order for the compound to

pass lipophilicity screening (Bhal *et al*., 2007). Log *D* is a pH dependent version of log *P* and it describes the octanol-water distribution coefficient for partitioning of ionisable species in biphasic media (Bhal *et al*., 2007). Log *D* is important since the pH of the body varies between different organs and so the ionic state of the compound of interest will vary depending on the pH of the immediate physiological conditions (Bhal *et al*., 2007). The log D_4 values are above five for the EPA, DHA and AA metabolites, except for the predicted metabolites 3, 7, 8 and 9 for EPA, and 8, 9 and 12 for DHA (Table 2.2). The log D_7 and D_9 values are below 5 for all the EPA, DHA and AA predicted metabolites (except metabolite 4 for AA). All MetaSite predicted metabolites for EPA, DHA and AA have molecular weights less than 500; less than 5 hydrogen bond donor atoms; and less than 10 nitrogen and oxygen atoms combined. This in combination with the fact that they have log D_7 and D_9 values less than 5 means that these metabolites have pharmacokinetic properties that would make them suitable for oral administration.

2.5 Conclusion

In silico studies are a good starting point during the determination of a compounds CYP-mediated phase 1 metabolism. However, these findings should be checked against literature and validated via *in vitro* studies. When performing *in silico* analyses, it is important to have a basic understanding of the mechanism by which the chosen software will perform its predictions. It is also important to have an understanding of the limitations of the chosen program. For the determination of FA metabolites *in silico*, MetaSite is a more efficient tool than SMARTCyp. This is because MetaSite is able to not only predict and rank the possible sites of metabolism, but it is also able to give information about the reaction type as well as monoisotopic masses and log *P* and log *D* values. Other advantages of MetaSite are that it is human specific and that it is not rule based, but rather, relies on the 3D structure of the different CYP isoforms (Cruciani *et al*., 2005). Since SMARTCyp is a rule- and 2D-based method, it has the disadvantage that highly reactive sites, which are not accessible in 3D space, are still ranked quite high (Rydberg *et al*., 2010). Another disadvantage of SMARTCyp is that it is bias toward the 3A4 isoform. The SMARTCyp reactivity parameter can be complemented with additional descriptors and empirical knowledge to increase accuracy

and create models for other CYP isoforms (Rydberg *et al*., 2010), but this process is complicated. However, if SMARTCyp is the chosen method for *in silico* metabolism, it would be far more accurate if the program was adapted to incorporate CYP isoforms known to metabolise the compound of interest.

In conclusion, both MetaSite and SMARTCyp predicted that EPA, DHA and AA will be metabolised by CYP enzymes through hydroxylation. MetaSite was also able to predict the formation of di-hydroxy- and epoxy-FAs. All MetaSite predicted metabolites for EPA, DHA and AA showed suitable pharmacokinetics for oral administration since they satisfied the criteria of the Ro5.

Chapter Three

In Vitro Metabolism of EPA, DHA and AA

3.1 Introduction

In vitro studies are useful for determining: the metabolism of compounds that do not have toxicological profiles; mechanisms of metabolism in more detail; potential compound-compound interactions; effects of environmental agents, ethnic background, gender, and genetics on the compounds' metabolism; and for biologically generating reference standards when chemically synthesized metabolite standards are not available (Wrighton *et al*., 1995; Scarth *et al*., 2010). Studies have shown that *in vitro* metabolism assays are as effective as *in vivo* assays and result in the same metabolite profile (Scarth *et al*., 2010). *In vitro* methods for the study of human liver drug metabolism can be divided into two categories, namely cellular models and drug-metabolising enzyme preparations (Wrighton *et al*., 1995). Cellular models include primary hepatocytes, liver slices, and hepatocyte derived cell lines; drug-metabolizing enzyme preparations include tissue homogenates, subcellular fractions (such as microsomal and cytosolic fractions), and isolated enzymes (Wrighton *et al*., 1995). The most commonly used system for *in vitro* metabolism studies has been the use of subcellular fractions (Wrighton *et al*., 1995).

Metabolism of many exogenous compounds (such as drugs) as well as many endogenous compounds (such as fatty acids) occurs in two stages, namely phase 1 and phase 2 (Glue and Clement, 1999). Phase 1 reactions encompass oxidation, reduction, and hydrolytic reactions, and lead to the conjugation of -OH, -COOH, -SH, -O- or NH_2 functional groups to the compound (Glue and Clement, 1999; Cruciani *et al*., 2005; Gonzalez and Tukey, 2005). These functional groups often dramatically alter the biological properties of the metabolite and may lead to either the inactivation of an active compound or, in some cases, the bioactivation of compounds (Gonzalez and Tukey, 2005). Phase 2 reactions involve the covalent conjugation of hydrophilic moieties (such as glutathione, glucuronic acid and sulphate) to the products formed during phase 1 (Lewis *et al*., 1998; Liska, 1998; Gonzalez and Tukey, 2005). The attachment sites for these hydrophilic moieties are usually the

oxygen, nitrogen and sulphur atoms added during phase 1 metabolism (Gonzalez and Tukey, 2005). The result of phase 2 metabolism is a compound with increased molecular weight and polarity, thus facilitating its elimination from the body (Gonzalez and Tukey, 2005).

CYPs are a family of heme-containing monooxygenases responsible for the majority of phase 1 metabolism (Yao *et al*., 2006). These enzymes are located in the endoplasmic reticulum within the living eukaryotic cell (Gonzalez and Tukey, 2005). When eukaryotic cells are broken up, closed vesicle-like structures containing CYP enzymes are formed from the endoplasmic reticulum, and these are known as microsomes (Pearce *et al*., 1996; De Graaf *et al*., 2002). Microsomes are therefore useful for the *in vitro* study of phase 1 metabolism (De Graaf *et al*., 2002). An advantage of using microsomes is that they are commercially available (from various animal species as well as humans) and can be easily preserved for long periods of time through storage at low temperatures (e.g., -80°C) (Wrighton *et al*., 1995; De Graaf *et al*., 2002; Jia and Liu, 2007). *In vitro* microsomal studies are advantageous over *in vivo* studies when determining the metabolites of a specific substrate since they normally result in a more concentrated, cleaner extract for analysis (Scarth *et al*., 2010). A disadvantage is that microsomes are not able to fully predict *in vivo* metabolism since they do not allow for phase 2 metabolism to occur (De Graaf *et al*., 2002). This is because they only posses UDP-glucuronyltransferases but lack the cofactor UDPGA and any other phase II enzymes and cofactors (De Graaf *et al*., 2002).

This chapter encompasses the use of human liver microsomes for the *in vitro* phase 1 metabolism of EPA, DHA and AA. A gas chromatography (GC) method was developed for the qualification of these PUFAs and their metabolites. This method was validated in terms of inter- and intra-day reproducibility, linearity and limit of detection (LOD). The microsomal system was optimised in terms of microsome and FA concentration. The concentrations of FA used were chosen such that they were high enough to generate detectable amounts of metabolite(s), but not so high that toxicity occurs (De Graaf *et al*., 2002).

3.2 Methods and Materials

3.2.1 Method validation

EPA, DHA and AA were purchased from Sigma-Aldrich®, Germany (product numbers: 44864; D2534; 10931). Solvents used were analytical grade and purchased from Sigma-Aldrich®, Germany. The analytical method for the detection of the FAs of interest was validated in terms of inter- and intra-day reproducibility, linearity, and LOD. FAs were dissolved in 1 ml dichloromethane (DCM) to a range of concentrations and derivatised using a fatty acid methyl ester (FAME) synthesis protocol adapted from Budge *et al*. (2006). Briefly, 3 ml Hilditch reagent (1.5% concentrated H_2SO_4 in MeOH dried over anhydrous Na_2SO_4) was added to samples which were then covered with N_2, capped, sealed with teflon tape, vortexed and placed at 100°C for 1 hour (vortexed at 30 minutes again to ensure proper mixing). Samples were allowed to cool to room temperature. Liquid-liquid extraction was performed by addition of 3 ml hexane and 1 ml MilliQ H_2O. Samples were vortexed, centrifuged at 857 *g* (Hettich EBA 20 centrifuge) for 5 minutes, and the top layer removed and kept. The hexane extraction was repeated an additional two times using 1 ml hexane each time. Anhydrous Na_2SO_4 was added. Samples were evaporated to dryness under N_2 and reconstituted in 100 µl hexane. GC (Agilent 7000 A), coupled to a flame ionization detector (FID), was used to analyse the samples. The column utilised was a Zebron™ ZB-WAX plus capillary GC column (length: 30 m, internal diameter: 0.32 mm, stationary film thickness: 0.25 µm) (Phenomenex, USA). Total run time was 40 minutes. Splitless injection was used with an injection temperature of 250°C. Initial oven temperature was 70°C and was held for 1 minute. The temperature was ramped at 40°C/minute to 170°C and then at 2.5°C/minute to 250°C and held for 4.5 minutes. Detection temperature was 300°C. For the inter- and intra-day reproducibility studies, the FAs were diluted such that their final concentration in the 100 µl hexane would be 200 µM. In the linearity studies, the final concentrations used were 25, 50, 100, 200, and 400 µM. Eicosadienoic acid (EDA) (Sigma-Aldrich®, Germany, product number: E3127) was used as an internal standard (IS) and was diluted such that its final concentration was 200 µM. The LODs were determined from linear regression curves of average peak height. The concentration at which a signal three times the baseline noise would be produced was taken to be the LOD.

3.2.2 Derivatisation and extraction optimisation

3.2.2.1 Derivatisation using 10% H_2SO_4/MeOH (v/v).

EPA was used for the optimisation of the derivatisation and extraction process. Microsomal incubation mixtures (1 ml) were set up containing 0.3 mg microsomes (Sigma-Aldrich®, Germany, product number: M0317), 50 µM EPA, 0.12 M potassium phosphate buffer (pH 7.4, with 5 mM $MgCl_2$), 5 mM glucose-6-phosphate (G6P) and 1 U/ml glucose-6-phosphate dehydrogenase (G6PDH). $NADP^+$ was omitted to prevent metabolism from occurring during this optimisation assay. G6P, G6PDH and $NADP^+$ were purchased from Calbiochem®. Two controls were set in place, one lacking microsomes and the other lacking EPA. A third control was also set up containing 50 µM EPA in DCM alone. Samples were incubated at 37°C for 15 minutes after which time 3 ml of a 10% H_2SO_4/MeOH (v/v) dried over anhydrous Na_2SO_4 solution was added. Samples were then capped with N_2, sealed with Teflon tape, vortexed and incubated at 100°C for 1 hour (vortexing again at 30 minutes). Samples were extracted into hexane and analysed by gas chromatography coupled to a flame ionisation detector (GC-FID) as described in section 3.2.1.

3.2.2.2 Optimisation to reduce contaminants

The assay was repeated, but this time 125 µl of a 0.2% H_2SO_4/MeOH (v/v) solution was added at the end of the 15 minutes incubation period at 37°C instead of the 10% H_2SO_4/MeOH (v/v) solution. Samples were extracted into DCM twice (2 ml DCM used for each extraction). The DCM was dried down under N_2 to a volume of 1.5 ml and 3 ml Hilditch reagent was added. Samples were capped with N_2, sealed with teflon tape, vortexed and placed at 100°C for 1 hour (vortexed at 30 minutes again to ensure proper mixing). Samples were cooled to room temperature, extracted into hexane and analysed via GC-FID as described in section 3.2.1.

3.2.3 Human liver microsomal system optimisation and PUFA metabolism

3.2.3.1 Identification of contaminating peaks

Incubation mixtures were set up in triplicate containing 0.3 mg/ml microsomes, 0.12 M potassium phosphate buffer (pH 7.4, with 5 mM $MgCl_2$), 5 mM G6P, 1 U/ml G6PDH and 1 mM $NADP^+$. These mixtures lacked any added FAs. Controls lacking microsomes were also prepared. Samples were derivatised through FAME synthesis using 10% H_2SO_4/MeOH (v/v) and extracted three times into hexane as previously described (section 3.2.1). An Agilent 7000 A GC-MS-QQQ coupled with the NIST 08 MS library was used to analyse the samples. The GC-MS running conditions were the same as those stipulated for GC-FID in section 3.2.1. MS was conducted in full scan mode using a transfer line temperature of 280°C and EI of 70 eV. GC-MS peaks were identified using MassHunter (Agilent Technologies).

3.2.3.2 *In vitro* metabolism of EPA using human liver microsomes

EPA was used for the optimisation of the human liver microsomal system. The *in vitro* metabolism conditions were adapted from Amet *et al.* (2002). Incubation mixtures (1 ml) were set up containing 0.3 mg microsomes, 50 µM EPA, 0.12 M potassium phosphate buffer (pH 7.4, with 5 mM $MgCl_2$), 5 mM G6P, 1 U/ml G6PDH and 1 mM $NADP^+$ (added to start the reaction). LA was used as a positive control. Three negative controls were established, one lacking microsomes and containing EPA, one lacking microsomes and containing LA, and the third containing microsomes and lacking FAs. The reaction was carried out for 15 minutes at 37°C and terminated by the addition of 3 ml 10% H_2SO_4/MeOH (v/v) dried over anhydrous Na_2SO_4. Derivatisation, extraction into hexane and GC-FID analysis were carried out as outlined in section 3.2.1. Samples were also analysed using GC-MS under the same conditions stipulated in section 3.2.3.1. GC-MS peaks were analysed using MassHunter.

3.2.3.3 Optimisation of i*n vitro* metabolism of EPA

The assay was repeated with an increased microsomal concentration of 0.6 mg/ml and FA concentration of 100 µM. EPA metabolism was performed in triplicate. LA was used as a

positive control and three negative metabolism controls were set up: one lacking microsomes and containing EPA, one lacking microsomes and containing LA, and the third containing microsomes and lacking FAs. Derivatisation and extraction into hexane were then carried out as outlined in section 3.2.1, but the hexane extraction was only performed twice instead of three times. Samples were analysed using GC-MS (under the conditions indicated in section 3.2.3.1) and peaks generated were identified using MassHunter.

3.2.3.4 DHA and AA metabolism

The *in vitro* metabolism of DHA and AA using human liver microsomes was performed in triplicate using the same method as stipulated for the *in vitro* metabolism of EPA outlined in section 3.2.3.3.

3.3 Results

3.3.1 Method validation

The analytical method for the detection of LA, EPA, DHA and AA involved derivatisation through the generation of FAMEs, liquid-liquid extraction into hexane and detection by GC-FID. This method was validated in terms of inter- and intra-day reproducibility, linearity, and LOD. The standard deviations for the average retention times and peak area ratios for the FAs were minimal, indicating that the method for the detection of LA, EPA, DHA and AA showed inter-day reproducibility (Table 3.1). For each FA, the average retention times and peak area ratios generated on the three consecutive days were similar, indicating that LA, EPA, DHA and AA showed intra-day reproducibility (Table 3.1). LA, EPA, DHA and AA resulted in a linear increase in average peak area ratio with increasing concentration from 25 to 400 µM (Figure 3.1). The LODs were defined as the concentration at which a signal three times baseline noise would be achieved, and were calculated using linear regression curves generated from average peak height (data not shown). The LODs were determined to be 92.61 nM, 169.52 nM, 131.20 nM and 203.77 nM for LA, EPA, DHA and AA respectively.

Table 3.1: Inter- and intra-day reproducibility of the detection of LA, EPA, DHA and AA by GC-FID.

	Day	Retention time (min)	Average peak area ratio*
LA	**1**	5.075 ± 0.001	0.349 ± 0.052
	2	5.074 ± 0.001	0.345 ± 0.047
	3	5.074 ± 0.001	0.347 ± 0.045
EPA	**1**	19.896 ± 0.002	0.861 ± 0.047
	2	19.890 ± 0.006	0.870 ± 0.049
	3	19.883 ± 0.013	0.869 ± 0.048
DHA	**1**	25.723 ± 0.005	1.401 ± 0.048
	2	25.718 ± 0.008	1.447 ± 0.048
	3	25.710 ± 0.021	1.444 ± 0.044
AA	**1**	20.781 ± 0.029	1.468 ± 0.154
	2	20.751 ± 0.017	1.471 ± 0.151
	3	20.785 ± 0.014	1.468 ± 0.139

FAMEs were synthesised and extracted into hexane. Samples were analysed using GC-FID. The assay was performed in triplicate on three consecutive days using 200 µM of the FA of interest and 200 µM EDA as an IS. *Average peak area ratio was calculated by taking the average of (FA peak area/EDA peak area).

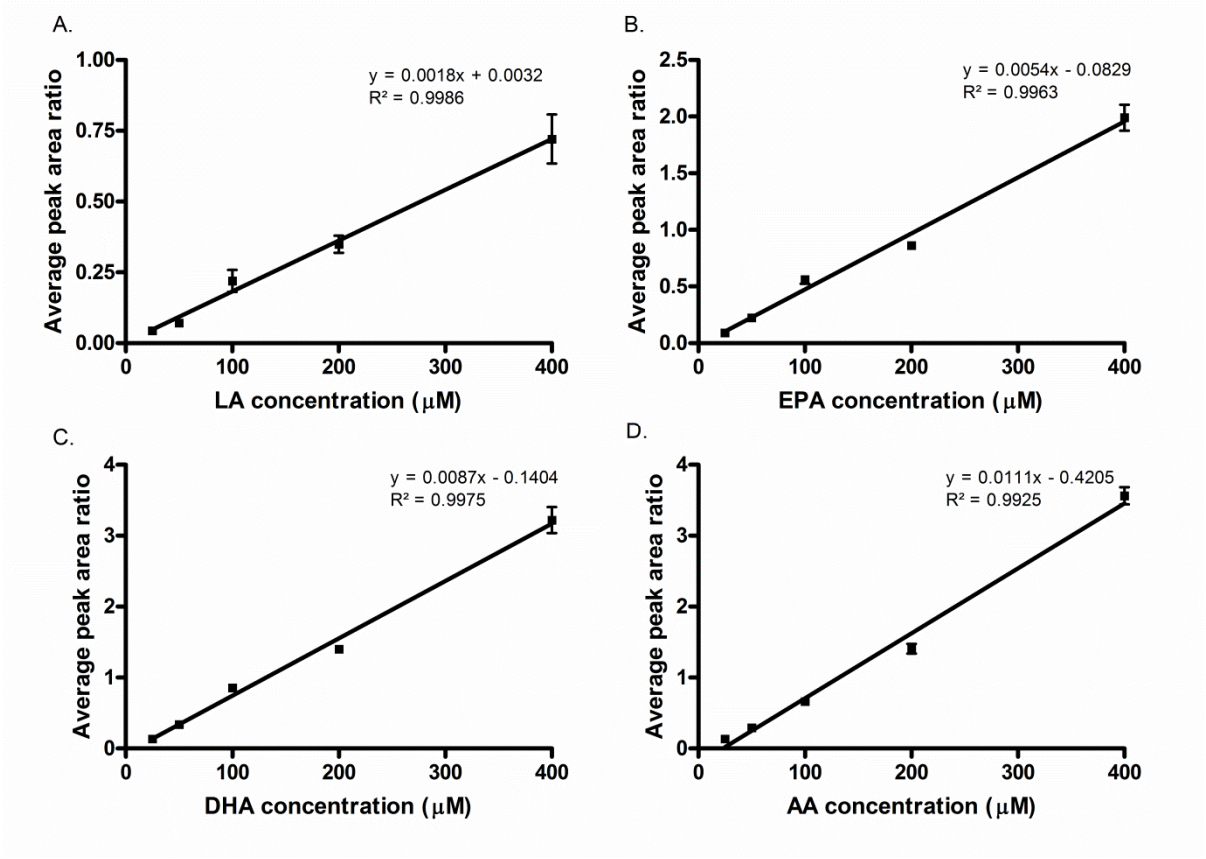

Figure 3.1: LA, EPA, DHA and AA GC-FID linearity.
EDA (200 μM) was used as an IS. FAMEs were synthesised through the use of Hilditch reagent, extracted into hexane and detected by GC-FID. The concentration range used for LA, EPA, DHA and AA was from 25 to 400 μM. Average peak area ratio was calculated by taking the average of (FA peak area/EDA peak area). Error bars indicate the standard deviation of the mean where *n=3*. A) LA linearity. B) EPA linearity. C) DHA linearity. D) AA linearity.

3.3.2 Derivatisation and extraction optimisation

Using the FAME synthesis protocol, hexane extraction and GC-FID detection method outlined in section 3.2.2.1, EPA resulted in a peak at 21.961 minutes in the control containing EPA dissolved in DCM (Figure 3.2A). This peak was also present in the total incubation mix and the control lacking microsomes but containing EPA (Figure 3.2B). It was absent in the control containing microsomes but lacking EPA (Figures 3.2A and B). This indicates that the peak represented EPA. When an initial extraction into DCM before FAME synthesis was performed, a decrease in peak areas for all the major peaks was observed, including EPA (Figure 3.3).

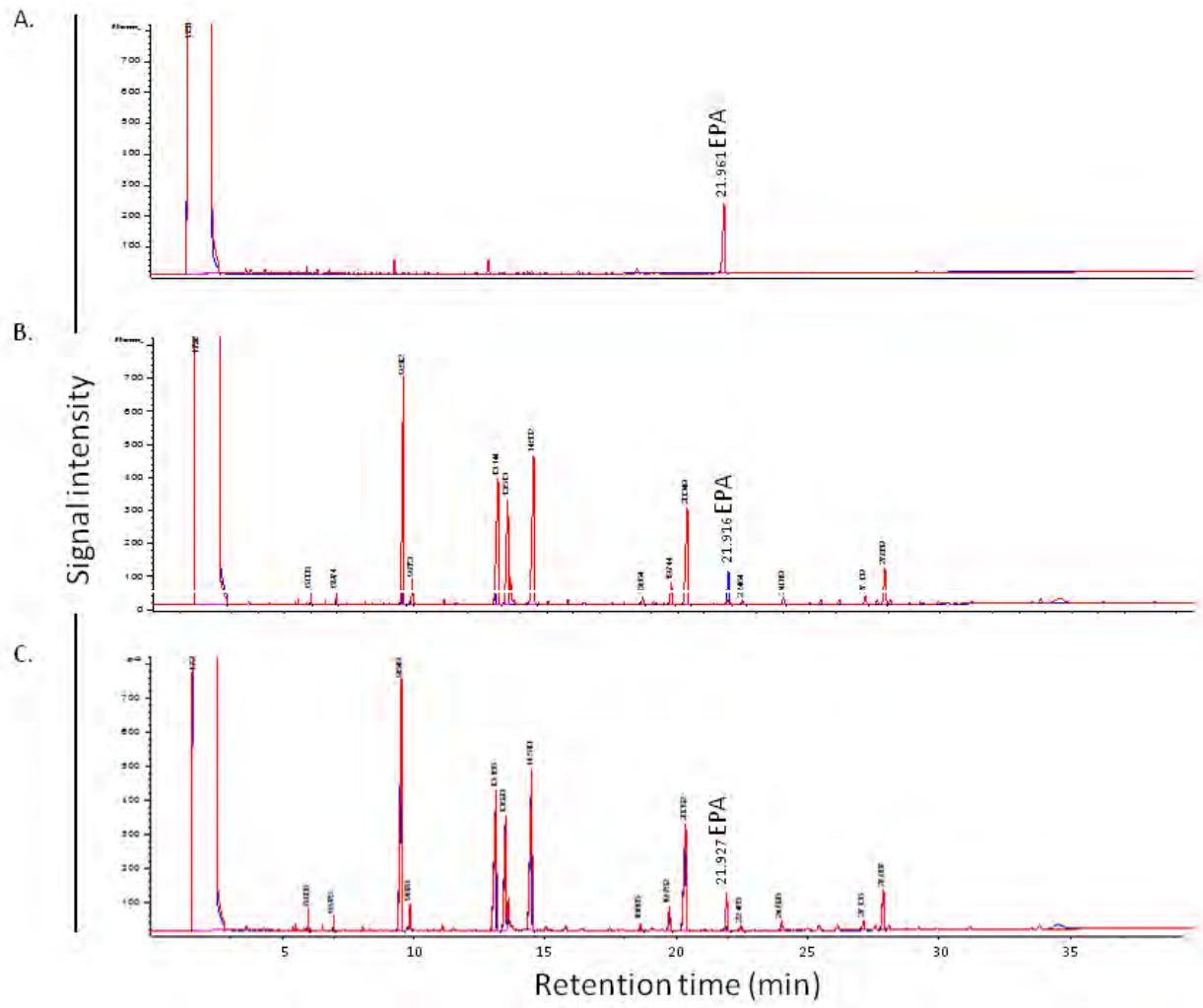

Figure 3.2: EPA extraction from the human liver microsomal system using 10% H_2SO_4/MeOH (v/v) for derivatisation.

An incubation mix was set up containing 0.3 mg microsomes, 50 µM EPA, 0.12 M potassium phosphate buffer (pH 7.4, with 5 mM $MgCl_2$), 5 mM G6P and 1 U/ml G6PDH. $NADP^+$ was omitted so as to prevent metabolism. EPA was derivatised by the addition of 10% H_2SO_4/MeOH (v/v) to this incubation mix and incubation at 100°C for 1 h. Liquid-liquid extraction into hexane was then carried out followed by GC-FID detection. A) Chromatogram produced for the control which contained EPA dissolved in DCM only (red) overlaid with the hexane blank (blue). B) Overlay of the chromatogram produced for the control containing microsomes but lacking EPA (red) and the control lacking microsomes but containing EPA (blue). C) Overlay of the chromatogram produced for the total incubation mix containing EPA (red) and the control containing microsomes but lacking EPA (blue).

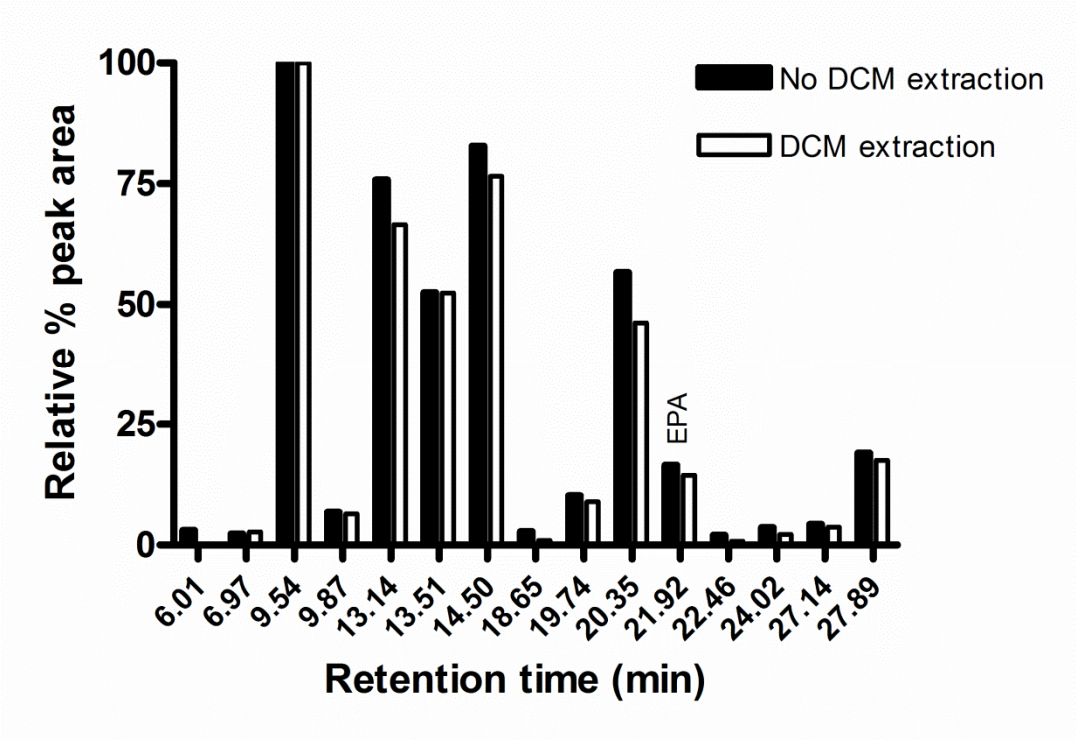

Figure 3.3: Effect of an initial DCM extraction on microsomal contamination.
An initial extraction into DCM was performed before FAME synthesis and extraction into hexane. The relative percent peak areas for the total incubation mix from the assay lacking an initial DCM extraction (section 3.2.2.1) and the assay in which an initial DCM extraction was performed before derivatisation are compared (section 3.2.2.2). The incubation mixes contained 0.3 mg/ml microsomes; 50 µM EPA; 0.12 M phosphate buffer (pH 7.4, with 5 mM $MgCl_2$); 5 mM G6P and 1 U/ml G6PDH. Relative percent peak area was calculated by allowing the largest peak (appearing at 9.54 min) to represent 100% and then expressing the other peak areas as a percentage relative to this peak.

3.3.3 Human liver microsomal system optimisation and PUFA metabolism

3.3.3.1 Identification of contaminating peaks

MassHunter was used to identify the contaminating peaks present in incubation mixes set up containing microsomes but lacking any added FAs. The main contaminants were various FAs, including EPA, DHA and AA (Table 3.2), with different forms of cholesterol forming minor contaminants.

Table 3.2: Contaminants from human liver microsomes.

Retention Time	Name	Formula	Area Sum Percent
5.552 ± 0.003	Myristic acid, ME	$C_{15}H_{30}O_2$	0.96 ± 0.10
7.347 ± 0.025	Palmitic acid, ME	$C_{17}H_{34}O_2$	2.75 ± 0.43
10.126 ± 0.097	Stearic acid, ME	$C_{19}H_{38}O_2$	22.08 ± 1.34
10.378 ± 0.021	Oleic acid, ME	$C_{19}H_{36}O_2$	14.55 ± 0.24
16.026 ± 0.049	Arachidonic acid, ME	$C_{21}H_{34}O_2$	23.43 ± 1.38
17.377 ± 0.043	Eicosapentaenoic acid, ME	$C_{21}H_{32}O_2$	0.77 ± 0.08
22.982 ± 0.025	Docosahexaenoic acid, ME	$C_{23}H_{34}O_2$	9.09 ± 0.50

Incubation mixes were set up containing microsomes but lacking any added FAs. FAME synthesis was performed followed by extraction into hexane and analysis by GC-MS and MassHunter. The major contaminants found are listed. These contaminants were not present in samples lacking microsomes. Average (± S.D.) retention time and area sum percent are given, *n = 3*.

3.3.3.2 *In vitro* metabolism of EPA PUFA

The initial EPA metabolism assay was conducted using 0.3 mg/ml microsomes and 50 µM FA in 0.12 M potassium phosphate buffer (pH 7.4, with 5 mM $MgCl_2$) with an NADPH generating system. The positive control, LA, produced a peak at 4.646 minutes in the control containing LA and lacking microsomes (Figure 3.4A). This peak was also present in the total incubation mix containing microsomes and LA, 0.12 M, but absent in the control containing microsomes and lacking FAs (Figure 3.4B). Through the use of MassHunter, a possible metabolite peak for LA was identified at 13.902 minutes (Figure 3.4B and C). This peak was identified as 12-OH-LA. It was absent in both the control containing LA and lacking microsomes, as well as the control containing microsomes and lacking FAs. The area sum percent for LA and 13-OH-LA in the total incubation mix were 2.41 and 0.25% respectively. EPA produced a peak at 18.383 minutes in the control containing EPA and lacking microsomes (Figure 3.5A). This peak was also present in the total incubation mix containing microsomes and EPA (Figure 3.5B). A peak for EPA was identified in the control containing microsomes but lacking FAs, but this peak had a smaller peak area than those samples which contained added EPA. No EPA metabolites were identified (Figure 3.5B).

EPA metabolism was repeated using an increased concentration of 0.6 mg/ml microsomes and 100 µM FAs. LA was identified at 4.488 minutes in the total incubation mix containing LA as well as the control containing LA and lacking microsomes. 12-OH-LA was identified at 13.098 minutes in the total incubation mix containing LA and was absent in both the control containing microsomes and lacking FAs and the control lacking microsomes and containing LA (Data not shown). The area sum percent for LA and 12-OH-LA in the total incubation mix were 1.47 and 0.34% respectively. EPA resulted in a peak at 17.381 ± 0.037 minutes in the total incubation mixes containing EPA and the control containing EPA and lacking microsomes. This peak was also visible in the control lacking EPA and containing microsomes, but it was greatly reduced having a peak area that was 7.35% the size of those present in the total incubation mix containing EPA. No peaks were identified that could represent EPA metabolites (Data not shown).

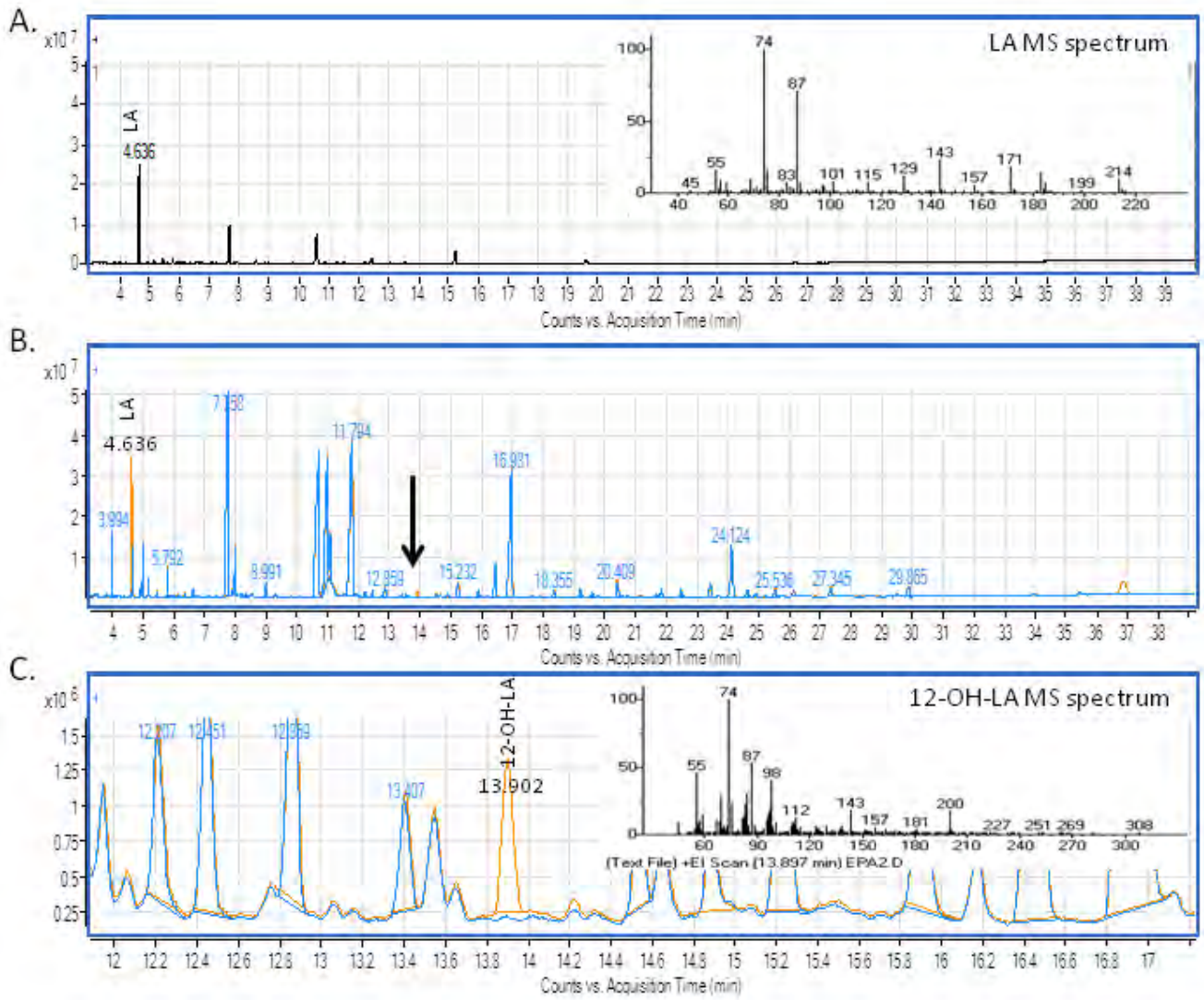

Figure 3.4: Initial *in vitro* metabolism of LA.

An incubation mix containing 50 µM LA and 0.3 mg/ml microsomes was set up in 0.12 M potassium phosphate buffer (pH 7.4, with 5 mM $MgCl_2$) with an NADPH generating system. Metabolism was allowed to occur for 15 min at 37°C and terminated by the addition of 10% H_2SO_4/MeOH (v/v). FAME synthesis was carried out followed by extraction into hexane and analysis via GC-MS. A) The control containing LA and lacking microsomes resulted in a peak for LA at 4.636 min. The spectrum for LA is shown as an inset. B) The chromatogram produced for the total incubation mix containing LA (orange) is overlaid with the control containing microsomes and lacking FAs (blue). LA produced a peak at 4.646 min. A peak at 13.902 min (highlighted by the arrow) was identified in the total incubation mix, but absent in the control. C) Zoomed in view showing metabolite peak at 13.902 min, identified as 12-OH-LA. The spectrum for this peak is shown as an inset.

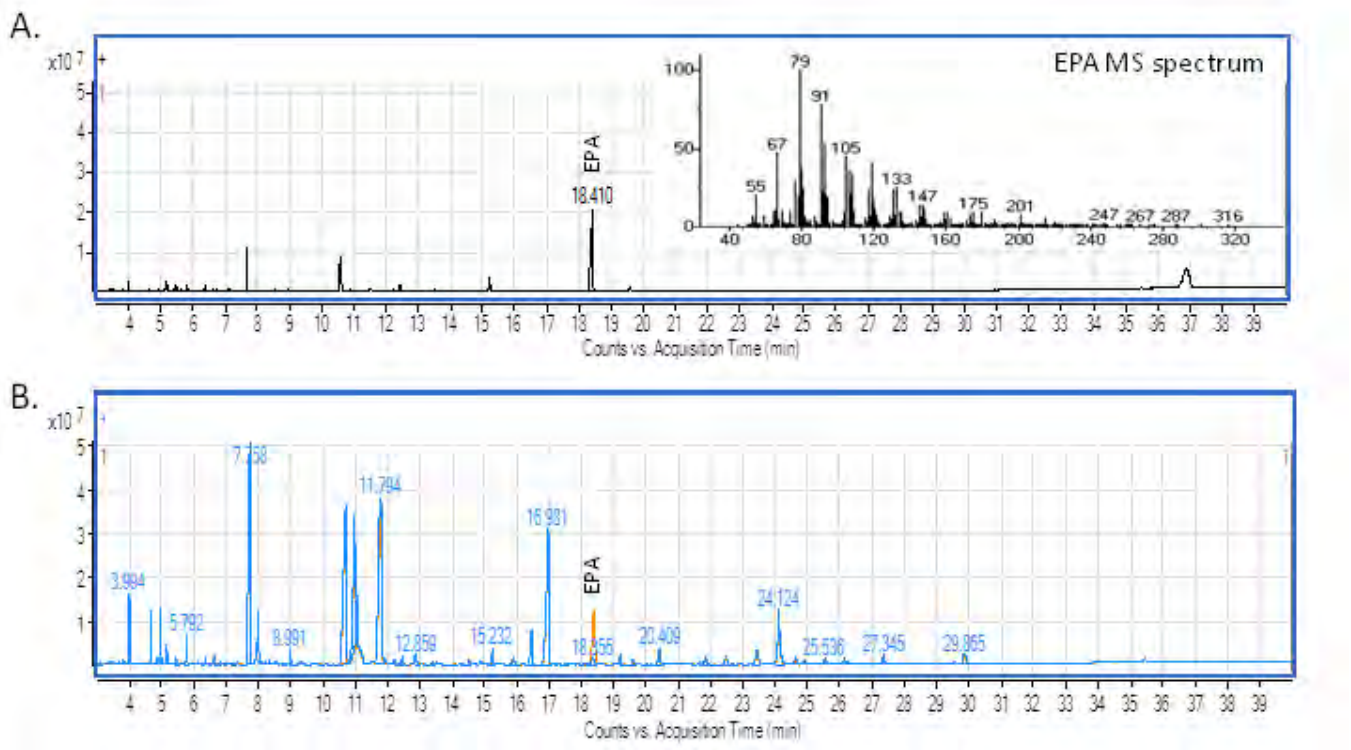

Figure 3.5: Initial *in vitro* metabolism of EPA.
An incubation mix containing 50 µM EPA and 0.3 mg/ml microsomes was set up in 0.12 M potassium phosphate buffer (pH 7.4, with 5 mM $MgCl_2$) with an NADPH generating system. Metabolism was allowed to occur for 15 min at 37°C and terminated by the addition of 10% H_2SO_4/MeOH (v/v). FAME synthesis was carried out followed by extraction into hexane and analysis via GC-MS. LA was used as a positive metabolism control (Figure 3.4). A) The control containing EPA and lacking microsomes produced a peak for EPA at 18.410 min. The spectrum for EPA is shown as an inset. B) The chromatogram produced for the total incubation mix containing EPA (orange) is overlaid with the control containing microsomes and lacking FAs (blue). EPA produced a peak at 18.383 min. No metabolite peaks for EPA were identified.

3.3.3.3 DHA and AA metabolism

DHA and AA *in vitro* metabolism were carried out in triplicate through the use of 0.6 mg/ml human liver microsomes and 100 µM FAs. The positive control, LA resulted in a peak at 4.427 ± 0.002 minutes in the total incubation mixes containing LA and the control containing LA and lacking microsomes. This peak was absent in the control containing microsomes and lacking LA. 12-OH-LA was present at 12.661 ± 0.004 minutes in the total incubation mixes containing LA, but was absent in the control containing LA and lacking microsomes as well as the control lacking LA and containing microsomes (Data not shown, but representative chromatogram can be seen in Figure 3.4). The area sum percent for LA and 12-OH-LA for replicate 1 were 1.54 and 0.57%, and for replicate 2 were 2.98 and 0.18% respectively. DHA

resulted in a peak at 22.454 ± 0.069 minutes in the three total incubation mix replicates containing DHA and the control containing DHA and lacking microsomes (Figure 3.6A and B). This peak was also present at 22.440 minutes in the control lacking DHA but containing microsomes and had a peak area 68.72% that of the DHA present in the total incubation mixes. No peaks that could represent DHA metabolites were identified. AA resulted in a peak at 15.651 ± 0.018 minutes in the total incubation mixes containing AA as well as the control containing AA and lacking microsomes (Figure 3.6C and D). This peak was also present in the control containing microsomes but lacking added AA. The area sum percent of AA in the control containing microsomes and lacking AA was 22.02% whilst the average area sum percent of the total incubation mixes containing AA was higher, being 27.47 ± 5.01%. No peaks were identified as AA metabolites.

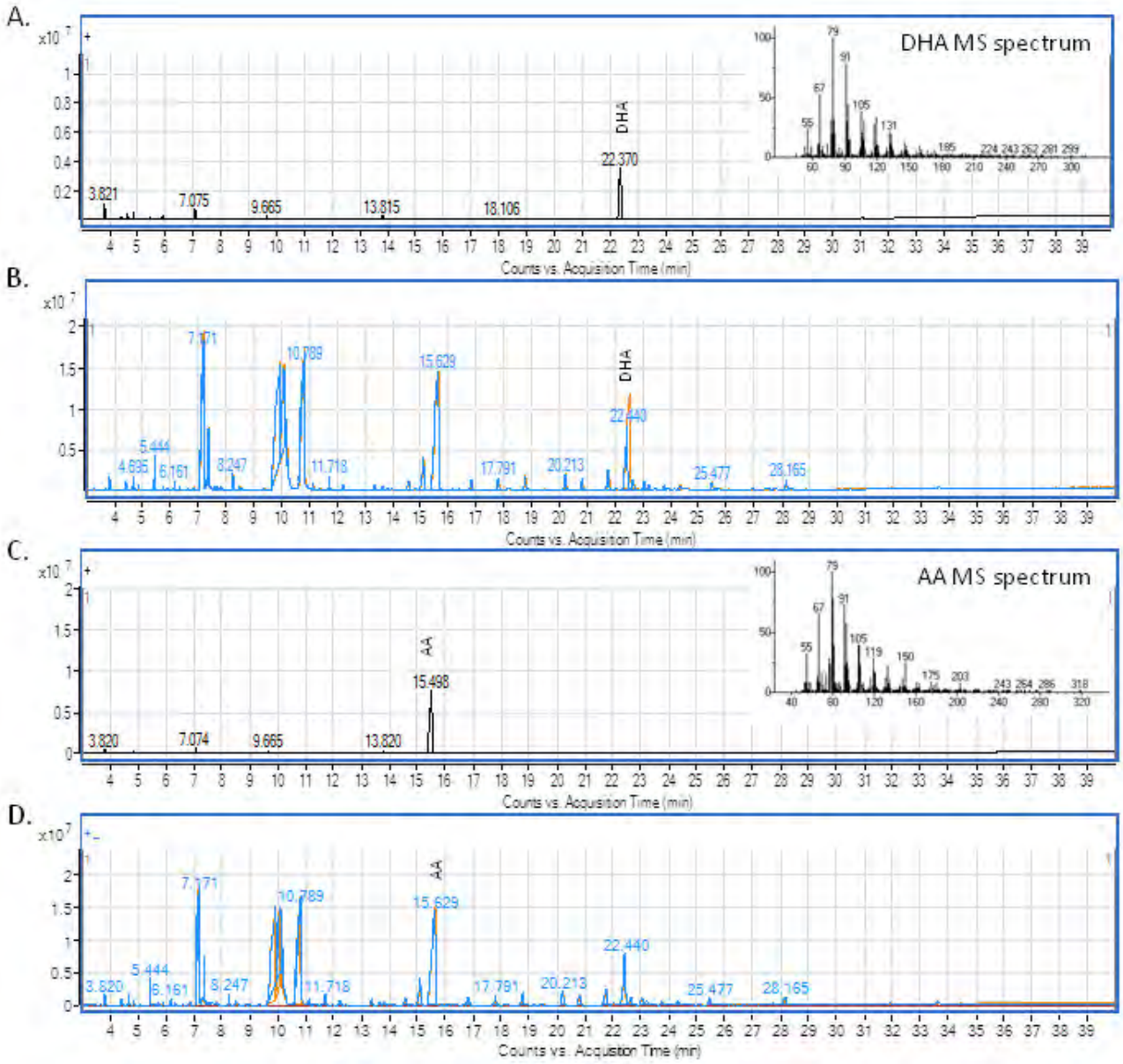

Figure 3.6: *In vitro* metabolism of DHA and AA.

Incubation mixes contained 100 µM FA (DHA or AA), 0.6 mg/ml microsomes, 0.12 M potassium phosphate buffer (pH 7.4, with 5 mM $MgCl_2$), and an NADPH generating system. Metabolism was allowed to occur for 15 min at 37°C and terminated by the addition of 10% H_2SO_4/MeOH (v/v). FAME synthesis was carried out followed by extraction into hexane and analysis by GC-MS. The assay was performed in triplicate. The chromatograms for one replicate from each FA are presented here. A) The control containing DHA and lacking microsomes produced a peak for DHA at 22.370 min. The spectrum for DHA is shown as an inset. B) The chromatogram produced for the total incubation mix containing DHA (orange) is overlaid with the control containing microsomes and lacking FAs (blue). DHA produced a peak at 22.440 min. No metabolite peaks for DHA were identified. C) The control containing AA and lacking microsomes produced a peak for AA at 15.498 min. The spectrum for AA is shown as an inset. D) The chromatogram produced for the total incubation mix containing AA (orange) is overlaid with the control containing microsomes and lacking FAs (blue). AA produced a peak at 15.629 min. No metabolite peaks for AA were identified.

3.4 Discussion

3.4.1 Method validation

Since the derivatisation of LA, EPA, DHA and AA through FAME synthesis; liquid-liquid extraction into hexane and analysis via GC-FID showed good linearity (Figure 3.1) in the selected concentration range (0 – 400 µM), and inter- and intra-day reproducibility (Table 3.1), as well as a LOD below the concentration range at which future experiments would be carried out, this method was deemed appropriate for LA, EPA, DHA and AA qualification.

3.4.2 Derivatisation and extraction optimisation

Numerous contaminating peaks were present in the total incubation mixes. This contamination was determined to be of microsomal origin since it was present in all samples containing microsomes, but absent in controls that lacked microsomes. In order to try and reduce this microsomal contamination, an initial extraction into DCM was performed, followed by derivatisation and extraction into hexane. This additional extraction step reduced the peak areas of the contaminating peaks, but also reduced the peak area for EPA (Figure 3.3). This reduction in peak area could therefore be linked to a loss of compounds due to the added extraction rather than a decrease in contaminating peaks alone. It was therefore decided to omit the initial DCM extraction in future assays so as to avoid loss of possible metabolites which may be present in small quantities.

3.4.3 Human liver microsomal system optimisation and PUFA metabolism

Contaminating peaks produced by the microsomes were identified using MassHunter. The main contaminants were found to be FAs. A concern was that EPA, DHA and AA were all found to be part of the microsomal contamination. A study performed by Waskell *et al.* (1982) using liver extracts from five male patients over the age of 45 found that polyunsaturated fatty acids comprised 42.6% of the total phospholipids from the liver microsomes, with EPA, DHA and AA representing 0.25, 5.75, and 14.6% of the total fatty acids respectively. This gives a ratio of EPA:DHA:AA of 1:23:58. The area sum percent for

EPA, DHA and AA present in microsomal contamination during this study were found to be 0.77 ± 0.08; 9.09 ± 0.50 and 23.43 ± 1.38% respectively (Table 3.2). This gives a ratio of EPA:DHA:AA of 1:12:30. Although the ratio is lower for this experiment, it still indicates that in human liver microsomes, the concentration of AA is greater than that of DHA which in turn is greater than that of EPA. Previous studies looking at the *in vitro* metabolism of FAs using microsomal systems have not reported that microsomal FAs are extracted along with the FAs being analysed and their metabolites (Amet *et al*., 2002; Fer *et al*., 2008a). Amet *et al*. (2002) and Fer *et al*. (2008a) both performed liquid-liquid extractions after microsomal incubations, using di-ethylether and ethyl acetate respectively. They analysed their fractions using HPLC-MS rather than GC-MS. This means that they did not need to derivatise their samples. It was thought that perhaps the derivatisation step used during this study resulted in the break down and release of FAs from the microsomes due to the lowered pH and increased temperature. However, an initial liquid-liquid extraction into DCM was unable to reduce the microsomal contamination. This implies that microsomal contamination should have been seen by Amet *et al*. (2002) and Fer *et al*. (2008a) who also performed liquid-liquid extractions.

LA is a 12-carbon FA and was chosen as a positive control during the *in vitro* metabolism assays since it has been found to be metabolised by CYPs in human liver microsomes (Clarke *et al*., 1994; Castle *et al*., 1995; Powel *et al*., 1996). The microsomal system was optimised in terms of protein and FA concentration. Initial metabolism studies conducted utilised 0.3 mg/ml microsomes and 50 µM FAs (LA or EPA). The *in vitro* metabolism of LA resulted in a peak corresponding to 12-OH-LA being produced in the total incubation mix containing LA (Figure 3.4). This peak was absent in the control containing microsomes and lacking LA, as well as the control lacking microsomes and containing LA. This indicates that the 12-OH-LA was produced through phase 1 CYP metabolism in the human liver microsomal system and not through spontaneous degradation or microsomal contamination. It can therefore be deduced that the conditions used were conducive to FA metabolism. Previous studies have reported 12-OH-LA to be the predominant LA metabolite produced in human liver microsomes (Clarke *et al*., 1994; Powel *et al*., 1996). The ω-hydroxylation of lauric acid has been found to be catalysed by CYPs of the 4A and 2E subfamilies (Clarke *et al*., 1994), with

the principle laurate ω-hydroxylating enzyme expressed in human liver proposed to be CYP4A11 (Powel *et al*., 1996).

EPA produced a peak in the total incubation mix containing EPA as well as the control containing EPA and lacking microsomes (Figure 3.5). However, no possible EPA metabolites were identified. Due to the low metabolism of LA and the fact that EPA was not metabolised, it was decided to increase the microsomal concentration from 0.3 mg/ml to 0.6 mg/ml and to double the concentration of PUFA used in order to try increase metabolism. It was also decided to only perform the hexane extraction twice instead of three times. The reason for this was that it was noticed that a white suspension would form at the interface between the buffer and hexane in all samples containing microsomes. This suspension would however be re-dissolved by the third extraction. Once again, 12-OH-LA was identified as a metabolite for LA, but no possible metabolite peaks for EPA were identified. The increased microsomal and PUFA concentration resulted in an increase in LA metabolism. This was evident since the area sum percent for LA decreased whilst the area sum percent for 12-OH-LA increased upon increase in microsomal and FA concentration, being 2.41% and 0.25% for LA and 12-OH-LA in the incubation mix containing 0.3 mg/ml microsomes and 50 µM LA, and 1.47% and 0.34% for LA and 12-OH-LA in the incubation mix containing 0.6 mg/ml microsomes and 100 µM LA. DHA and AA *in vitro* metabolism were therefore conducted using 0.6 mg/ml microsomes and 100 µM PUFA. Performing the hexane extraction twice instead of three times reduced the microsomal contamination; therefore the hexane extraction was performed twice in future studies.

During the *in vitro* metabolism of DHA and AA, no metabolite peaks were identified (Figure 3.6). LA was used as a positive control (in duplicate) and was metabolised to 12-OH-LA. The area sum percent for LA and 12-OH-LA for replicate 1 were 1.54 and 0.57%, and for replicate 2 were 2.98 and 0.18% respectively. Since the LA peak area was smaller in replicate 1 than in replicate 2 whilst the 12-OH-LA peak area was larger in replicate 1 than in replicate 2, it is evident that LA metabolism took place to a greater extent in replicate 1 than in replicate 2.

This was unexpected since the assay parameters were the same in both experiments and so it would be expected that a similar degree of metabolism would occur.

Since the ω-hydroxylation of lauric acid has been found to be catalysed by CYPs of the 4A family (Clarke *et al*., 1994), it can be deduced that these enzymes were active in the human liver microsomes. CYP4A enzymes exhibit (ω-1)-hydroxylase activities when using EPA and DHA as substrates (Arnold *et al.,* 2010). It was therefore expected that possible metabolites that would be produced during the *in vitro* metabolism of EPA and DHA using human liver microsomes would be 20-hydroxyeicosapentaenoic acid (20-HEPE) and 22-hydroxydocosahexaenoic acid (22-HDoHE) respectively. Other possible metabolites for EPA and DHA that were anticipated were 17, 18-epoxyeicosatetraenoic acid (17, 18-EpETE) and 19, 20-epoxydocosapentaenoic acid (19, 20-EpDPE) respectively. The reason for this is that the n-3 double bond that distinguishes EPA and DHA from their n-6 counterparts is a predominant site of epoxidation for many CYP isoforms, including several members of the CYP4A subfamily (Arnold *et al.,* 2010; Konkel and Shunck, 2011). The CYP4A subfamily is a major 20- hydroxyeicosatetraenoic acid (20-HETE) producing enzyme subfamily in mammals, showing an evident regioselectivity in favour of hydroxylating the terminal methyl group during AA metabolism (Arnold *et al*., 2010). It was therefore expected that the *in vitro* metabolism of AA would result in the formation of 20-HETE, the main AA product of CYP4A catalysed reactions (Arnold *et al*., 2010).

Environmental factors such as drugs, diet, and lifestyle have a considerable influence on the expression and activity of CYP enzymes (Glue and Clement, 1999). Levels of the different CYP isoforms therefore vary greatly among hepatic microsome samples depending on exposure to inducers or inhibitors prior to microsomal preparations (Wrighton *et al*., 1995). Thus, a reason why EPA, DHA and AA were not metabolised may be that the CYP isoforms required for their metabolism were not induced prior to microsomal fractionation or were present in quantities that were insufficient for metabolism to occur.

Other factors resulting in considerable variability in CYP expression include age, gender, race and genetic factors (Glue and Clement, 1999). CYP genetic polymorphisms and differences in gene regulation result in inter-individual differences in CYP expression (Gonzalez and Tukey, 2005), and individuals with genetically low levels of enzyme activity (poor metabolizers) have been discovered (Glue and Clement, 1999). Thus, the source from which the microsomes were isolated could have had genetic polymorphisms which resulted in them being poor metabolizers of FAs.

Conclusion

An analytical method (GC-FID/MS) was optimised for FA analysis and validated in terms of inter- and intra-day reproducibility, linearity and LOD. The human liver microsomal system was optimised for FA metabolism in terms of microsomal and FA concentration. The system resulted in the metabolism of the positive control, LA, to 12-OH-LA. However, it was unable to metabolise EPA, DHA and AA. This may be due to low expression or absence of the CYP isoforms responsible for their metabolism. Contamination from the microsomes, mainly in the form of FAs, was a confounding factor. It was therefore decided to purchase metabolites for future comparative studies, using *in silico* analysis as a basis for metabolite choice.

Chapter Four

Effect of PUFAs on colon cancer cell viability

4.1 Introduction

In vitro studies have previously found a correlation between PUFAs and cancer. EPA and DHA have been found to have inhibitory effects on carcinogenesis (Ligo *et al*., 1997; Chamras *et al*., 2002; Schley *et al*., 2005; Bougnoux *et al*., 2010; Lu *et al*., 2010). The affects of AA are controversial, with some studies indicating that it promotes cancer (Schley *et al*., 2005; Ligo *et al*., 1997), some that it has no impact on cancer cell growth (Lu *et al*., 2010), and others that it inhibits carcinoma (Schonberg *et al.,* 2006; Habermann *et al*., 2009). The correlation between PUFAs and colon cancer is of particular interest since diet and nutrition have been shown to play an important role in the cause and primary prevention of colon carcinoma (Matsuura *et al*., 2006). EPA, DHA and AA have been found to have inhibitory effects on colon carcinoma *in vitro* (Schonberg *et al.,* 2006; Habermann *et al*., 2009). SW480 and SW620 are paired colon carcinoma cell lines. SW480 was established from a primary adenocarcinoma of the colon in a 50 year old male whilst SW620 was isolated a year later from a metastasis of the same tumor in the lymph node (Leibovitz *et al*., 1976). These cell lines were therefore chosen for this study as it allowed for the comparison of the effect of PUFAs on different stages of the same tumor. Studies comparing the effects of EPA, DHA and AA on carcinoma to the effects of their CYP metabolites have not been conducted to date. This chapter therefore aimed to address this topic in the colon carcinoma cell lines, SW480 and SW620. Since the human liver microsomal system was unable to metabolise our PUFAs of interest, we decided to move the study forward by purchasing known CYP metabolites. The selection of a metabolite was based on knowledge gaps in the literature, *in silico* predictions and availability. The metabolite of choice was 17, 18-epoxyeicosatetraenoic acid (EpETE), which is formed through the CYP epoxidation of EPA at the n-3 double bond.

This chapter describes the assessment of the cytotoxicity of EPA, DHA and AA towards SW480 and SW620 cells and aims to compare the cytotoxicity of EPA with its CYP

metabolite, 17, 18-EpETE, towards SW480 cells through the use of WST-1 cell viability assay and real-time cell analysis.

4.2 Methods

4.2.1 Cell lines and culture conditions

The paired colon carcinoma cell lines, SW480 and SW620 (European Collection of Cell Cultures, catalogue numbers: 87092801 and 87051203 respectively), were maintained in culture at 37°C in complete medium containing Leibovitz's medium (L-15) (Sigma-Aldrich®, Germany) supplemented with 10% (v/v) heat-inactivated foetal calf serum (FCS) (Lonza, USA), 1 mM L-glutamine (Sigma-Aldrich®, Germany), and 100 U/ml penicillin, 100 µg/ml streptomycin and 12.5 µg/ml amphotericin (PSA) (Sigma-Aldrich®, Germany).

4.2.2 Effect on cell viability

Cell viability upon treatment with EPA, DHA and AA (SW480 and SW620 cells) or 17, 18-EpETE (SW480 cells) was assessed by means of WST-1 assay, according to manufacturer's instructions. The method was validated through the assessment of the interference of the compounds of interest with the assay. L-15 media was placed in a 96-well plate (100 µl/well) and incubated with a range (0 – 200 µM) of concentrations of sulindac sulfide (SuS), 5-fluorouracil (5FU), AA, DHA, EPA and 17, 18-EpETE at 37°C for 96 hours. After incubation, 10 µl WST-1 reagent (Roche, Switzerland) was added to each well and incubated at 37°C for 4 hours. The absorbance at 440 nm was determined using a Powerwave spectrophotometer (BioTek). The assay was performed in triplicate. A spectral absorbance scan (λ: 250 – 900 nm) was conducted for each compound in triplicate using a concentration of 400 µM (dissolved in 100 µl DMSO). SuS, 5FU and DMSO were from Sigma-Aldrich®, Germany. 17, 18-EpETE was from Cayman Chemical, USA (product number: 50861). For WST-1 assays, cells were seeded at 3 000 cells/well in complete medium in a 96-well plate and allowed to adhere for 24 hours. Cells were treated with a range of concentrations (0 – 200 µM) of EPA, DHA or AA (SW480 and SW620 cells) or 17, 18-EpETE (SW480 cells) and incubated at 37°C

for 96 hours. SuS (0 – 200 µM) was used as a positive control and 0.5% DMSO (v/v) was used as a vehicle control. After treatment, 10 µl WST-1 reagent was added to each well and incubated at 37°C for 4 hours. The absorbance at 440 nm was determined with complete medium containing WST-1 reagent used as a blank. Cell viability was normalized and expressed as a percent of the maximum response. Average cell viability was plotted against log concentration. Each compound was assayed in triplicate in three independent experiments during assessment of EPA, DHA and AA. 17, 18-EpETE was assayed in triplicate. The EC_{50} values were determined by non-linear regression and compared using an *F* test (p = 0.05) (GraphPad Prism Version 4, GraphPad Software, San Diego California, www.graphpad.com). A two-tailed, unpaired t-test (p = 0.05) was performed in order to asses if there was a significant difference between the effects of 17, 18-EpETE and EPA at each concentration.

4.2.3 Real-time analysis of the effect of EPA and 17, 18-EpETE on cell viability

The real-time cell analyzer xCELLigence System (Roche, Switzerland) was used to monitor cell proliferation rates. SW480 cells were seeded at 12 000 cells/well in complete medium in a 96-well plate and incubated at 37°C for 96 hours (until a cell index above 0.7 had been reached). Cells were treated with a range of EPA and 17, 18-EpETE concentrations (0 – 100 µM) and incubated at 37°C for 96 hours. SuS (0 – 100 µM) and 5FU (627.1 µM) were used as positive controls and 0.5% DMSO was used as a vehicle control. The assay was performed in triplicate. One-way ANOVA followed by a Tukey multiple comparisons test was performed to assess the variance between treatments (p = 0.05). Microelectronic plates (E-Plates) integrated with gold microelectrode arrays were employed during real-time cell analysis using the xCELLigence System. Low AC voltage was applied to the plate and produced a small electric field between the electrodes, which was impeded by the presence of adherent cells (Abassi *et al*., 2009).

Measured cell-electrode impedance was converted to a parameter termed cell index (CI) according to the following equation (RTCA software 1.2. Roche, Switzerland):

$$\text{CI} = max_{i=1,\ldots N}\left(\frac{R_{cell}(f_i)}{R_b(f_i)} - 1\right)$$

where $R_b(f)$ and $R_{cell}(f)$ are the frequency-dependent electrode resistances (a component of impedance) without cells or with cells present, respectively (Abassi *et al*., 2009). *N* is the number of the frequency points at which the impedance is measured (Abassi *et al*., 2009). Under the same physiological conditions, the $R_{cell}(f)$ value increases with increasing cell attachment, leading to an increase in the value for CI (Abassi *et al*., 2009). Decrease in CI correlates generally well to cell death (Gerets *et al*., 2012).

4.3 Results

4.3.1 WST-1 method validation

When increasing concentrations of SuS, 5FU, AA, EPA, DHA and 17, 18-EpETE were incubated with WST-1 in the absence of cells there was no change in the absorbance at 440 nm (Figure 4.1). This suggested that the compounds did not react with WST-1 reagent to produce a product that absorbed light at 440 nm. A spectral absorbance scan of solutions of the compounds indicated that these compounds did not absorb light at 440 nm, but were found to absorb light in the UV range as indicated by the peak absorbance between 200 and 300 nm (Figure 4.1). SuS also resulted in a peak in absorbance between 300 and 400 nm, however this was below the 440 nm used for WST-1 assays. Therefore, the WST-1 assay was deemed a suitable assay to assess cell viability of SW480 and SW620 cells upon treatment with the PUFAs, using SuS and 5FU as positive controls. The media did however absorb light at this wavelength, having an average absorbance of 0.189 ± 0.016 (Figure 4.1). Complete medium containing WST-1 was therefore used as a blank in future WST-1 assays.

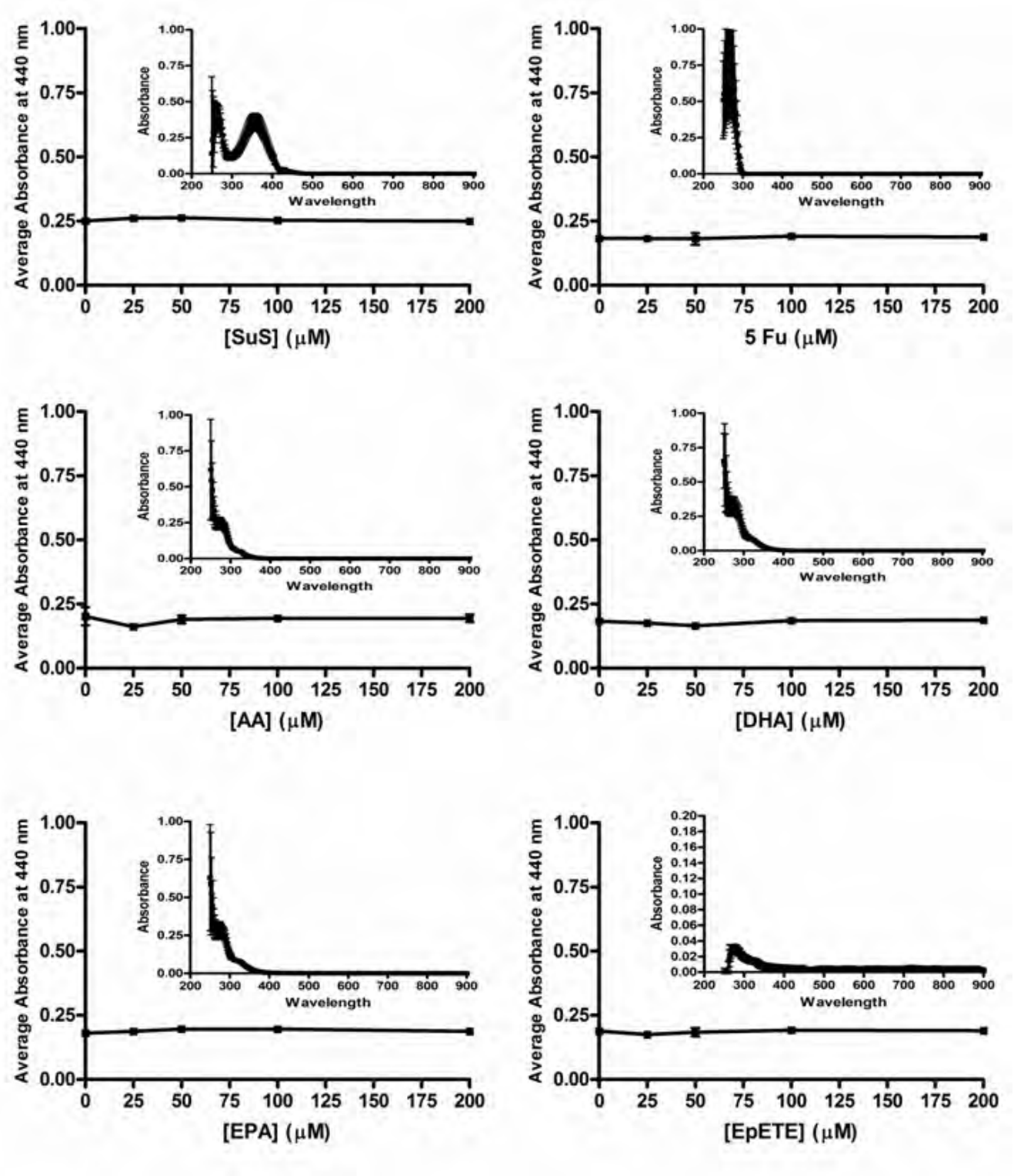

Figure 4.1: WST-1 method validation.

A range (0 – 200 μM) of SuS, 5FU, AA, DHA, EPA and 17, 18-EpETE concentrations were incubated at 37°C for 96 h. WST-1 reagent (10 μl) was added to each well, incubated at 37°C for 4 h, and absorbance read at 440 nm. Average absorbance at 400 nm was plotted against concentration. Error bars indicate the standard deviation of the mean where *n = 3*. A spectral scan (λ: 250 – 900 nm) for each compound was performed using a concentration of 400 μM. Average absorbance was plotted against wavelength and shown as an inset. Error bars indicate the standard deviation of the mean where *n = 3*.

4.3.2 Effect of EPA, DHA and AA on SW480 and SW620 cell viability

SW480 and SW620 cells were incubated with a range (0 – 200 µM) of concentrations of EPA, DHA and AA for 96 hours at 37°C. The average percentage cell viability of SW480 (Figure 4.2) and SW620 (Figure 4.3) cells was found to decrease with increasing concentrations of these PUFAs. This suggested that EPA, DHA and AA reduced SW480 and SW620 cell viability in a concentration dependant manner. The EC_{50} values for EPA, DHA and AA in SW480 cells were found to be similar (*F* test, $p > 0.05$), being 60.49 µM, 49.12 µM and 49.31 µM respectively. The EC_{50} values for EPA, DHA and AA in SW620 cells were found to be significantly different (*F* test, $p < 0.05$), being 62.41 µM, 45.54 µM and 36.23 µM respectively. Between cell lines, the EC_{50} values for EPA and DHA were not significantly different (*F* test, $p > 0.05$), whilst the EC_{50} value for AA was significantly lower in SW620 cells than in SW480 cells (*F* test, $p < 0.05$). The positive control, SuS, resulted in an EC_{50} value of 61.65 µM in SW480 cells and 60.12 µM in SW620 cells.

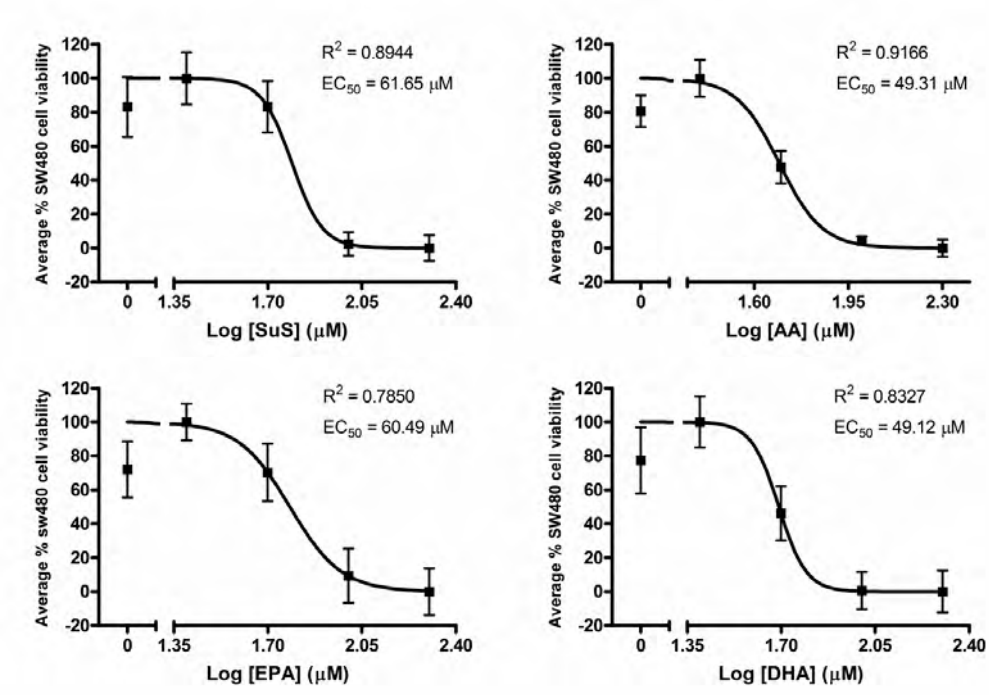

Figure 4.2: Effect of EPA, DHA and AA on SW480 cell viability.
SW480 cells were seeded at 3 000 cells/well in a 96-well plate. Viability was assessed via WST-1 assay after treatment with a range (0 – 200 µM) of EPA, DHA and AA concentrations for 96 h. Cell viability was normalized and expressed as a percent of the maximum response. Average cell viability was plotted against log concentration. Error bars indicate the standard deviation of the mean where *n = 9*. A sigmoidal dose-response curve (variable slope) was fitted using GraphPad. An *F* test ($p > 0.05$) indicated that the EC_{50} values for AA, EPA and DHA were not significantly different.

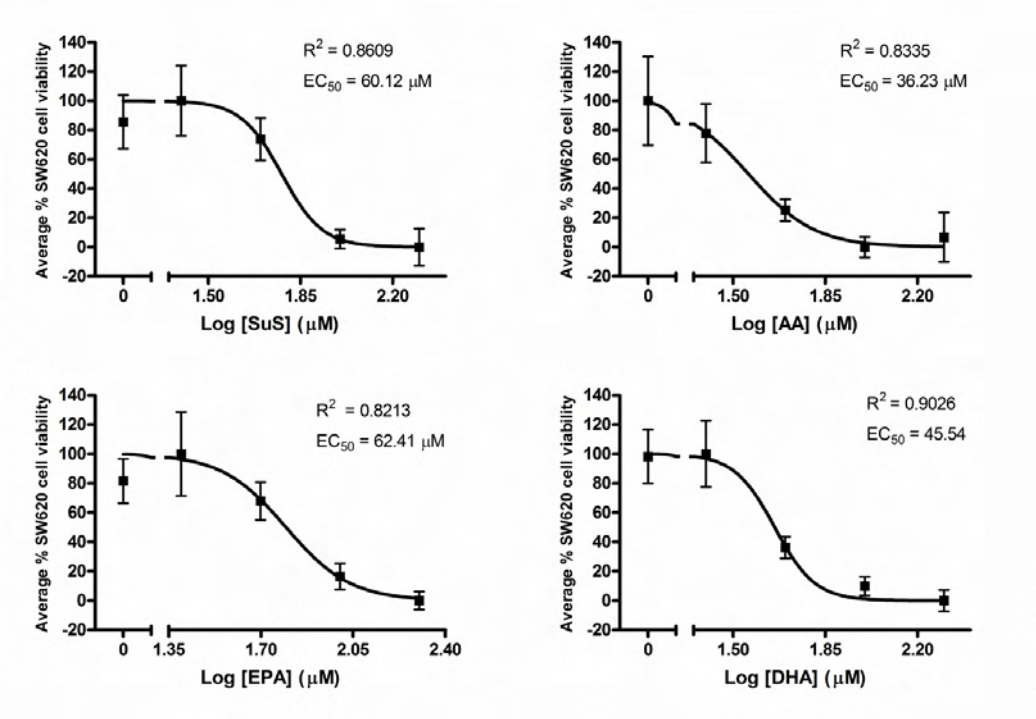

Figure 4.3: Effect of EPA, DHA and AA on SW620 cell viability.
SW620 cells were seeded at 3 000 cells/well in a 96-well plate. Viability was assessed via WST-1 assay after treatment with a range (0 – 200 µM) of EPA, DHA and AA concentrations for 96 h. Average cell viability was plotted against log concentration. Error bars indicate the standard deviation of the mean where *n = 9*. A sigmoidal dose-response curve (variable slope) was fitted using GraphPad. An *F* test ($p < 0.05$) indicated that the EC_{50} values for AA, EPA and DHA were significantly different from each other.

4.3.3 Effect of 17, 18-EpETE on SW480 cell viability

SW480 cells were incubated with a range (0 – 200 µM) of 17, 18-EpETE concentrations for 96 hours at 37°C. A decrease in average percentage cell viability was observed with increasing 17, 18-EpETE concentrations (Figure 4.4). This suggested that 17,18-EpETE reduced SW480 cell viability in a concentration dependant manner. The EC_{50} value was determined to be 23.23 µM. This EC_{50} value for 17, 18-EpETE was significantly different to the EC_{50} determined for EPA previously (60.49 µM) (*F* test, $p < 0.05$). A two-tailed, unpaired t-test showed that the reduction in SW480 cell viability by 17, 18-EpETE and EPA was significantly different at both the 25 µM and 50 µM concentrations ($p < 0.05$).

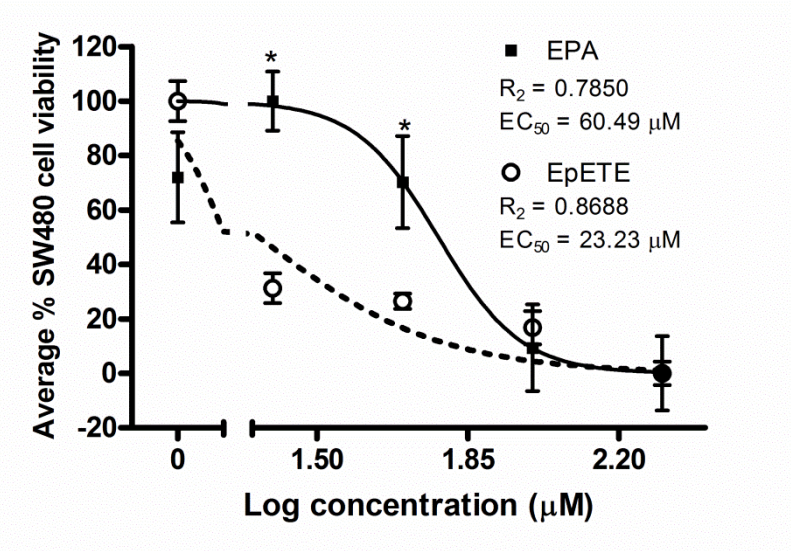

Figure 4.4: Comparison of the effect of EPA and 17, 18-EpETE on SW480 cell viability.
Cells were seeded at 3 000 cells/well in a 96-well plate. Viability was assessed via WST-1 assay after treatment with a range (0 – 200 μM) of 17, 18-EpETE concentrations for 96 h. Cell viability was normalized and expressed as a percent of the maximum response. Average cell viability for 17, 18-EpETE was plotted against log concentration together with EPA results previously generated for SW480 cells (Figure 4.2). Error bars indicate the standard deviation of the mean where *n = 3* for 17, 18-EpETE and *n = 9* for EPA. A sigmoidal dose-response curve (variable slope) was fitted using GraphPad. A two-tailed, unpaired t-test was performed to assess the variance between replicates at each concentration using a significance level of p = 0.05. Significant difference between EPA and 17, 18-EpETE at a particular concentration is indicated by an asterisk. An *F* test ($p < 0.05$) indicated that the EC_{50} values for EPA and 17, 18-EpETE were significantly different.

4.3.4 Real-time analysis of the effect of EPA and 17, 18-EpETE on cell viability

SW480 cells were treated with a range (0 – 100 μM) of concentrations of EPA and 17, 18-EpETE for 96 hours. Cells were monitored using the real-time cell analyzer xCELLigence System. A decrease in CI over time (from 124.9 – 190.9 hours) was observed for all concentrations of EPA and 17, 18-EpETE used (Figure 4.5A). This decrease in CI corresponded to an increase in cell death. This suggested that EPA and 17, 18-EpETE reduced cell viability of SW480 cells over time. However, the DMSO vehicle control also resulted in a decrease in CI, and hence a decrease in SW480 cell viability, over time. The average cell death rates for EPA and 17, 18-EpETE were not significantly different to the DMSO vehicle control (One-way ANOVA and Tukey multiple comparisons test, $p > 0.05$) (Figure 4.5B). The rate of cell death for 5FU (627.1 μM) was significantly different to the DMSO vehicle control (One-way ANOVA and Tukey multiple comparisons test, $p < 0.05$) (Figure 4.5B).

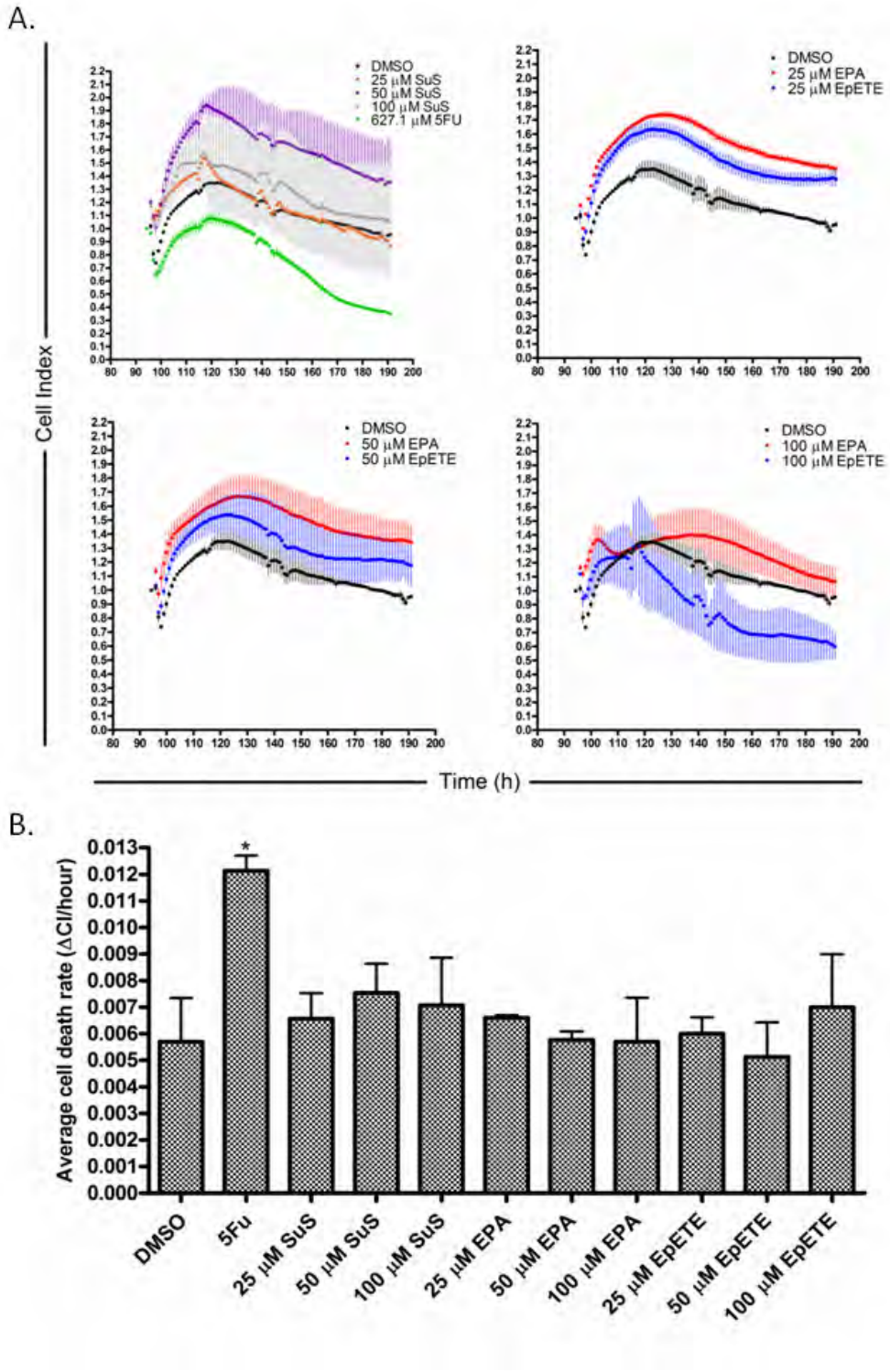

Figure 4.5: Real-time analysis of SW480 cells treated with EPA and 17, 18-EpETE.
The real-time cell analyzer xCELLigence System was used to monitor cell proliferation rates. SW480 cells were seeded at 12 000 cells/well in a 96-well plate, incubated at 37°C for 96 h and then treated with a range of EPA and 17, 18-EpETE concentrations (0 – 100 µM) for 96 h. A) CI over time is reported. Each data point was normalised against the time just before compound addition (96 h). Error bars indicate the standard deviation of the mean where *n = 3.* B) Cell death rates were determined as the gradient from the linear portions of the graphs in A (Time 124.9067 – 190.9078 h). Error bars indicate the standard deviation of the mean where *n = 3.* One-way ANOVA followed by a Tukey multiple comparisons test was performed to assess the variance between treatments (p = 0.05). Significant difference is indicated by an asterisk.

4.4 Discussion

4.4.1 EPA, DHA and AA reduced SW480 and SW620 cell viability in a concentration dependant manner

SuS resulted in a decrease in SW480 and SW620 cell viability, having an EC_{50} of 61.65 µM and 60.12 µM respectively. Previous studies have also found SuS to be toxic towards colon cancer cell lines in the micromolar range, having an EC_{50} in SW480 and SW620 cells around 200 ± 110 µM (Chan *et al*., 1998; Karaguni *et al*., 2002).

EPA, DHA and AA were found to reduce SW480 (Figure 4.2) and SW620 (Figure 4.3) cell viability in a concentration dependent manner, with AA and DHA exhibiting greater cytotoxic effects than EPA in both cell lines (Figure 4.2 and 4.3). The effect of AA on carcinogenesis is a controversial topic, with some studies reporting it to promote carcinogenesis (Ligo *et al*., 1997; Schley *et al*., 2005) and others stating that it has inhibitory effects on carcinogenesis (Schonberg *et al.,* 2006; Engelbrecht *et al*., 2008; Habermann *et al*., 2009). EPA, DHA and AA have previously been found to inhibit SW480 and SW620 cell viability in a concentration-dependent manner (Schonberg *et al.,* 2006). This concentration-dependent cytotoxicity has also been reported for EPA, DHA and AA in other colon cancer cell lines (Engelbrecht *et al*., 2008; Habermann *et al*., 2009). A study by Schonberg *et al*. (2006) found that SW620 cells were more sensitive to EPA, DHA and AA than SW480 cells, with DHA exhibiting the strongest effect in both cell lines. They reported cell viabilities of 23, 50 and 56% in SW480 cells and 5, 25 and 25% in SW620 cells after exposure to 70 µM DHA, EPA and AA respectively for 144 hours (Schonberg *et al*., 2006).

EC_{50} values for EPA, DHA and AA were in the micromolar range in both cell lines. The EC_{50} values for EPA, DHA and AA were not significantly different in SW480 cells (*F* test, $p > 0.05$), but were significantly different in SW620 cells (*F* test, $p < 0.05$). Between cell lines, the EC_{50} values for EPA and DHA were not significantly different (*F* test, $p > 0.05$), whilst the EC_{50} value for AA was significantly lower in SW620 cells than in SW480 cells (*F* test, $p < 0.05$). This supports previous findings for AA that showed it to be more toxic towards SW620 cells than

SW480 cells (Schonberg *et al*., 2006). EC_{50} values for EPA, DHA and AA have not been previously reported in SW480 and SW620 cells, but have been reported in two other colon carcinoma cell lines, namely LT97 and HT29. After treatment with PUFAs for 72 hours, EPA, DHA and AA were found to have EC_{50} values in LT97 cells of approximately 100 µM, 140 µM and 110 µM respectively (Habermann *et al*., 2009). In HT29 cells, EPA, DHA and AA were found to have EC_{50} values of approximately 190 µM, 130 µM and 240 µM (Habermann *et al*., 2009). This suggested that EPA, DHA and AA were more toxic towards SW480 and SW620 cells than LT97 and HT29 cells. However, EPA, DHA and AA cytotoxicity has been found to be time-dependent, with greater exposure time resulting in increased toxicity towards cancer cell lines (Schonberg *et al*., 2006; Habermann *et al*., 2009). Therefore, the decreased cytotoxicity seen in LT97 and HT29 cells during the study by Habermann *et al*. (2009) in comparison to the cytotoxicity towards SW480 and SW620 cells observed during this study may have been due to a decreased exposure time (72 hours in comparison to 96 hours in the current study). Habermann *et al*. (2009) found the toxicity of AA to be significantly different between the two colon cell lines tested. This, together with our findings that AA toxicity was significantly different between SW480 and SW620 cells suggested that AA toxicity was dependent on the cell line. They also found that the effect of DHA was not significantly different between cell lines (Habermann *et al*., 2009). This, together with our findings that DHA toxicity was not significantly different between SW480 and SW620 cells suggested that DHA toxicity was not dependent on the cell line.

Blood plasma concentrations of EPA, DHA, and AA have been reported to be 19.4 ± 1.5 µg/ml, 10.1 ± 0.4 µg/ml and 137 ± 8 µg/ml respectively in subjects consuming a fish-based diet (Pawlosky *et al*., 2003). Since the duodenum is the major site of fat absorption (Besnard and Niot, 2000), it is expected that the levels of these PUFAs will be lower in the colon. EC_{50} values for EPA, DHA and AA were determined in µM during this study and have been converted to µg/ml here for easier comparison. EPA EC_{50} values determined in this study were lower than EPA blood plasma levels, being 18.30 µg/ml (60.49 µM) and 18.88 µg/ml (62.41 µM) in SW480 and SW620 cells respectively. AA EC_{50} values were also lower than AA blood plasma levels, being 15.01 µg/ml (49.31 µM) and 11.03 µg/ml (36.23 µM) in SW480 and SW620 cells respectively. However, DHA EC_{50} values were higher than DHA blood

plasma levels, being 16.14 µg/ml (49.12 µM) and 14.96 µg/ml (45.54 µM) in SW480 and SW620 cells respectively, thus suggesting that the DHA concentration required for effective inhibition of colon carcinoma will not be reached on a physiological level.

4.4.2 Comparison of toxicity of EPA and 17, 18-EpETE in SW480 cells

The human liver microsomal system was unable to metabolise our PUFAs of interest, therefore we decided to move the study forward by purchasing known CYP metabolites. Metabolite selection was based on knowledge gaps in the literature, *in silico* predictions and availability. The metabolite of choice was 17, 18-EpETE, which is formed through the CYP epoxidation of EPA at the n-3 double bond. The reasons why an EPA epoxide, and specifically 17, 18-EpETE, was chosen were as follows. Firstly, CYP epoxygenases have been found to be upregulated in human tumors (Xu *et al.*, 2011). Secondly, EPA showed lower toxicity towards both cell lines (Figure 4.2 and 4.3) in comparison to DHA and AA and epoxides tend to be more toxic than their parent compounds (Born *et al*., 1997). Thirdly, 17, 18-EpETE was ranked, by MetaSite during the *in silico* analysis (Table 2.2, EPA metabolite 12), as the most likely EPA epoxide to form during phase 1 CYP-mediated metabolism of EPA. Fourthly, the n-3 double bond distinguishes ω-3 FAs from their ω-6 counterparts and is known to be a predominant site of epoxidation for many CYP isoforms, including several members of the CYP4A subfamily (Arnold *et al.,* 2010; Konkel and Shunck, 2011). Lastly, the effects of EPA epoxides on colon carcinoma have not previously been reported. Since EPA showed similar toxicity towards SW480 and SW620 cells (*F* test, $p > 0.05$), future comparative studies of EPA and 17, 18-EpETE were conducted in one cell line only. SW480 was the cell line of choice since it was isolated from the primary tumor (Leibovitz *et al*., 1976).

WST-1 analysis found that 17, 18-EpETE reduced SW480 cell viability in a concentration dependant manner, resulting in a significantly greater decrease in SW480 cell viability than EPA at a concentration of 25 µM and 50 µM (Figure 4.4) (T-test, $p < 0.05$). The EC_{50} for 17, 18-EpETE (23.23 µM) was significantly lower than the EC_{50} previously determined for EPA

(60.49 µM) in SW480 cells (*F* test, $p < 0.05$). The increased toxicity seen for 17, 18-EpETE was anticipated since epoxides have been known to be more reactive and toxic than their parent compounds (Born *et al*., 1997). Many toxic epoxides mediate their effects through direct interaction of the epoxide moiety with cellular components (Born *et al*., 1997).

Real-time analysis found that all concentrations of EPA and 17, 18-EpETE (25, 50 and 100 µM) used resulted in a decrease in CI over time (Figure 4.5A). This decrease in CI can be correlated to an increase in cell death. The vehicle control also resulted in a decrease in CI over time. The decrease in cell viability observed in the vehicle control may be due to the length of the assay. Cells were seeded at 12 000 cells/well in a 96-well plate and incubated for 96 hours before compound addition, and then a further 96 hours after compound addition. Thus, cells may have become over confluent during this time, leading to cell death, or perhaps the nutrients required for growth were depleted during this time since the media was not changed (only 50 µl media was added to the original 150 µl media upon compound addition).

4.5 Conclusion

EPA, DHA and AA were found to reduce SW480 and SW620 cell viability in a concentration dependent manner. EC_{50} values for all three PUFAs were in the micromolar range for both cell lines, with EPA having a higher EC_{50} value in both cell lines in comparison to DHA and AA.

SW480 cell viability was reduced in a concentration dependant manner upon treatment with 17, 18-EpETE. The metabolite, 17, 18-EpETE, was found to be significantly more toxic towards SW480 cells than the parent compound, EPA. Since a significant difference in cytotoxicity in SW480 cells was observed for EPA and 17, 18-EpETE, the effects of these two PUFAs on SW480 cell biology were compared in the forthcoming chapter. This entailed an

analysis of the effect of EPA and 17, 18-EpETE on apoptosis, reactive oxygen species (ROS) production, cell migration, and anchorage independent growth.

Chapter Five

Comparison of the biological effects of EPA and its CYP metabolite 17, 18-EpETE on SW480 cells

5.1 Introduction

The ability to evade apoptosis and activate metastasis are two important hallmarks of cancer (Jiang *et al*., 1998; Hanahan and Weinberg, 2011). Cancer cells display unregulated growth and are less prone to apoptosis (Jiang *et al*., 1998). Compounds that lead to apoptosis in tumour cells are therefore sought after in cancer prevention and treatment (Jiang *et al*., 1998). EPA has previously been shown to induce apoptosis in cancer cell lines, including those of leukemic, pancreatic and colon carcinoma (Chiu and Wan, 1999; Lai *et al*., 2006; Giros *et al*., 2009; Fukui *et al*., 2013). EPA induced apoptosis has been found to be mediated by caspases, with both the intrinsic and extrinsic apoptotic pathways being implicated (Giros *et al*., 2009; Fukui *et al*., 2013). ROS have been shown to induce apoptosis and decrease cell proliferation in cancer cells (Simon *et al*., 2000; Pelicano *et al*., 2004). The production of ROS has been proposed as a possible mechanism for EPA-induced cell death in cancer cells (Field and Schley, 2004; Larsson *et al*., 2004). This has been supported through studies showing that co-treatment with EPA and an antioxidant, such as vitamin E, reduces the cytotoxic effects of EPA *in vitro* and *in vivo* (Chajès *et al*., 1995; Latham *et al*., 2001; Fukui *et al*., 2013).

Metastasis is the major cause of mortality in cancer patients (Iwamoto *et al*., 1998) and progression of colon cancer is particularly associated with metastasis formation (Sack *et al*., 2011). Thus the suppression of metastasis is an important aspect in the treatment of colorectal cancer. EPA has been found to inhibit colon carcinoma metastasis *in vivo* and *in vitro* (Iwamoto *et al*., 1998; Hawcroft *et al*., 2012). In a mouse model of MDA-MB-231 human breast cancer cell metastasis to bone, a fish oil diet enriched in EPA and DHA has been found to inhibit breast cancer cell metastasis to bone (Mandal *et al*., 2010).

Anoikis resistance, or survival in the absence of attachment to extracellular marix, is a prerequisite for the development of tumor metastases (Kim *et al*., 2012). The study of a compounds ability to reduce anoikis resistance is therefore important since it encompasses the eradication of circulating tumor cells and the prevention of tumor metastasis. Anchorage-independent *in vitro* cell growth is the ability of cancer cells to form colonies under conditions that don't allow for cell adhesion, such as culture in semisolid media (Mori *et al*., 2009). Anchorage-independent cell growth is considered to be fundamental in cancer biology since it has been found to be linked to *in vivo* tumor cell aggressiveness (including tumorigenic and metastatic potentials), and has been used as a marker for *in vitro* transformation (Mori *et al*., 2009).

This chapter aimed to compare the effects of EPA and its CYP metabolite, 17, 18-EpETE, on apoptosis, ROS production, and two important components of metastasis, namely, migration and anchorage independent cell growth in SW480 cells. The doses used and choice of assays were selected based on the previous cytotoxicity assays and the amount of compound available.

5.2 Methods

5.2.1 Detection of apoptosis in EPA and 17, 18-EpETE treated cells

Annexin V apoptosis detection kit: sc-4252 AK (Santa Cruz) was used for the apoptosis assay and the method was adapted from Xie *et al*. (2011). SW480 cells were seeded at a concentration of 7.6×10^5 cells/well into a 24 well plate and allowed to adhere overnight. Cells were treated with 25 µM EPA or 25 µM 17, 18-EpETE and incubated at 37°C for 24 hours. DMSO (0.5 %) was used as a vehicle control and 5FU (5 mM) was used as a positive control. After 24 hours, media with floating cells was collected. Adherent cells were washed with phosphate buffered saline (PBS) and detached with ACCUTASE (Sigma-Aldrich®, Germany). Collected media containing floating cells was added to quench ACCUTASE. Cells were harvested by centrifugation (1 125 *g* for 5 minutes) and resuspended in single cell suspension in 1 × assay buffer (catalogue number: sc-4252 AK, Santa Cruz) at a

concentration of 1×10^6 cells/100 µl. Annexin V-FITC (0.5 µg) was added and samples were incubated at 4°C in the dark for 1 hour. Cells were washed with 1 ml PBS to remove unbound Annexin V, collected by centrifugation (1 125 *g* for 5 minutes) and resuspended in single cell suspension in PBS at a concentration of 1×10^6 cells/100 µl. Propidium iodide (PI) (0.25 µg) was added and samples were analysed using a FACSAria II flow cytometer (BD Biosciences). A blue laser with an excitation wavelength of 488 nm and emission wavelengths of 519 nm and 628 nm was used for Annexin V-FITC and PI respectively. The following controls were included: untreated and unstained cells; untreated cells stained with Annexin V only; untreated cells stained with PI only; untreated cells permeabilized with Triton X-100 and stained with PI only. The assay was performed in triplicate. FlowJo software (TreeStar Inc.) was used for data analysis.

5.2.2 Effect of EPA and 17, 18-EpETE on reactive oxygen species (ROS) production in SW480 cells

The detection of ROS production in treated SW480 cells was adapted from de la Mare *et al*. (2012). SW480 cells were seeded into a black-walled, glass bottom 96 well plate (1×10^4 cells/well) and allowed to adhere overnight. Cells were treated with 0.5% DMSO (vehicle control), or 25, 50, or 100 µM EPA or EpETE and incubated at 37°C for 24 hours. Cells were washed twice with PBS and 100 µM 2', 7'-dichlorofluorescein diacetate (DCFH-DA) was added. DCFH-DA is deacetylated by esterase in the cytosol to produce DCFH, which then undergoes ROS-mediated oxidation to form the fluorescent species, DCF (Wu *et al*., 2010). Fluorescence acquisition (Ex: λ485/Em: λ535 nm) was carried out every 10 minutes for 2 hours in a plate reader (BioTek) at 37°C. Intracellular ROS levels were calculated using the following equation:

$$F = [(F_{120} - F_i)/F_{120} \times 100]$$

where F_{120} represents the fluorescence at 120 minutes and F_i represents the initial fluorescence at time zero. The addition of 100 µM H_2O_2 to untreated cells at time zero served as a positive control. The experiment was carried out in triplicate. One-way ANOVA

(p = 0.05) was performed followed by a Tukey multiple comparisons test (p = 0.05) in order to assess if there was a significant difference in intracellular ROS levels.

5.2.3 Effect of EPA and 17, 18-EpETE on SW480 cell migration

SW480 cell migration was monitored by wound healing assay using a protocol adapted from Sade *et al*. (2012). Rat collagen (100 µg/ml) was used to coat the bottom of wells in a 96-well plate. SW480 cells were seeded at 1×10^6 cells/well in complete medium and allowed to adhere for 24 hours such that a confluent monolayer was formed. The monolayer of cells was scratched with a sterile toothpick and debris removed by washing twice with sterile PBS. Cells were incubated for 12 hours at 37°C in complete medium containing 25 µM EPA or 17, 18-EpETE. DMSO (0.5%) was used as a vehicle control and 5FU (600 µM) was used as a positive control. The progress of wound healing was monitored with microphotographs of ×5 magnification taken at 0, 6 and 12 hours with the Zeiss Axio Vert.A1 microscope. Wound area was calculated using ImageJ software and normalised against wound area at 0 hours which represented 100%. One-way ANOVA (p = 0.05) was performed followed by a Tukey multiple comparisons test (p = 0.05) in order to assess if there was a significant difference in migration between treated and vehicle control cells.

5.2.4 Effect of EPA and 17, 18-EpETE on anchorage-independent cell growth in SW480 cells

5.2.4.1 Soft agar assay

The method for assessing the effect of EPA and 17, 18-EpETE on SW480 anchorage-independent cell growth by soft agar assay was adapted from Dhawan *et al*. (2005). Base layers of 100 µl of 0.6% (w/v) agar (Sigma-Aldrich®, Germany) in complete Roswell Park Memorial Institute medium (RPMI) (Sigma-Aldrich®, Germany) containing 10% FCS and 100 U/ml penicillin, 100 µg/ml streptomycin and 12.5 µg/ml amphotericin (PSA) were prepared in 96-well plates. After the base layer had solidified, a 100 µl top layer was applied. This consisted of 0.3% (w/v) agar in complete RPMI and SW480 cells in single cell suspension at a concentration of 500 cells/well. Once this top layer had solidified, 50 µl complete RPMI and

an appropriate concentration of test compound was added to each well. EPA and 17, 18-EpETE were tested at a concentration of 25 µM. DMSO (0.5%) was used as a vehicle control and 5FU (600 µM) was used as a positive control. The plate was incubated at 37°C with 9% CO_2 for 24 days. Cells were given fresh complete RPMI every 4 days (50 µl/well), with half the cells receiving complete RPMI alone and the other half receiving complete RPMI containing test compounds. Microphotographs of ×10 magnification were taken on day 0 and day 24 with the DSZ5000X inverted biological microscope and the number of colonies having a diameter of 50 µm counted on day 24. One-way ANOVA followed by a Tukey multiple comparisons test was performed to assess the variance between the DMSO vehicle control and cells treated initially with EPA and 17, 18-EpETE ($p = 0.05$).

5.2.4.2 Tumorsphere assay

SW480 cells were grown in Dulbecco's Modified Eagle Medium (DMEM) containing 2% (v/v) B-27 supplement, PSA, 10 µg/ml insulin, 20 ng/ml EGF, 20 ng/ml bFGF and 4 ng/ml heparin (Sigma-Aldrich®, Germany). Cells were stained with PI and sorted by fluorescence activated cell sorting (FACS) on the FACSAria II instrument (BD Biosciences) such that 500 live cells/well were seeded in single cell suspension in a 96-well plate with Ultra-low Attachment surface (Corning Inc.). Half the samples were treated on day 0 and half were treated on day 3, with cells not receiving treatment on day 3 being given fresh medium at this timepoint. EPA and 17, 18-EpETE were used at a concentration of 25 µM. DMSO (0.5%) was used as a vehicle control and 5FU (600 µM) was used as a positive control. The plate was incubated at 37°C with 9% CO_2 for 6 days. Microphotographs of ×10 magnification were taken on day 0, 3 and 6 with the DSZ5000X inverted biological microscope. WST-1 assay was performed on day 6 to assess cell viability. Briefly, 10 µl WST-1 reagent was added to each well and incubated at 37°C for 4 hours. The absorbance at 440 nm was determined with complete DMEM containing WST-1 reagent used as a blank. Cell viability was normalized and expressed as a percent of the DMSO vehicle control which represented 100% viability. The number of colonies having a diameter of 100 µm and greater were counted on day 6.

5.3 Results

5.3.1 Analysis of the mechanism of EPA and 17, 18-EpETE mediated cell death

SW480 cells were treated with 25 µM EPA or 17, 18-EpETE for 24 hours, stained with Annexin V-FITC and PI, and analysed by flow cytometry to detect apoptotic cells (Figure 5.1). This concentration was used since it was the lowest concentration that resulted in a significant difference in cell viability between EPA and 17, 18-EpETE treated cells (Figure 4.4). For the DMSO control, 2.12% of cells stained Annexin V-/PI+, 5.50% of cells stained Annexin V+/PI+ and 0.79% of cells stained Annexin V+/PI-. Treatment with EPA resulted in 3.94% of cells stained Annexin V-/PI+, 6.01% of cells stained Annexin V+/PI+ and 0.46% of cells stained Annexin V+/PI-. Treatment with 17, 18-EpETE resulted in 2.02% of cells stained Annexin V-/PI+, 5.77% of cells stained Annexin V+/PI+ and 0.62% of cells stained Annexin V+/PI-. Cells stained Annexin V-/PI+ represent necrotic cells, cells stained Annexin V+/PI+ represent late apoptotic cells and cells stained Annexin V+/PI- represent early apoptotic cells. Since the percentages for EPA and 17, 18-EpETE were similar to the DMSO control, treatment with these compounds did not result in an increase in necrotic and apoptotic cells under the conditions tested. This trend was similar for all replicates. Treatment with 5 mM 5FU resulted in 4.96% of cells stained Annexin V-/PI+, 14.4% of cells stained Annexin V+/PI+ and 1.2% of cells stained Annexin V+/PI-. This indicated an increase in necrotic and apoptotic cells after 5FU treatment relative to the DMSO control.

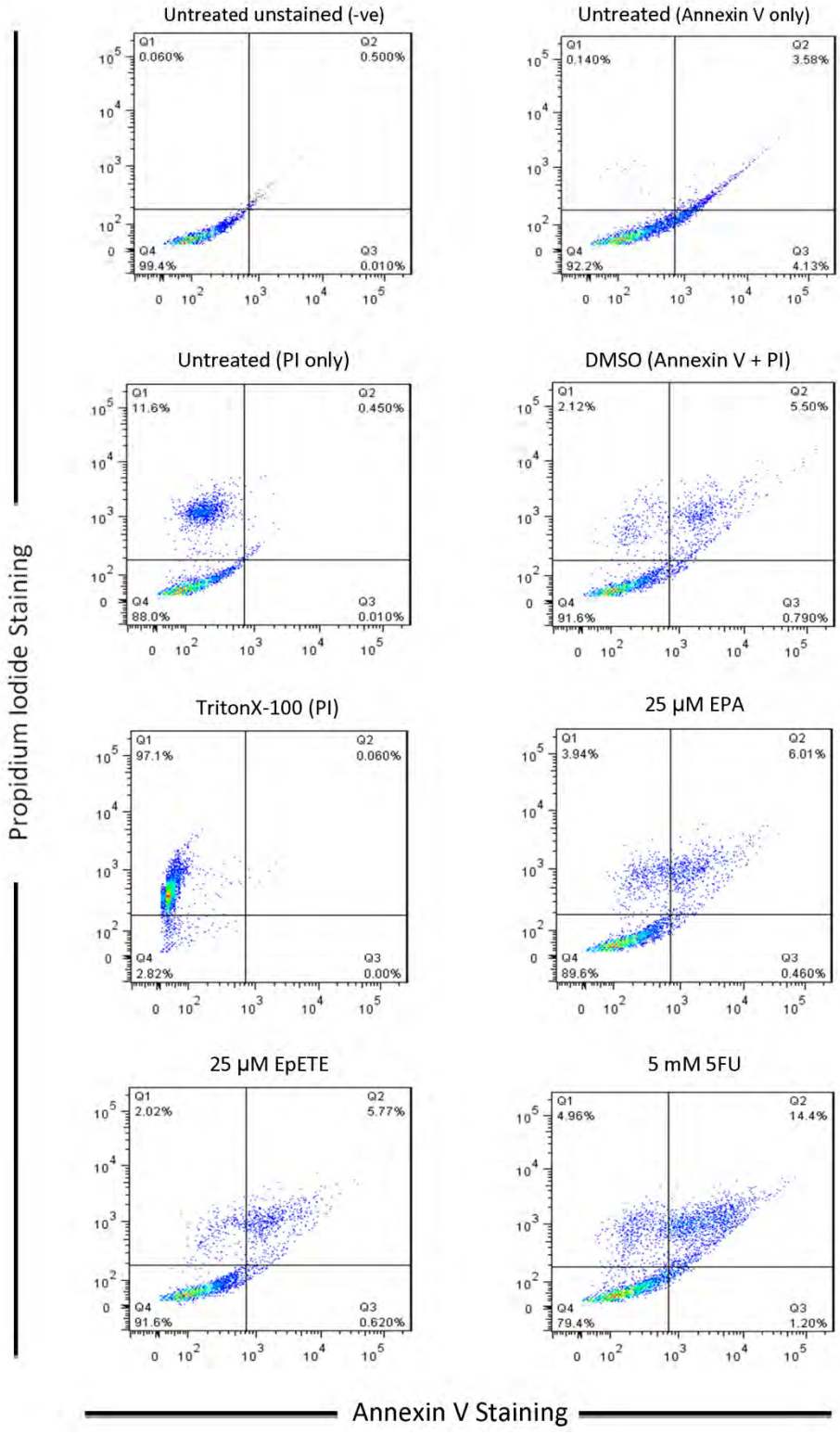

Figure 5.1: Apoptosis analysis of SW480 cells treated with EPA and 17, 18-EpETE.
SW480 cells were seeded at 7.6 × 10^5 cells/well in a 24 well plate, allowed to adhere overnight and treated with 25 µM EPA or 17, 18-EpETE for 24 h. DMSO (0.5%) was used as a vehicle control and 5FU (5 mM) was used as a positive control. After 24 h, floating and adherent cells were collected and stained with Annexin V-FITC and PI. Analysis was carried out using a FACSAria II flow cytometer and FlowJo software. For the PI positive control, cells were permeabilized with Triton X-100 before staining with PI (no annexin V). The gates were set according to the untreated unstained sample. The assay was performed in triplicate. Representative graphs from one set of replicates are shown. The same trend was exhibited in all replicates. Q1: Annexin V-/PI+ (necrotic), Q2: Annexin V+/PI+ (late apoptotic), Q3: Annexin V+/PI- (early apoptotic), Q4: Annexin V-/PI-.

5.3.2 Effect of EPA and 17, 18-EpETE on ROS production in SW480 cells

SW480 cells were treated with a range (0 – 100 µM) of concentrations of EPA or 17, 18-EpETE for 24 hours. ROS production was monitored after this incubation period through the ROS dependent conversion of DCFH-DA to the fluorescent species DCF (Wu *et al*., 2010). H_2O_2 served as a positive control and showed a linear increase in fluorescence with increasing time (Figure 5.2A). Fluorescence increased over time for both the DMSO control and cells treated with EPA or 17, 18-EpETE (Figure 5.2A). Intracellular ROS levels were calculated using the fluorescent values obtained at 120 minutes (Figure 5.2B). All concentrations of 17, 18-EpETE, as well as 50 µM and 100 µM EPA, resulted in decreased intracellular ROS levels relative to the DMSO control. Intracellular ROS levels were only significantly lower than the DMSO control for 25 µM 17, 18-EpETE (One-way ANOVA, Tukey multiple comparisons test, $p < 0.05$).

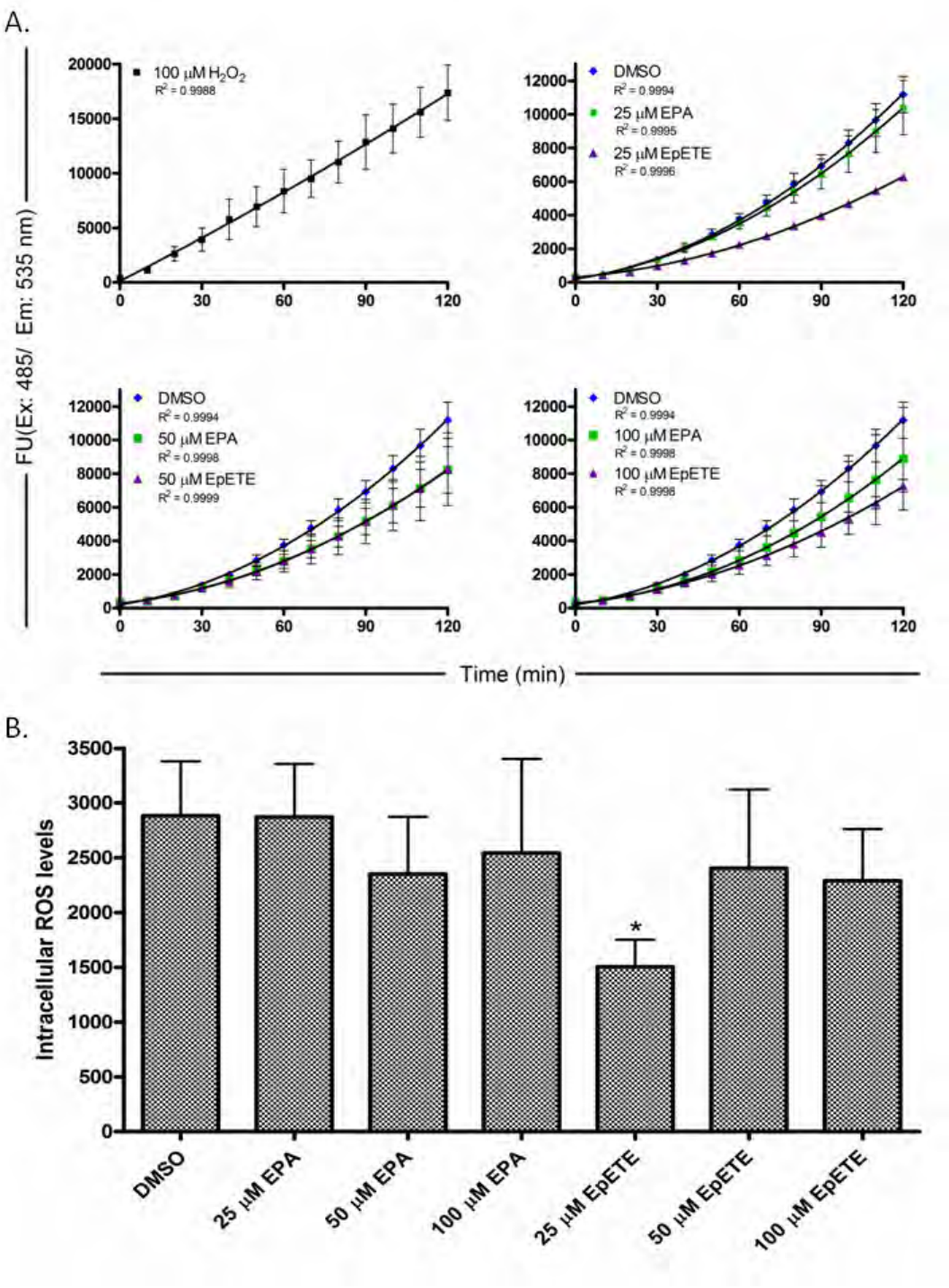

Figure 5.2: Effect of EPA and 17, 18-EpETE on ROS production in SW480 cells.
DCFH-DA was used to assess the formation of ROS in SW480 cells in the presence and absence of EPA and 17, 18-EpETE. SW480 cells were incubated with a range of concentrations of EPA or 17, 18-EpETE for 24 h. DCFH-DA was added to a final concentration of 100 μM and ROS production monitored through the formation of DCF. Fluorescence readings were taken every 10 min for 2 h using an excitation wavelength of 485 nm and an emission wavelength of 535 nm. A) Change in fluorescence over time. Each concentration is plotted on a separate graph for clarity. Error bars indicate the standard deviation of the mean where *n = 3.* B) Intracellular ROS levels were calculated using the following equation: $[(F_{120} - F_i)/F_{120} \times 100]$, where F_{120} represents the fluorescence at 120 min and F_i represents the initial fluorescence at time zero. One-way ANOVA (p = 0.05) was performed followed by a Tukey multiple comparisons test (p = 0.05) in order to assess the variance between treatments. Significant difference is indicated by an asterisk.

5.3.3 Effect of EPA and 17, 18-EpETE on SW480 cell migration

Wounds were created in confluent monolayers of SW480 cells using a sterile toothpick. Wound closure was monitored for 12 hours after treatment with 25 µM EPA or 17, 18-EpETE with microphotographs taken at 0, 6 and 12 hours (Figure 5.3A). DMSO (0.5%) was used as the vehicle control and 5FU (600 µM) was used as a positive control. ImageJ software was used to determine wound area, which was normalised against the wound area at time 0 which represented 100%. A time dependent decrease in percentage wound area from 0 to 12 hours was seen for the DMSO vehicle control (Figure 5.3B). Treatment with EPA or 17, 18-EpETE resulted in a decrease in percentage wound area from 0 to 6 hours, with no change in percentage wound area between 6 and 12 hours (Figure 5.3B). The decrease in percentage wound area between 0 and 12 hours for EPA and 17, 18-EpETE treated cells was slightly lower than for the DMSO control. EPA and 17, 18-EpETE therefore resulted in a minor decrease in SW480 cell migration, with the effect being more pronounced between 6 and 12 hours. The decrease in wound area was however not significantly different between EPA, 17, 18-EpETE and the DMSO control (One-way ANOVA, Tukey multiple comparisons test, $p > 0.05$). The positive control, 5FU, was used at a concentration previously found to be non-toxic to SW480 cells after 24 hours of exposure (data not shown). The decrease in wound area between 0 and 12 hours was significantly less in 5FU treated cells than in the DMSO control (One-way ANOVA, Tukey multiple comparisons test, $p < 0.05$). (Figure 5.3B). Therefore, 5FU inhibited SW480 cell migration.

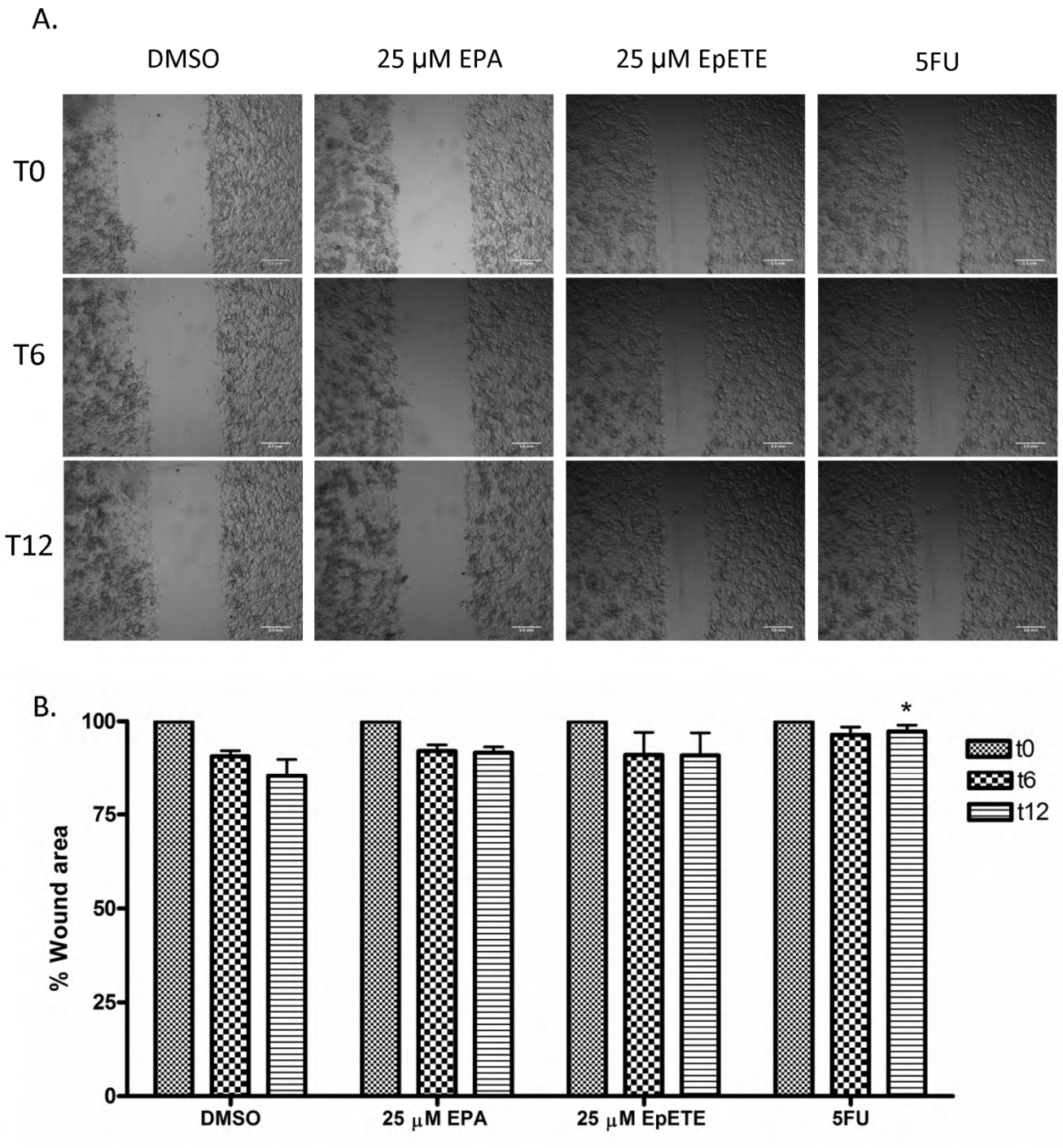

Figure 5.3: Migration of SW480 cells after treatment with EPA and 17, 18-EpETE.
SW480 cells were seeded at 1 × 10^6 cells/well in complete medium in 96-well plates precoated with rat collagen. A sterile toothpick was used to make a wound in confluent monolayers of SW480 cells. Cells were treated with 25 µM EPA or 17, 18-EpETE. DMSO (0.5%) was used as a vehicle control and 5FU (600 µM) was used as a positive control. A) Microphotographs of ×5 magnification taken at 0, 6 and 12 h to monitor wound closure. B) Wound area was calculated using ImageJ software and normalised against the wound area at 0 h which represented 100%. Error bars indicate the standard deviation of the mean where *n = 3*. The reduction in wound area was not significantly different between EPA, 17, 18-EpETE and the DMSO control (One-way ANOVA, Tukey multiple comparisons test, $p > 0.05$). The reduction in wound area was significantly different between 5FU and the DMSO control over the 12 h incubation period (One-way ANOVA, Tukey multiple comparisons test, $p < 0.05$). Significant difference is indicated by an asterisk.

5.3.4 Effect of EPA and 17, 18-EpETE on anchorage-independent cell growth in SW480 cells

5.3.4.1 Soft agar assay

SW480 cells were grown in 0.3% (w/v) agar for 24 days and effect of 25 μM EPA and 17, 18-EpETE on colony formation assessed. After 24 days, SW480 cells had formed colonies in the DMSO vehicle control (7.67 ± 0.47 colonies/500 cells seeded) (Figure 5.4A and B). Initial treatment with EPA and 17, 18-EpETE significantly reduced the number of colonies formed by day 24, relative to the DMSO vehicle control, with the number of colonies formed being 1.67 ± 0.47 colonies/500 cells seeded for both EPA and 17, 18-EpETE (One-way ANOVA, Tukey multiple comparisons test, $p < 0.05$) (Figure 5.4B). The reduction in colony formation was not significantly different between EPA and 17, 18-EpETE (One-way ANOVA, Tukey multiple comparisons test, $p > 0.05$). Weekly treatment with EPA and 17, 18-EpETE inhibited the formation of any colonies (Figure 5.4A and B). Treatment with 5FU (both initially and weekly) led to no colonies being formed by day 24 (Figure 5.4A and B).

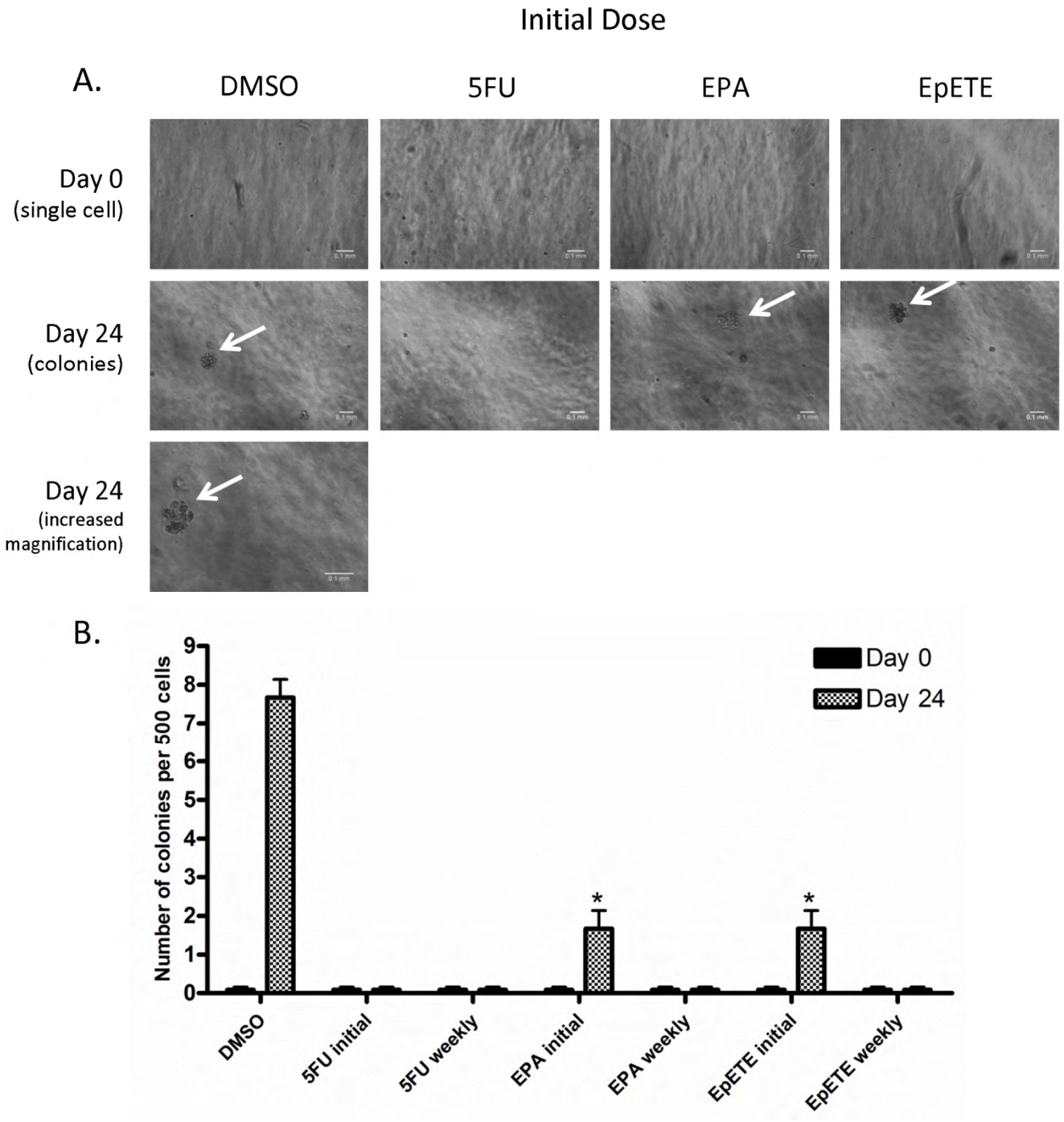

Figure 5.4: Effect of EPA and 17, 18-EpETE on SW480 anchorage independent cell growth in the soft agar assay.

Cells were seeded at 500 cells per well into 0.3% (w/v) agar in complete RPMI and treated with 25 µM EPA or 17, 18-EpETE. Fresh media was given every 4 days, with half the samples receiving media alone and the other half receiving media containing test compound. DMSO (0.5%) was used as a vehicle control and 5FU (600 µM) as a negative control. A) Microphotographs taken on day 0 and day 24 for samples receiving an initial dose of test compounds. Colonies are indicated with arrows. B) Number of colonies formed after 24 days in samples dosed initially and weekly. Colonies having a diameter of 50 µm and greater were counted. Error bars indicate the standard deviation of the mean where *n = 3.* One-way ANOVA followed by a Tukey multiple comparisons test was performed to assess the variance between the DMSO vehicle control and cells treated initially with EPA and 17, 18-EpETE ($p = 0.05$). Significant difference is indicated by an asterisk.

5.3.4.2 Tumorsphere assay

SW480 cells were sorted using flow cytometry and live cells seeded in single cell suspension at a concentration of 500 cells/well in a 96-well plate. The number of colonies formed by day 6 was found to increase with increased cell concentration (Figure 5.5A). EPA treatment either on day 0 (tumorsphere seeding) or day 3 (post tumorsphere formation), significantly reduced SW480 tumorsphere viability (Figure 5.5B) as well as the number of colonies formed (Figure 5.5C) by day 6, relative to the DMSO control (One-way ANOVA, Tukey multiple comparisons test, $p < 0.05$). Treatment with 17, 18-EpETE on day 0 and day 3 reduced tumorsphere viability (Figure 5.5B) by day 6 relative to the DMSO control, however, this reduction was not significantly different (One-way ANOVA, Tukey multiple comparisons test, $p > 0.05$). Treatment with 17, 18-EpETE resulted in a decrease in the number of colonies formed (Figure 5.5C) by day 6 relative to the DMSO control, but the decrease was only significant for treatment on day 3 (One-way ANOVA, Tukey multiple comparisons test, $p < 0.05$). Colony formation and tumorsphere viability were significantly lower in cells treated with EPA on day 0 in comparison to cells treated with 17, 18-EpETE on day 0 (One-way ANOVA, Tukey multiple comparisons test, $p < 0.05$). Colony formation and tumorsphere viability were similar in cells treated with EPA on day 3 in comparison to cells treated with 17, 18-EpETE on day 3 (One-way ANOVA, Tukey multiple comparisons test, $p > 0.05$). An observation made was that colonies formed by day 6 were smaller in samples treated with EPA or 17, 18-EpETE in comparison to the DMSO control. The colonies were also smaller in samples treated with EPA or 17, 18-EpETE on day 0 compared to those treated with EPA or 17, 18-EpETE on day 3 (Figure 5.5D and E). 5FU treatment on day 0 and day 3 both significantly reduced cell viability (Figure 5.5B) relative to the DMSO control (One-way ANOVA, Tukey multiple comparisons test, $p < 0.05$). Treatment with 5FU on day 0 did not allow for any colonies to form, whilst treatment on day 3 significantly reduced the number of colonies formed relative to the DMSO control (Figure 5.5C) (One-way ANOVA, Tukey multiple comparisons test, $p < 0.05$).

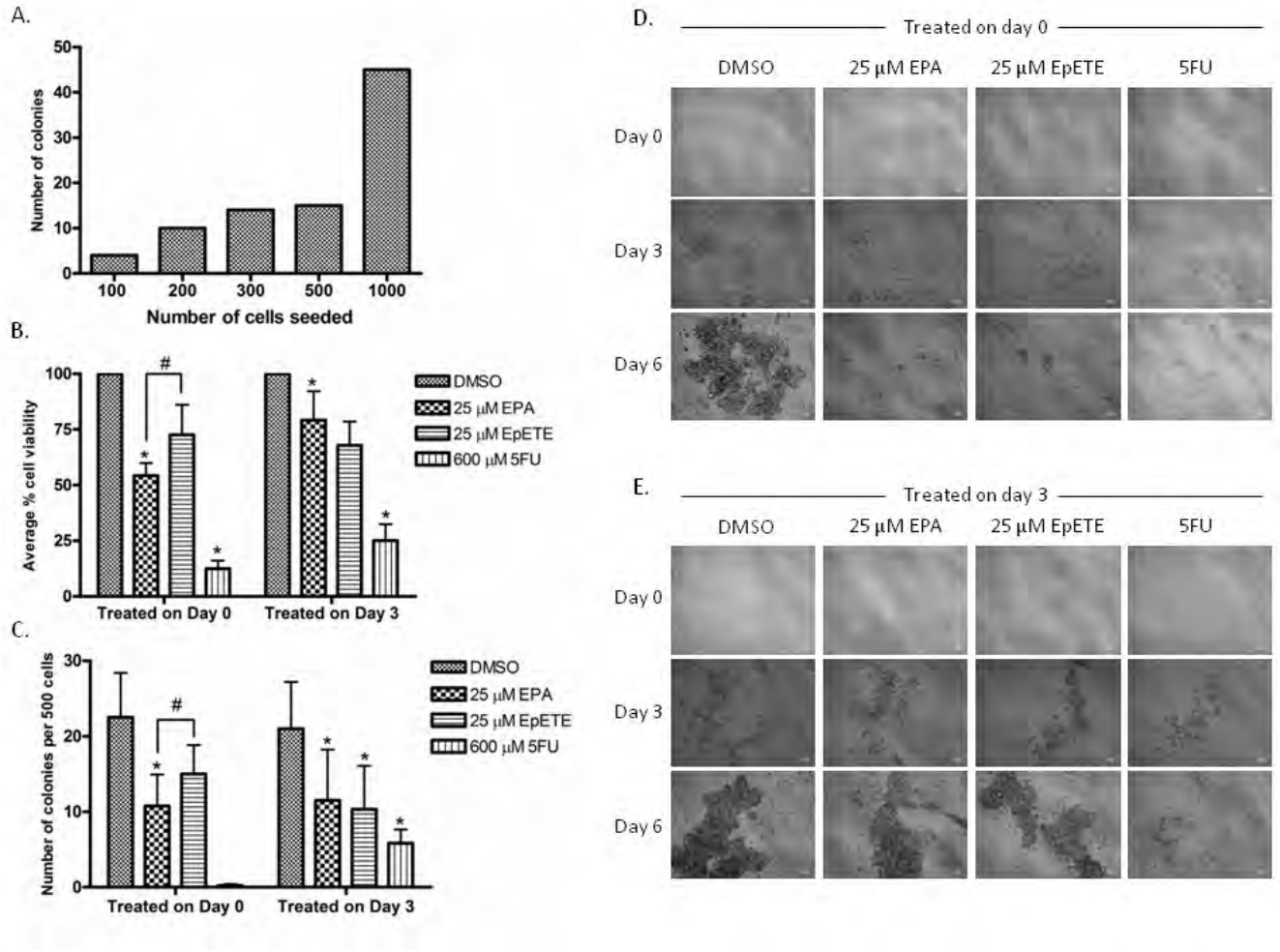

Figure 5.5: Effect of EPA and 17, 18-EpETE on SW480 anchorage independent cell growth using the tumorsphere assay.

Live cells were seeded in single cell suspension by FACS at a concentration of 500 cells/well in complete DMEM in a 96-well plate with Ultra-low Attachment surface. Samples were treated at seeding (day 0) or on day 3 with 25 μM EPA or 17, 18-EpETE. DMSO (0.5%) was used as a vehicle control and 5FU (600 μM) was used as a positive control. Error bars indicate the standard deviation of the mean where *n = 6*. One-way ANOVA followed by a Tukey multiple comparisons test was performed to assess the variance in average percent cell viability and colony number between DMSO and each treatment for cells treated on day 0 and day 3 ($p = 0.05$). Significant difference relative to the DMSO control is indicated by an asterisk. Significant difference between EPA and 17, 18-EpETE is indicated by a hash sign. A) Number of colonies formed on day 6 with increasing number of cells seeded. B) Cell viability on day 6 assessed by WST-1 assay. C) Colonies having a diameter of 100 μm and greater were counted on day 6. D) Microphotographs taken on day 0, 3 and 6 of cells treated on day 0. E) Microphotographs taken on day 0, 3 and 6 of cells treated on day 3.

5.4 Discussion

5.4.1 Apoptosis and ROS production in EPA and 17, 18-EpETE treated cells

Cancer cells have been found to have increased ROS levels relative to non-cancerous cells (Pelicano *et al*., 2004; Lu *et al*., 2007). These increased ROS levels have been attributed, in part, to oncogenic stimulation, increased metabolic activity, and mitochondrial malfunction (Pelicano *et al*., 2004). The persistent increased oxidative stress in cancer cells stimulates cell proliferation, induces genomic instability and promotes mutations (since the ROS serve as an endogenous source of DNA-damaging agents) and leads to development of drug resistance (Pelicano *et al*., 2004; Zhang *et al*., 2008). A decrease in ROS may therefore lead to a decrease in cell proliferation rate, but may not necessarily result in cell death or apoptosis. Treatment with 17, 18-EpETE at a concentration of 25 µM significantly decreased ROS production and cell viability of SW480 cells (Figure 4.4), but did not result in apoptosis in these cells over 24 hours. The decreased cell viability may therefore be representative of a decreased cell proliferation rate. The differential effects of EPA and 17, 18-EpETE (25 µM) on ROS production may account for the significant decrease in cell viability in 17, 18-EpETE treated cells compared to EPA treated cells (25 µM) (Figure 4.4) since at this concentration 17, 18-EpETE was found to significantly reduce ROS levels whilst ROS levels remained constant for EPA relative to the DMSO control.

Since cancer cells are under increased intrinsic ROS stress, and ROS are chemically active and can inflict cellular damage, cancer cells are vulnerable to further increases in ROS levels (Pelicano *et al*., 2004). Increased ROS levels have been shown to induce apoptosis and decrease cell proliferation in many different cell systems under both physiologic and pathologic conditions (Simon *et al*., 2000; Pelicano *et al*., 2004). The apoptosis inducing ability of 17, 18-EpETE in cancer cell lines has not previously been reported in literature. Previous studies have shown that EPA induced apoptosis in several colorectal cell lines, including SW480 cells (Clarke *et al*., 1999; Giros *et al*., 2009). A study by Giros *et al*. (2009) found that treatment of SW480 cells with 60 µM EPA for 24 hours significantly increased the number of apoptotic cells relative to the vehicle control. This significant increase in apoptosis was also seen in other colorectal cell lines (Caco-2, HT-29, HCT116 and LoVo)

(Giros *et al*., 2009). Treatment with 50 μM EPA for 24 hours was found to significantly increase apoptosis in HT29 colon carcinoma cells (Clarke *et al*., 1999). Both the intrinsic and extrinsic pathways have been implicated in EPA-induced apoptosis through the down-regulation of X-linked inhibitor of apoptosis protein (XIAP) and FLICE-like inhibitory protein (FLIP) respectively (Giros *et al*., 2009). A study in MCF-7 cells found that incubation with EPA (10 μM, 24 hours) did not significantly increase the percent of apoptotic cells relative to the vehicle control (Chamras *et al*., 2002). The concentrations of EPA at which apoptosis occurred were greater than the concentration used during this study (and the concentration used in the study of MCF-7 cells which showed no increase in apoptosis with EPA treatment).

5.4.2 EPA and 17, 18-EpETE reduced SW480 cell migration and anchorage independent growth

EPA and 17, 18-EpETE resulted in a similar reduction in SW480 cell migration relative to the DMSO control from 0 to 12 hours, with the greatest reduction being from 6 to 12 hours (One-way ANOVA, Tukey multiple comparisons test, $p > 0.05$). This indicated that the effect of these PUFAs on SW480 cell migration was greater after incubation with these PUFAs for more than 6 hours and that EPA and 17, 18-EpETE reduced cell migration with the same efficacy. The effects of EPA and 17, 18-EpETE on cell migration have not previously been reported in SW480 and SW620 cells. The findings in this study support those of previous studies which have shown EPA to inhibit cell migration in the micromolar concentration range in different cell lines *in vitro*. M38 mouse colorectal cancer cell migration has been shown to be inhibited by EPA in a dose dependent manner (Volpato *et al*., 2012). In N87 gastric cancer cells, treatment with EPA (0.5 μM – 5 μM) has been shown to significantly inhibit macrophage-activated cell migration (Wu *et al*., 2012). Treatment with 165 nM EPA significantly reduced MDA-MB-231 breast cancer cell migration over 21 hours *in vitro* (Mandal *et al*., 2010). Previous studies have not, however, reported that the ability of EPA to reduce cell migration increases with time, as observed during this study. Another possible reason why the effect of EPA and 17, 18-EpETE was greater from 6 to 12 hours could be that SW480 cells have a low migration rate (Sabauste *et al*., 2009), and therefore it may take

longer for the effects of the PUFAs to become evident than if they were used to treat a highly migratory cell line such as the SW620 cell line (Sabauste *et al*., 2009).

The effect of EPA and 17, 18-EpETE on SW480 anchorage independent cell growth was assessed during this study using two assays, namely, soft-agar and tumorsphere assay. Both assays found that treatment with EPA and 17, 18-EpETE at a concentration of 25 µM inhibited anchorage independent growth of SW480 cells. Tumorsphere assays differ from soft agar assays in that they are serum free. The ability of cancer cells to form anchorage independent colonies under serum-free tumorsphere conditions reflects their stem-like characteristics (Wang *et al*., 2010; Zhang *et al*., 2012). Normally, very few cells within a tumor have the capacity to start a new tumor (Erickson and Hubbard, 2010). Those cells that are capable of initiating new tumors are known as cancer stem cells (CSCs) and are of great interest because they may not be killed by conventional chemotherapies and could be the cause of disease recurrence (Erickson and Hubbard, 2010). The ability of a compound to target CSCs is therefore of great importance. Tumorsphere assays are often used to isolate cancer stem cells (CSCs) in order to characterize them or to assess the effect of compounds on the CSC population (Qiang *et al*., 2009). The ability of EPA and 17, 18-EpETE to reduce colony formation under serum free conditions during this study therefore implicates these PUFAs as potential CSC targeting agents.

The soft agar assay found that the extent of inhibition was similar for EPA and 17, 18-EpETE (Figure 5.4). This was supported by the results obtained for treatment on day 3 during the tumorsphere assay which showed that EPA and 17, 18-EpETE reduced colony formation and cell viability relative to the DMSO control to a similar extent in SW480 cells (Figure 5.5). Colony formation and cell viability was, however, significantly lower in cells treated with EPA on day 0 in comparison to cells treated with 17, 18-EpETE on day 0 during the tumorsphere assay (One-way ANOVA, Tukey multiple comparisons test, $p < 0.05$). This suggested that EPA prevented colony formation to a greater extent than 17, 18-EpETE if colonies had not already formed prior to treatment, but after colonies had formed, treatment with EPA and 17, 18-EpETE resulted in the same reduction in colony growth. Perhaps a reason why this

significant difference was not seen during the soft agar assay was due to the time differences between the assays (the soft agar assay was conducted for 24 days whilst the tumorsphere assay was conducted for 6 days). The increased exposure time during the soft agar assay may have resulted in a loss of significant difference between EPA and 17, 18-EpETE since the effects of PUFAs have been found to be time dependent (Schonberg *et al*., 2006; Habermann *et al*., 2009). Another possible explanation could be that EPA is more effective at targeting CSCs than 17, 18-EpETE, before colony formation, since the significant difference between EPA and 17, 18-EpETE was observed under serum free tumorsphere conditions.

The effect of 17, 18-EpETE on anchorage-independent cancer cell growth has not previously been reported, but EPA has been shown to inhibit anchorage independent growth. A recent study conducted by Yang *et al*. (2012) found that EPA significantly inhibited anchorage independent cell proliferation in a concentration dependent manner in SW620 cells relative to the vehicle control (10 μM - 70 μM, 3 days). The concentration used during this study was within the concentration range used by Yang *et al*. (2012), therefore supporting their findings.

Since migration and anchorage independent growth are important components of metastasis (Steeg, 2003), our findings supported previous *in vivo* and *in vitro* studies which have shown that EPA, in the micromolar range, reduced cancer cell metastasis in a range of cancer types. Dietary administration of EPA has been found to reduce metastasis of MC-26 mouse colorectal cancer cells to the liver *in vivo*, and inhibit MC-26 migration in a concentration (50 – 200 μM) dependant manner *in vitro* (Hawcroft *et al*., 2012). A diet high in EPA has been found to significantly reduce the number and size of liver metastatic foci of rat colon cancer cells, ACL-15, *in vivo* (Iwamoto *et al*., 1998). These effects were explained by low expression of vascular cell adhesion molecule 1 resulting in decreased tumor cell adhesion to the capillary bed, and decreased cell proliferation at the secondary site (Iwamoto *et al*., 1998).

5.5 Conclusion

Treatment with 25 μM EPA and 17, 18-EpETE for 24 hours did not result in apoptosis in SW480 cells. EPA (50 μM and 100 μM) and 17, 18-EpETE (25 μM, 50 μM and 100 μM) resulted in decreased intracellular ROS levels relative to the DMSO control, with this decrease being significant for 25 μM 17, 18-EpETE. SW480 cell migration was inhibited to a similar extent by treatment with EPA and 17, 18-EpETE, with the greatest inhibition being seen between 6 and 12 hours of treatment. EPA and 17, 18-EpETE reduced colony formation and cell viability of SW480 cells under anchorage independent conditions, with this reduction in cell viability being significantly greater for EPA than for 17, 18-EpETE in cells treated on day 0 of the tumorsphere assay.

Chapter Six

Conclusions and Future Work

6.1 Overview

This study aimed to assess the effects of EPA, DHA, AA and their CYP metabolites on the paired colon carcinoma cell lines, SW480 and SW620. An overview of the scientific method employed and results obtained during this study is summarised in Figure 6.1 and addressed in more detail in the sections that follow.

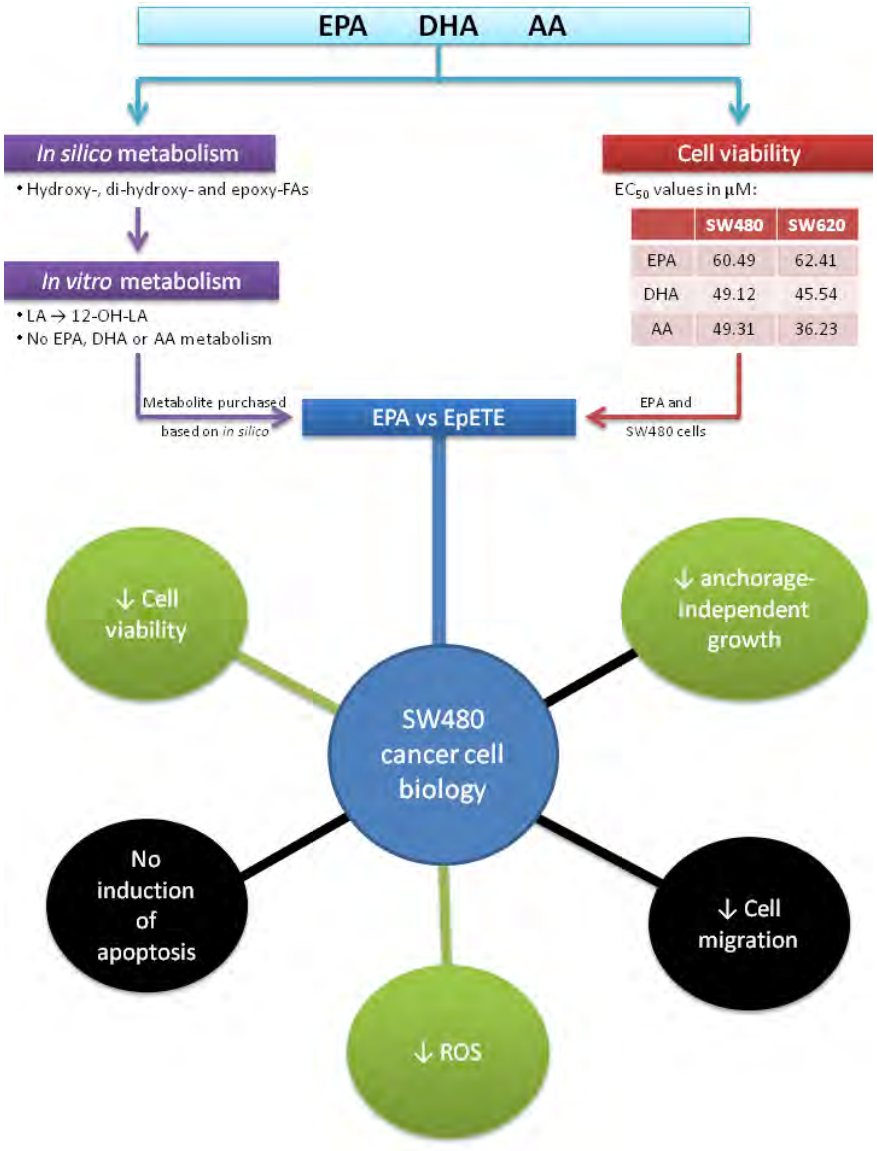

Figure 6.1: Outline of the scientific method followed and results achieved during this study.
A significant difference between the effect of EPA and 17, 18-EpETE is represented in green; a similar effect between EPA and 17, 18-EPETE is represented in black. A decrease is indicated by a downward arrow.

6.2 *In silico* predicted metabolites of EPA, DHA and AA were suitable for oral administration

EPA, DHA and AA were metabolised *in silico* using two software programs, namely MetaSite and SMARTCyp. Predicted metabolites included hydroxy-, di-hydroxy- and epoxy-FAs, and these metabolites satisfied the criteria of the Ro5, thus making them suitable for oral administration (Table 2.1 and 2.2). Future *in silico* studies could encompass the use of computational software programmes that are able to forecast potential toxicity issues. An example of such a programme is DEREK (Deductive Estimation of Risk from Existing Knowledge) (LHASA Ltd., Leeds, UK) which is a rule-based system that uses known structure-toxicity relationships and mechanisms to make quantitative predictions about a compound (Greene, 2002). Another software programme that may be of interest is OncoLogic (LogiChem Inc., USA) which is a rule-based system that is able to predict the carcinogenic potential of chemical structures (Greene, 2002). These software programmes would be helpful in predicting the potential toxicity and carcinogenicity of EPA, DHA and AA metabolites towards non-cancerous tissues.

6.3 GC-MS method for PUFA detection was developed and validated

A GC-MS method for the detection of EPA, DHA, AA, LA and their CYP-metabolites was developed and validated in terms of inter- and intra-day reproducibility, linearity, and LODs (Chapter 3). GC is generally the preferred method for the separation and quantification of FAs in the form of FAMEs (Amet *et al*., 2002). However, this method has some drawbacks that need to be taken into account. Firstly, FAMEs may be lost during derivatisation or injection due to their volatile nature; secondly, since the conversion of FAs to methyl esters requires that the samples be exposed to high temperatures, thermal degradation or structural modification of unsaturated FAs is a possibility; lastly, when using FID the FA is unable to be recovered for further analysis since it is destroyed (Amet *et al*., 2002). High performance liquid chromatography (HPLC) may provide an alternative method for the separation and quantification of PUFAs in future studies. An advantage to the use of HPLC would be that PUFAs would not need to be derivatised prior to detection (Amet *et al*., 2002; Fer *et al*., 2008a).

6.4 Human liver microsomal system resulted in the metabolism of LA to 12-OH-LA

In vitro metabolism through the use of human liver microsomes resulted in the metabolism of the positive control, LA, to 12-OH-LA. This indicates that the system was functional. However, it was unable to metabolise the longer chained PUFAs EPA, DHA or AA. CYPs have large and fluid substrate binding sites, causing them to have slow catalytic rates since they are promiscuous in their capacity to bind and metabolise multiple substrates (Gonzalez and Tukey, 2005). For this reason, perhaps a longer incubation period would have resulted in metabolism. For example, De Graaf *et al*. (2002) used an incubation period of 2 hours when metabolising their drugs of interest.

Options for future work could involve the use of isolated CYP isoforms or the use of hepatocytes (Jia and Liu, 2007). The specific CYP isoform of interest, such as the known FA metaboliser CYP4A, could be obtained through purification from an appropriate tissue or through complementary DNA (cDNA) expression systems (Wrighton *et al*., 1995). Using specific isoforms would only allow for the study of phase 1 metabolism and would selectively determine the metabolites formed by the chosen isoforms, thus resulting in a metabolite profile that may be substantially different to that seen *in vivo* (Jia and Liu, 2007). The use of hepatocytes, however, would allow for both phase 1 and phase 2 metabolism since all the potential metabolic pathways are intact and available, thereby giving a good indication of the metabolites that would be produced *in vivo* (Wrighton *et al*., 1995; De Graaf *et al*., 2002). Also, the use of hepatocytes would allow for the induction of the enzymes necessary for PUFA metabolism upon incubation with these compounds, thereby ensuring metabolism would occur (De Graaf *et al*., 2002). Hepatocytes could therefore also be used in order to identify which metabolising enzymes are induced in the presence of our PUFAs of interest (Wrighton *et al*., 1995). In a study performed by De Graaf *et al*. (2002) different *in vitro* techniques were used to metabolise three unnamed compounds and the resulting metabolites were compared to *in vivo* findings. Their study showed that hepatocytes resulted in a greater percent of the parent compound being metabolised in comparison to microsomes. It also showed that a compound that was not metabolised by the liver microsomes was able to be metabolised through the use of hepatocytes, thus

supporting the suggestion of using hepatocytes in future studies. Drawbacks to the use of hepatocytes include their phenotypic instability, restricted accessibility and short functional period (Nussler *et al*., 2001; Castell *et al*., 2006). Transformed human hepatic cell lines are more readily available, easier to maintain in culture and remain functionally active for long periods of time, and therefore provide an alternative to hepatocytes during *in vitro* metabolism studies (Nussler *et al*., 2001). However, previous studies have found cell lines to be of limited use in metabolism assays since they don't accurately reflect the metabolic potential of their parent cell (Wrighton *et al*., 1995). For example, expression levels of genes coding for CYPs and some important phase II enzymes have been found to be significantly different in the hepatic cell line HepG2 in comparison to human liver samples, with activity and expression of phase I enzymes reported to be highly significantly lower in HepG2 cells (Wilkening *et al*., 2003). Hepatocytes are therefore the preferred model for *in vitro* metabolism studies.

6.5 EPA, DHA and AA reduced SW480 and SW620 cell viability in a concentration dependent manner

EPA, DHA and AA were found to reduce the cell viability of SW480 (Figure 4.2) and SW620 (Figure 4.3) cells in a concentration dependent manner, having EC_{50} values in the micromolar range. Previous studies have reported that these PUFAs reduce the cell viability of human colon (Engelbrecht et al., 2008; Habermann et al., 2009), breast and lung cancer cells in a concentration dependent manner (Bègin *et al*., 1986). Future studies could therefore be extended to include other cell lines. Since the effect of these PUFAs has previously been found to be time-dependent (Schonberg *et al*., 2006; Habermann *et al*., 2009), future studies should assess the effect of PUFA exposure time on SW480 and SW620 cell viability.

6.6 SW480 cell viability was significantly lower in 17, 18-EpETE treated cells than EPA treated cells

WST-1 assay showed that treatment with 17, 18-EpETE significantly reduced SW480 cell viability in comparison to EPA at lower concentrations, with the EC_{50} values being 23.23 µM and 60.49 µM for 17, 18-EpETE and EPA respectively (Figure 4.4). Real-time analysis found that EPA and 17, 18-EpETE reduced SW480 cell viability, however, these reductions were not significantly different to the vehicle control (Figure 4.5). Future studies would need to optimise the real-time cell viability assay in terms of cell number and treatment time. The effect of replacing media with fresh media upon compound addition should also be investigated. A confounding factor when using the xCELLigence System to determine cytotoxicity is that any change in the cell status, such as a change in morphology, will lead to a change in the CI (Gerets *et al*., 2012) which may be read as cell death. Future studies should therefore also monitor cell morphology in order to determine whether cytotoxicity results are being skewed by changes in cell morphology.

Intracellular levels of 17, 18-EpETE are tightly regulated and its metabolism occurs relatively rapidly (Fleming, 2011). The soluble epoxide hydrolase (sEH) is the most important EpETE-metabolising enzyme and converts 17, 18-EpETE to 17, 18-dihydroxyeicosatetraenoic acid (DHEQ) through the addition of a water molecule (Fleming, 2011) (Figure 6.2). Future studies would need to investigate if the increased toxicity seen for 17, 18-EpETE in comparison to EPA was due to 17, 18-EpETE itself or its sEH metabolite 17, 18-DHEQ. This could be achieved through the use of sEH inhibitors such as 4-[4-(3-adamantan-1-yl-ureido)-cyclohexyloxy]-benzoicacid (Hwang *et al*., 2007). It is proposed that sEH inhibition would increase 17, 18-EpETE toxicity since epoxides are generally more biologically active than their diol metabolites (Fleming, 2011). Future studies involving CYP epoxygenase inhibitors such as 17-ODYA (Jiang *et al*., 2005) would also be of interest in order to determine if the cytotoxic effects observed by EPA were due to EPA itself or if EPA was metabolised to 17, 18-EpETE which then resulted in the observed cytotoxicity. If the latter was the case, it could be used to explain the decreased cytotoxicity observed in EPA since EPA would need to be metabolised to 17, 18-EpETE before any cytotoxic effects could occur.

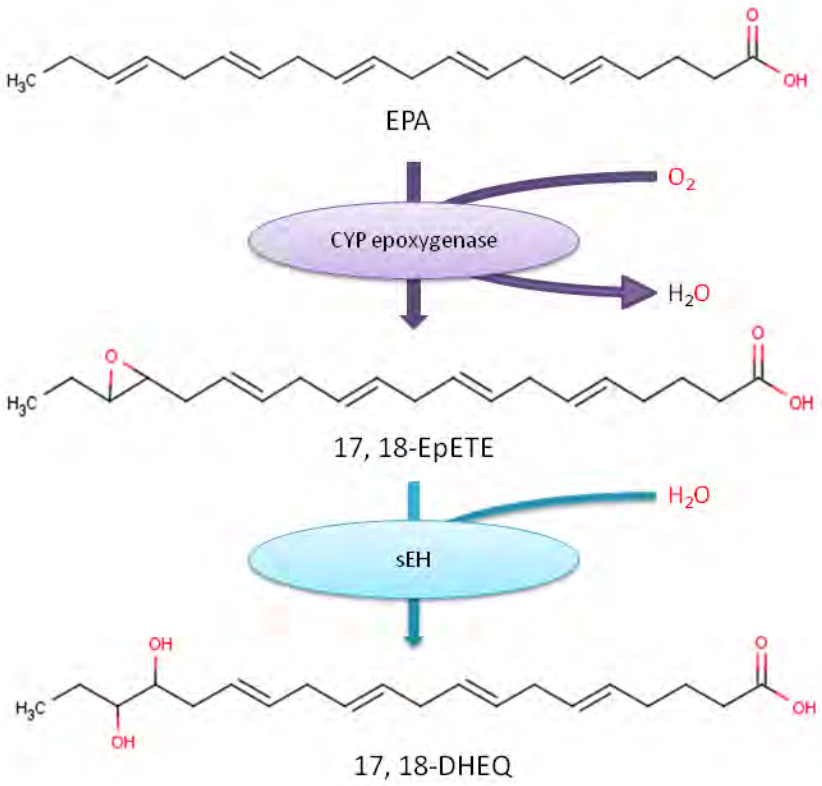

Figure 6.2: EPA metabolism.
EPA is metabolised by cytochrome P450 epoxygenases to 17, 18-EpETE which is metabolised to its corresponding diol by the soluble epoxide hydrolase (sEH). EpETE: epoxyeicosatetraenoic acid. DHEQ: Dihydroxyeicosatetraenoic acid. (Adapted from Fleming 2011).

The EPA and 17, 18-EpETE dependant decrease in SW480 cell viability observed during this study may be linked to a decrease in cell proliferation rate. This could be investigated in future studies through the assessment of the effect of EPA and 17, 18-EpETE on the distribution of SW480 cells in the various phases of the cell cycle and could be determined by flow cytometry with propidium iodide staining (de la Mare *et al*., 2012). Treatment of the human pancreatic cell line MIA PaCA-2 with 50 µM EPA has been found to result in cell cycle arrest and accumulation of cells in S-phase (Lai *et al*., 1996). The fluorescent dye carboxyflourescein diacetate succinimidyl ester (CFDA-SE) would also be useful in determining if the decrease in cell viability observed is due to a decrease in cell proliferation rate. The membrane permeable CFDA-SE diffuses into cells and cellular esterases cleave the acetate groups to produce a highly fluorescent and membrane impermeable CFSE that can

be detected by flow cytometry (Banks *et al*., 2011). The CFSE fluorescence intensity (FI) is sequentially halved after cell division and therefore provides an indirect measure of the number of divisions a cell has undergone (Banks *et al*., 2011). Up to eight rounds of cell division can be monitored before the CFSE FI is reduced to the background flourescence level of unstained cells (Banks *et al*., 2011).

Studies assessing the link between EPA, CYP epoxidation and carcinogenesis have not been conducted to date. A study performed by Cui *et al*. (2011) assessed the effect of four EPA epoxides (17,18-, 14,15-, 11,12- and 8,9-EpETE) on the non-cancerous bEND.3 cell line established from mouse brain endothelial cells. They did not, however, compare their results to the parent compound, EPA. The metabolite, 17, 18-EpETE, significantly inhibited bEND.3 cell proliferation, whilst 8, 9- and 11, 12-EpETE stimulated proliferation, and 14, 15-EpETE had no effect relative to the DMSO control (10 µM, 24 hours) (Cui *et al*., 2011). These differential effects highlight the possible relevance of the ω-3 double bond in EPA which is transformed in the production of 17, 18-EpETE.

Jiang *et al*. (2007) assessed the effects of AA epoxides, epoxyeicosatrienoic acids (EETs), on carcinoma; however, their study was limited as they didn't compare these effects to those of the parent compound. CYP2J2 is the predominant human AA epoxygenase that generates all four epoxyeicosatrienoic acids (EETs), namely 5,6-; 8, 9-; 11,12-; and 14,15-EET, through the addition of an epoxide group to one of the four double bonds of AA (Jiang *et al.*, 2007; Xu *et al.*, 2011). Transfection with a recombinant adeno-associated virus vector containing the CYP2J2 cDNA in a sense direction (rAAV-CYP2J2), or addition of exogenous EETs was found to increase cell proliferation in eight cancer cell lines (ScaBER, SiHa, U251, A549, Tca-8113, Ncl-H446, HepG2, and the colon carcinoma cell line LS-174) (Jiang *et al*., 2005).

The current study was limited to one metabolite due to the high cost and limited commercial availability of these metabolites. Another limitation was that only a small amount of metabolite was able to be purchased, and therefore the study was carried out on

a single cell line. Future studies therefore need to look at the effect of DHA and AA epoxides, and should incorporate both SW480 and SW620 cells in order to compare the effect of these compounds on the primary tumor and its metastatic counterpart. The effect of different PUFA epoxide isoforms should also be investigated to see if the position of epoxidation has an effect on function.

6.7 EPA and 17, 18-EpETE did not induce apoptosis in SW480 cells at a concentration of 25 µM over 24 hours

At a concentration of 25 µM, EPA and 17, 18-EpETE did not result in apoptosis in SW480 cells over a 24 hour incubation period (Figure 5.1). This result alone, however, is not sufficient to conclude that EPA and 17, 18-EpETE do not induce apoptosis in SW480 cells since our study only looked at a single concentration of the PUFAs and a single incubation period. Future studies using a range of concentrations therefore need to be performed in order to confirm if EPA and 17, 18-EpETE result in apoptosis in SW480 cells at concentrations greater than 25 µM and to determine at which concentration apoptotic effects begin to be exhibited. The effect of increased incubation time also needs to be addressed and the mechanism of apoptosis should be investigated in order to determine if the parent compound and metabolite activate the same pathways.

6.8 The EPA epoxide, 17, 18-EpETE, significantly reduced ROS production in SW480 cells

EPA and 17, 18-EpETE reduced ROS production in SW480 cells, with this reduction being significantly different to the vehicle control for cells treated with 25 µM 17, 18-EpETE (Figure 5.2). A possible reason why 17, 18-EpETE resulted in a significant reduction in ROS whilst EPA did not, could be linked to the enzyme sEH. Since sEH is the main enzyme responsible for 17, 18-EpETE metabolism it may possibly be upregulated in 17, 18-EpETE treated cells (Fleming, 2011). sEH and microsomal epoxide hydrolases (mEH) belong to the same family of C-X bond hydrolases which involve an alkyl-enzyme intermediate (Lacourciere and Armstrong, 1994). mEH have been found to participate in the removal of reactive oxygen species (Cheong *et al*., 2009). sEH may therefore be responsible for the

significant decrease in ROS in 17, 18-EpETE treated cells. Future studies could test this hypothesis through the use of sEH inhibitors such as 1-(1-methanesulfonyl-piperidin-4-yl)-3-(4-trifluoromethoxy-phenyl)-urea (TUPS) (Aboutabl *et al*., 2011).

Increased ROS levels have been shown to reduce cell viability and induce apoptosis in many different cell systems (Simon *et al*., 2000; Pelicano *et al*., 2004), and an increase in ROS has been proposed as a mechanism of EPA mediated apoptotic cell death in cancer cells (Fukui *et al*., 2013). Treatment of the pancreatic cell line MIA-PaCa-2 with 100 µM EPA was found to increase intracellular ROS accumulation (Fukui *et al*., 2013). Co-treatment with the antioxidant vitamin E and EPA suppressed intracellular ROS accumulation and cell death, showing that EPA reduced cell viability in MIA-PaCa-2 cells through the production of ROS (Fukui *et al*., 2013). Treatment of two breast carcinoma cell lines, namely HBL-100 and ZR-75, with 66 µM EPA was found to significantly decrease cell proliferation and increase the concentration of cellular lipid hydroperoxides relative to the vehicle control (Chajès *et al*., 1995). Simultaneous addition of vitamin E (10 µM) and EPA resulted in a significant decrease of cellular lipid hydroperoxides relative to EPA treated cells as well as a restoration in cell proliferation (Chajès *et al*., 1995). This suggested that the inhibitory effects of EPA on proliferation of HBL-100 and ZR-75 cells were linked to the formation of lipid peroxidation products.

Prospective studies need to explore the link between ROS, cell viability and apoptosis. This could be achieved by assessing the effect of co-treatment with PUFAs and anti-oxidants on ROS production, cell viability and apoptosis (Chajès *et al*., 1995; Fukui *et al*., 2013). The ability of the PUFAs to mop up ROS also needs to be assessed. This could be achieved by generating ROS in cells through incubation with 5FU (Zhang *et al*., 2008) followed by incubation with the PUFAs. Future studies should expand the test concentrations to include concentrations lower than 25 µM and between 25 µM and 100 µM.

6.9 EPA and 17, 18-EpETE reduced SW480 cell migration and anchorage independent growth

The reduction in SW480 cell migration was similar for EPA and 17, 18-EpETE treated cells. Future time and concentration studies should be performed to assess if EPA and 17, 18-EpETE continue to exert similar effects on SW480 cell migration at increased exposure time and concentrations. Exposure studies could be achieved by pre-incubating cells with EPA and 17, 18-EpETE for different lengths of time before seeding for the wound healing assay. Transwell migration assays may also be helpful in future studies.

EPA has been implicated as a potential CSC targeting compound due to its ability to inhibit cell proliferation and induce apoptosis under anchorage independent conditions in carcinoma cell lines (Chamras *et al*., 2002; Erickson and Hubbard *et al*., 2010; Yang *et al*., 2012). The current study supported this hypothesis since EPA was found to reduce SW480 cell growth under serum free tumorsphere conditions (Figure 5.5). A self renewal assay performed by Erickson and Hubbard (2010) on PyV-mT breast cancer cells provides further evidence to support the hypothesis that EPA is able to target CSC. Primary tumorspheres from cultures treated with 5 µM EPA were dissociated and the resultant cells re-cultured with 5 µM EPA. EPA was found to significantly reduce the formation of secondary tumorspheres relative to the vehicle control and primary tumorspheres (Erickson and Hubbard *et al*., 2010). The reduction in primary and secondary tumorsphere formation suggested that EPA may be able to target the tumor initiating CSC subpopulation as well as terminally differentiated tumor cells. Further evidence that EPA may be able to target CSCs has been provided by a study that found that EPA reduced the expression of CD44 protein, as well as CD44 mRNA, in MDA-MB-231 breast cancer cells *in vitro* and *in vivo* (Mandal *et al*., 2010). CD44 is a cell surface adhesion protein that has been reported to promote the progression of cancer metastasis (Weber *et al*., 2002; Ouhit *et al*., 2007) and is a putative marker of colon and breast CSCs (Lei *et al*., 2008; Wang *et al*., 2012). Future studies to compare the effect of EPA and 17, 18-EpETE on colon CSCs need to be performed. This could be addressed through the use of anchorage independent assays performed using cells that are CD44+, sorted by fluorescence-activated cell sorting (FACS). CD133 is also a putative

marker of colon CSCs (Wang *et al*., 2012) and could therefore be used in combination with CD44 in order to isolate colon CSCs. The use of self renewal assays would also be a helpful tool.

An important consideration to take into account for the anchorage independent growth data is that cell viability was not assessed during the soft agar assay but was assessed during the tumorsphere assay. Future studies need to conduct a WST-1 assessment of cell viability at the end of the soft agar assay and look at the effect of time and PUFA concentration on the inhibition of anchorage independent growth by EPA and 17, 18-EpETE in SW480 cells.

Future studies could be expanded to address the effect of EPA and 17, 18-EpETE on anchorage independent growth in a range of cancer cell lines as well as their effect on apoptosis under anchorage independent conditions. EPA has been found to inhibit anchorage independent growth in breast carcinoma. Soft-agar analysis of anchorage-independent cell growth in MCF-7 breast cancer cells showed that EPA (10 µM and 100µM for 14 days) significantly reduced colony formation relative to the vehicle control (Chamras *et al*., 2002). In PyV-mT breast cancer cells, EPA (5 µM treatment for 2 weeks) has been shown to significantly reduce the number of tumorspheres formed as well as cell proliferation relative to the vehicle control (Erickson and Hubbard *et al*., 2010). EPA has been found to induce apoptosis in SW620 cells grown under anchorage independent conditions (Yang *et al*., 2012).

EPA and 17, 18-EpETE may play a role in the inhibition of cancer metastasis since they were able to inhibit two fundamental processes that underpin cancer metastasis, namely cell migration and anchorage-independent growth, in SW480 cells during this study. The effects of EPA and 17, 18-EpETE on other aspects of metastasis, such as invasion, should be compared in SW480 cells in future studies. *In vivo* animal models would be an important tool in assessing the effect on metastasis in future work (Iwamoto *et al*., 1998; Hawcroft *et al*., 2012).

The effect of the AA CYP metabolites, EETs, on metastasis has previously been reported. EETs were found to promote metastasis in human breast cancer cell lines (Jiang *et. al.*, 2007). These findings are limited, however, as the effect of the metabolites was not compared with the parent compound. Addition of exogenous EET regioisomers or overexpression of CYP2J2 or CYP102 F87V with an associated increase in EET production has been found to result in a significant increase in transwell migration and invasion into matrigel in human breast cancer cell lines in comparison to untreated cells and vehicle controls (Jiang *et. al.*, 2007). Transfection with rAAV-antiCYP2J2 or administration of 17-ODYA was shown to significantly inhibit the migration and invasion in human breast cancer cells (Jiang *et. al.*, 2007). Future studies should look at comparing the effects of DHA and AA to the effects of their CYP epoxides on cancer cell metastasis.

6.10 Effects of PUFA on non-cancerous tissues

The effects of EPA, DHA, AA and 17, 18-EpETE on non-cancerous tissues was not addressed in this study and should be looked at in future work. Previous studies have found EPA, DHA and AA to be non-toxic towards non-cancerous cell lines. Engelbrecht *et al.* (2008) looked at the effect of various FAs, including AA and DHA, on colon carcinoma cells (CACO2-2) and "normal" colon epithelium cells (NCM460). Although AA (10 µM, 48 hours) reduced cell viability in CACO-2 cells, this reduction was not significant (Engelbrecht *et al*., 2008). DHA (10 µM, 48 hours), however, significantly reduced the cell viability of CACO-2 cells (Engelbrecht *et al*., 2008). AA and DHA (10 µM, 48 hours) increased cell viability in NCM460 cells, with this increase being significant for DHA (Engelbrecht *et al*., 2008). At a concentration of 24 µM, EPA, DHA and AA have been found to significantly inhibit growth of MCF-7 breast cancer cells, but not MCF-10A non-cancerous human mammary epithelial cells (Grammatikos *et al*., 1994). The incubation periods used were different for the two cell lines, being 7 days for MCF-7 and 4 days for MCF-10A. This may have confounded their findings since the effects of PUFAs have been found to be time dependent (Schonberg *et al*., 2006; Habermann *et al*., 2009). In terms of ROS production, supplementation with 66 µM EPA or DHA in the human breast cancer cell lines HBL-100 and ZR-75 resulted in a significant increase in lipid hydroperoxides relative to the vehicle control (Chajès *et al*., 1995).

Supplementation of non-cancerous human skin fibroblasts with EPA or DHA did not increase the amount of lipid hydroperoxides (Chajès *et al*., 1995). Supplementation with DHA and EPA did not induce apoptosis in the normal human colon mucosal epithelial cells NCM460 (Giros *et al*., 2009).

6.11 Final conclusions

In conclusion, the dietary intake of EPA, DHA and AA may be beneficial to one's health due to the negative effects that these PUFAs have on colon carcinoma, exhibited by the decrease in SW480 and SW620 colon cell viability during this study. Supplementation with the EPA metabolite, 17, 18-EpETE, may prove to be more beneficial than the intake of EPA since it was found to significantly reduce SW480 cell viability relative to EPA treated cells at lower concentrations. However, due to the high cost of the metabolite, this may not be a feasible option at present. Since, at lower concentrations, 17, 18-EpETE significantly decreased SW480 cell viability relative to EPA, the dietary intake of EPA may have variable benefits between individuals due to inter-individual differences in metabolism. Age, gender, race and genetic factors considerably influence the expression of CYPs (Glue and Clement, 1999; Gonzalez and Tukey, 2005), and individuals with low levels of enzyme activity (poor metabolisers) would benefit less than individuals that are good metabolisers. EPA and 17, 18-EpETE were also found to reduce SW480 cell migration and anchorage-independent growth, thereby supporting their possible use in colon cancer prevention. Future studies are needed in order to further understand the negative effects of PUFAs on carcinoma and to determine the mechanisms by which these effects occur.

Reference List

Abassi, Y. A., Xi, B., Zhang, W., Ye, P., Kirstein, S. L., Gaylord, M. R., Feinstein, S. C., Wang, X. and Xu, X. 2009. Kinetic cell-based morphological screening: Prediction of mechanism of compound action and off-target effects. *Chemistry and Biology*, **16** (7): 712-723.

Aboutabl, M. E., Zordoky, B. N., Hammock, B. D. and El-Kadi, A. O. 2011. Inhibition of soluble epoxide hydrolase confers cardioprotection and prevents cardiac cytochrome P450 induction by benzo(a)pyrene. *Journal of Cardiovascular Pharmacology*, **57** (3): 273-281.

Adas, F., Berthou, F., Salaün, J., Dréano, Y. and Amet, Y. 1999. Interspecies variations in fatty acid hydroxylations involving cytochromes P450 2E1 and 4A. *Toxicology Letters*, **110**: 43-55.

Almeida, C. A. and Barry, S. A. 2010. Cancer: Basic science and clinical aspects. Wiley-Blackwell, United States of America, 405pp.

Amet, Y., Adas, F. and Berthou, F. 2002. High performance liquid chromatography of fatty acid metabolites improvement of sensitivity by radiometric, fluorimetric and mass spectrometric methods. *Analytica Chimica Acta,* **465**: 193-198.

Ananthaswamy, H. N and Pierceall, W. E. 1990. Molecular mechanisms of ultraviolet radiation carcinogenesis. *Photochemistry and Photobiology*, **52** (6): 1119-1136.

Arnold, C., Konkel, A., Fischer, R. and Schunck, W. 2010. Cytochrome P450-dependent metabolism of ω-6 and ω-3 long-chain polyunsaturated fatty acids. *Pharmacological Reports*, **62**: 536-547.

Banks, H. T., Sutton, K. L., Thompson, W. C., Bocharov, G., Roose, D., Schenkel, T. and Meyerhans, A. 2011. Estimation of cell proliferation dynamics using CFSE data. *Bulletin of Mathematical Biology*, **73** (1): 116-150.

Bartsch, H., Nair, J. and Owen, R. W. 1999. Dietary polyunsaturated fatty acids and cancers of the breast and colorectum: emerging evidence for their role as risk modifiers. *Carcinogenesis*, **20** (12): 2209-2218.

Bègin, M. E., Ells, G., Das, U. N. and Horrobin, D. F. 1986. Differential killing of human carcinoma cells supplemented with n-3 and n-6 polyunsaturated fatty acids. *Journal of the National Cancer Institute*, **77** (5): 1053-1062.

Bertram, J. S. 2001. The molecular biology of cancer. *Molecular Aspects of Medicine,* **21**: 167-223.

Besnard, P. and Niot, I. 2000. Chapter 6: Role of Lipid-Binding Proteins in Intestinal Absorption of Long-Chain Fatty Acids. In Christophe, A. B. and de Vriese, S. (Eds.), *Fat Digestion and Absorption* (pp. 96-118). United States of America: AOCS Press.

Bhal, S. K., Kassam, K., Peirson, I. G. and Pearl, G. M. 2007. The rule of five revisited: Applying log *D* in place of log *P* in drug-likeness filters. *Molecular Pharmaceutics*, **4** (4): 556-560.

Born, S. L., Rodriquez, P. A., Eddy, C. L. and Lehman-McKeeman, L. D. 1997. Synthesis and reactivity of coumarin 3,4-epoxide. *Drug Metabolism and Disposition*, **25** (11): 1318-1324.

Bougnoux, P. 1999. n-3 Polyunsaturated fatty acids and cancer. *Current Opinion in Clinical Nutrition and Metabolic Care*, **2** (2): 121-126.

Bougnoux, P., Hajjaji, N., Maheo, K., Couet, C. and Chevalier, S. 2010. Fatty acids and breast cancer: Sensitization to treatments and prevention of metastatic re-growth. *Progress in Lipid Research*, **49**: 76-86.

Budge, S. M., Iverson, S. J. And Koopman, H. N. 2006. Studying trophic ecology in marine ecosystems using fatty acids: A primer on analysis and interpretation. Marine Mammal Science, 22 (4): 759-801.

Campbell Marotta, L. L. and Polyak, K. 2009. Cancer stem cells: a model in the making. *Current Opinion in Genetics and Development*, **19**: 44-50.

Castell, J. V., Jover, R., Martínez-Jiménez, C. P. and Gómez-Lechón, M. J. 2006. Hepatocyte cell lines: their use, scope and limitations in drug metabolism studies. *Expert Opinion on Drug Metabolism and Toxicology*, **2** (2): 183-212.

Castle, P. J., Merdink, J. L., Okita, J. R., Wrighton, S. A. and Okita, R. T. 1995. Human liver lauric acid hydroxylase activities. *Drug Metabolism and Disposition*, **23** (10): 1037-1043.

Chajés, V., Sattler, W., Stranzl, A. and Kostner, G. M. 1995. Influence of n-3 fatty acids on the growth of human breast cancer cells in vitro: relationship to peroxides and vitamin-E. *Breast Cancer Research and Treatment*, **34** (3): 199-212.

Chamras, H., Ardashian, A., Heber, D. and Glaspy, J. 2002. Fatty acid modulation of MCF-7 human breast cancer cell proliferation, apoptosis and differentiation. *Journal of Nutritional Biochemistry*, **13**: 711-716.

Chan, T. A., Morin, P. J., Vogelstein, B. and Kinzler, K. W. 1998. Mechanisms underlying nonsteroidal antiinflammatoy drug-mediated apoptosis. *Proceedings of the National Academy of Sciences*, **95**: 681-686.

Chapple, C. 1998. Molecular-genetic analysis of plant cytochrome P450-dependent monooxygenases. Annual *Review of Plant Physiology and Plant Molecular Biology*, **49:** 311-343.

Cheong, A. W., Lee, Y. L., lui, W. M., Yeung, W. S. and Lee, K. F. 2009. Oviductal microsomal epoxide hydrolase (EPHX1) reduces reactive oxygen species (ROS) level and enhances preimplantation mouse embryo development. *Biology of Reproduction*, **81** (1); 126-132.

Chen, J., Capdevila, J. and Harris, R. C. 2001. Cytochrome P450 epoxygenase metabolism of arachidonic acid inhibits apoptosis. *Molecular and Cellular Biology*, **21** (18): 6322-6331.

Chiu, L. C. M. and Wan, J. M. F. 1999. Induction of apoptosis in HL-60 cells by eicosapentaenoic acid (EPA) is associated with downregulation of bcl-2 expression. *Cancer Letters*, **145**: 17-27.

Ciotta, C., Ceccotti, S., Aquilina, G., Humbert, O., Palombo, F., Jiricny, J. and Biqnami, M. 1998. Increased somatic recombination in methylation tolerant human cells with defective DNA mismatch repair. *Journal of Molecular Biology*, **276** (4): 705-719.

Clarke, R. G., Lund, E. K., Latham, P., Pinder, A. C. and Johnson, I. T. 1999. Effect of eicosapentaenoic acid on the proliferation and incidence of apoptosis in the colorectal cell line HT29. *Lipids*, **34**: 1287-1295.

Clarke, S. E., Baldwin, S. J., Bloomer, J. C., Ayrton, A. D., Sozio, R. S. and Chenery, R. J. 1994. Determination of cytochrome P450 2E1 and 4A in hepatic microsomes. *Chemical Research in Toxicology*, **7** (6): 836-842.

Crawford, M., Galli, C., Visioli, F., Renaud, S., Simopoulos, A. P. and Spector, A. A. 2000. Role of plant-derived omega-3 fatty acids in human nutrition. *Annals of Nutrition and Metabolism*, **44**: 263-265.

Cruciani, G., Carosati, E., De Boeck, B., Ethirajulu, K., Mackie, C., Howe, T. and Vianello, R. 2005. MetaSite: Understanding metabolism in human cytochromes from the perspective of the chemist. *Journal of Medicinal Chemistry*, **48** (22): 6970-6979.

Cui, P. H., Petrovic, N. and Murray, M. 2011. The ω-3 epoxide of eicosapentaenoic acid inhibits endothelial cell proliferation by p38 MAP kinase activation and cyclin D1/CDK4 down-regulation. *British Journal of Pharmacology*, **162**: 1143-1155.

De Graaf, I. A. M., Van Meijeren, C. E., Pektas, F. and Koster, H. J. 2002. Comparison of *in vitro* preparations for semi-quantitative prediction of *in vivo* drug metabolism. *Drug Metabolism and Disposition*, **30**: 1129-1136.

De la Mare, J., Lawson, J. C., Chiwakata, M. T., Beukes, D. R., Edkins, A. L. and Blatch, G. L. 2012. Quinones and halogenated monoterpenes of algal origin show anti-proliferative effects against breast cancer cells *in vitro*. *Investigational New Drugs*, **30** (6): 2187-2200.

Dhawan, P., Singh, A. B., Deane, N. G., No, Y., Shiou, S., Schmidt, C., Neff, J., Washington, M. K. and Beauchamp, R. D. 2005. Claudin-1 regulates cellular transformation and metastatic behaviour in colon cancer. *The Journal of Clinical Investigation*, **115** (7): 1765-1776.

Domanski, T. L. and Halpert, J. R. 2001. Analysis of mammalian cytochrome P450 structure and function by site-directed mutagenesis. *Current Drug Metabolism*, **2**: 117-137.

Dove-Edwin, I. and Thomas, H. J. W. 2001. The prevention of colorectal cancer. *Alimentary Pharmacology and Therapeutics*, **15**: 323-336.

Engelbrecht, A. M., du Toit-Kohn, J. L., Ellis, B., Thomas, M., Nell, T. and Smith, R. 2008. Differential induction of apoptosis and inhibition of the PI3-kinase pathway by saturated, monounsaturated and polyunsaturated fatty acids in a colon cancer cell model. *Apoptosis*, **13**: 1368-1377.

Erickson, K. L. and Hubbard. N. E. 2010. Fatty acids and breast cancer: The role of stem cells. *Prostaglandins, Leukotrienes and Essential Fatty Acids*, **82**: 237-241.

Eshleman, J. R., Lang, E. Z., Bowerfind, G. K., Parsosns, R., Vogelstein, B., Willson, J. K., Veigl, M. L., Sedwick, W. D. and Markowitz, S. D. 1995. Increased mutation rate at the hprt locus accompanies microsatellite instability in colon cancer. *Oncogene*, **10** (1): 33-37.

Etsuro, O. 2000. Hormone-dependent cancer: Its carcinogenic mechanism and the treatment. Hormone-dependent cancer and nuclear receptor. *Biotherapy*, **14** (11): 1069-1075.

Fauser, J. K., Prisciandaro, L. D., Cummins, A. G. and Howarth, G. S. 2011. Fatty acids as potential adjunctive colorectal chemotherapeutic agents. *Cancer Biology and Therapy*, **11** (8): 724-731.

Fer, M., Corcos, l., Drèano, Y., Plee-Gautier, E., Salaun, J. P., Berthou, F. and Amet, Y. 2008a. Cytochromes P450 from family 4 are the main omega hydroxylating enzymes in humans: CYP4F3B is the prominent player in PUFA metabolism. *Journal of Lipid Research*, **49**: 2379-2389.

Fer, M., Drèano, Y., Lucas, D., Corcos, L., Salaün, J., Berthou, F. and Amet, Y. 2008b. Metabolism of eicosapentaenoic and docosahexaenoic acids by recombinant human cytochromes P450. *Archives of Biochemistry and Biophysics*, **471**: 116-125.

Field, C. J. and Schley, P. D. 2004. Evidence for potential mechanisms for the effect of conjugated linoleic acid on tumor metabolism and immune function: lessons from n-3 fatty acids. *The American Journal of Clinical Nutrition*, **79**: 1190S-1198S.

Fleming, I. 2011. The cytochrome P450 pathway in angiogenesis and endothelial cell biology. *Cancer Metastasis Reviews*, **30**: 541-555.

Fukui, M., Kang, K. S., Okada, K. and Zhu, B. T. 2013. EPA, an omega-3 fatty acid, induces apoptosis in human pancreatic cancer cells: Role of ROS accumulation, caspase-8 activation, and autophagy induction. *Journal of Cellular Biochemistry*, **114**: 192-203.

Gerets, H. H. J., Tilmant, K., Gerin, B., Chanteux, H., Depelchin, B. O., Dhalluin, S. and Atienzar, F. A. 2012. Characterization of primary human hepatocytes, HepG2 cells, and HepaRG cells at the mRNA level and CYP activity in response to inducers and their predictivity for the detection of human hepatotoxins. *Cell Biology and Toxicology*, **28**: 69-87.

Giros, A., Grzybowski, M., Sohn, V. R., Pons, E., Fernandez-Morales, J., Xicola, R. M., Sethi, P., Grzybowski, J., Goel, A., Boland, C. R., Gassull, M. A. and Llor, X. 2009. Regulation of colorectal cancer cell apoptosis by the n-3 polyunsaturated fatty acids docosahexaenoic and eicosapentaenoic. *Cancer Prevention Research*, **2**: 732-742.

Gleissman, H., Yang, R., Martinod, K., Lindskog, M., Serhan, C., Johnsen, J. and Kogner, P. 2010. Docosahexaenoic acid metabolome in neural tumors: identification of cytotoxic intermediates. *The Journal of the Federation of American Societies for Experimental Biology*, **24**: 906-915.

Gonzalez, F. J. and Tukey, R. H. 2005. Chapter 3: Drug Metabolism. In Goodman, L. S., Limbird, L. E., Milinoff, P. B. and Ruddon, R. W. (Eds.), *Goodman and Gilman's The Pharmacological Basis of Therapeutics* (11th ed., pp. 71-91). New York: McGraw-Hill, Health Profession Division.

Glue, P. and Clement, R. P. 1999. Cytochrome P450 enzymes and drug metabolism – Basic concepts and methods of assessment. *Cellular and Molecular Neurobiology*, **19** (3): 309-323.

Grammatikos, S. I., Subbaiah, P. V, Victor, T. A. and Miller, W. M. 1994. n-3 and n-6 fatty acid processing and growth effects in neoplastic and non-cancerous human mammary epithelial cell lines. *British Journal of Cancer*, **70**: 219-227.

Greene, N. 2002. Computer systems for the prediction of toxicity: an update. *Advanced Drug Delivery Reviews*, **54**: 417-431.

Guadamillas, M. C., Cerezo, A. and del Pozo, M. A. 2011. Overcoming anoikis – pathways to anchorage-independent growth in cancer. *Journal of Cell Science*, **124**: 3189-3197.

Guengerich, F. P. 2001. Common and uncommon cytochrome P450 reactions related to metabolism and chemical toxicity. *Chemical Research in Toxicology*, **14** (6): 611-641.

Guengerich, F. P. 2006. Cytochrome P450s and other enzymes in drug metabolism and toxicity. *The American Association of Pharmaceutical Scientists*, **8** (1): 101-111.

Habermann, N., Christian, B., Luckas, B., Pool-Zobal, B. L., Lund, E. K. and Glei, M. 2009. Effects of fatty acids on metabolism and cell growth of human colon cell lines of different transformation state. *BioFactors*, **35** (5): 460 – 467.

Hamburger, A., W. and Salmon, S., E. 1977. Primary bioassay of human tumor stem cells. *Science*, **197** (4302): 461-463.

Hanahan, D. and Weinberg, R. A. 2011. Hallmarks of cancer: The next generation. *Cell*, **144**: 646-674.

Hawcroft, G., Volpato, M., Marston, M., Ingram, N., Perry, S. L., Cockbain, A. J., Race, A. D., Munarini, A., Belluzzi, A., loadman, P. M., Coletta, P. L. And Hull, M. A. 2012. The omega-3 polyunsaturated fatty acid eicosapentaenoic acid inhibits mouse MC-26 colorectal cancer cell liver metastasis via inhibition of PGE2-dependent cell motility. *British Journal of Pharmacology*, **166** (5): 1724-1737.

Hornberg, J. J., Bruggeman, F. J., Westerhoff, H. V. and Lankelma, J. 2006. Cancer: A systems biology disease. *BioSystems*, **83**: 81-90.

Huggins, C. 1963. The hormone-dependent cancers. *The Journal of the American Medical Association*, **186** (5): 481-483.

Hur, S., Lee, H., Kim, Y., Lee, B. H., Shin, J. and Kim, T. Y. 2008. Sargaquinoic acid and sargachromenol, extracts of *Sargassum sagamianum*, induce apoptosis in HaCaT cells and mice skin: Its potentiation of UVB-induced apoptosis. *European Journal of Pharmacology*, **582**: 1-11.

Hwang, S. H., Tsai, H., Liu, J., Morisseau, C. and Hammock, B. D. 2007. Orally bioavailable potent soluble epoxide hydrolase inhibitors. *Journal of Medicinal Chemistry*, **50** (16): 3825-3840.

Iwamoto, S., Senzaki, H., Kiyozuka, Y., Ogura, E., Takada, H., Hioki, K. and Tsubura, A. 1998. Effects of fatty acids on liver metastasis of ACL-15 rat colon cancer cells. *Nutrition and Cancer*, **31** (2): 143-150.

Jackson, A. L. and Loeb, L. A. 2001. The contribution of endogenous sources of DNA damage to the multiple mutations in cancer. *Mutation Research/Fundamental and Molecular Mechanisms of Mutagenesis*, **477**: 7-21.

Jemal, A., Siegal, R., Xu, J. and Ward, E. 2010. Cancer Statistics. *CA: A Cancer Journal for Clinicians*, **60**: 277-300.

Jia, L. and Liu, X. 2007. The conduct of drug metabolism studies considered good practice (II): *In vitro* experiments. *Current Drug Metabolism*, **8** (8): 822-829.

Jiang, J., Chen, C., Card, J. W., Yang, S., Chen, J., Fu, X., Ning, Y., Xiao, X., Zeldin, D. C. and Wang, D. W. 2005. Cytochrome P450 2J2 promotes the neoplastic phenotype of carcinoma cells and is up-regulated in human tumors. *Cancer Research*, **65**: 4707-4715.

Jiang, J., Ning, Y., Chen, C., Ma, D., Liu, Z., Yang, S., Zhou, J., Xiao, X., Zhang, X. A., Edin, M. L., Card, J. W., Wang, J., Zeldin, D. C. and Wang, D. W. 2007. Cytochrome P450 epoxygenase promotes human cancer metastasis. *Cancer Research*, **67**: 6665-6674.

Jiang, W. G., Bryce, R. P. and Horrobin, D. F. 1998. Essential fatty acids: molecular and cellular basis of their anti-cancer action and clinical implications. *Critical Reviews in Oncology/Hematology*, **27**: 179-209.

Karaguni, I. M., Glusenkamp, K. H., Langerak, A., Geisen, C., Ullrich, V., Winde, G., Moroy, T. and Muller, O. 2002. New indene-derivatives with anti-proliferative properties. *Bioorganic and Medicinal Chemistry Letters*, **12**: 709-713.

Kim, D., Chung, K. and Lee, J. 1998. Stimulatory effects of high-fat diets on colon cell proliferation depend on the type of dietary fat and site of the colon. *Nutrition and Cancer*, **30** (2): 118-123.

Kim, J. H., Choi, Y. W., Park, C., Jin, C. Y., Lee, Y. J., Park, D. J., Kim, S. G., Kim, G. Y., Choi, I. W., Hwang, W. D., Jeong, Y. K., Kim, S. K. and Choi, Y.H. 2010. Apoptosis induction of human leukemia U937 cells by gomisin N, a dibenzocyclooctadiene lignin, isolated from *Schizandra chinensis* Baill. *Food and chemical Toxicology*, **48**: 807-813.

Kim, Y., Koo K. H., Sung, J. K., Yun, U. and Kim, H. 2012. Anoikis Resistance: An essential prerequisite for tumor metastasis. *International Journal of Cell Biology*, **2012:** 1-11.

Konkel, A. and Schunck, W. 2011. Role of cytochrome P450 enzymes in the bioactivation of polyunsaturated fatty acids. *Biochimica et Biophysica Acta*, **1814**: 210-222.

Korolev, D., Balakin, K. V., Nikolsky, Y., Kirillov, E., Ivanenkov, Y. A., Savchuk, N. P., Ivashchenko, A. A. and Nikolskaya, T. 2003. Modeling of human cytochrome P450-mediated dug metabolism using unsupervised machine learning approach. *Journal of Medicinal Chemistry*, **46**: 3631-3643.

Kubens, B. S. and Zänker, K. S. 1998. Differences in the migration capacity of primary human colon carcinoma cells (SW480) and their lymph node metastatic derivatives (SW620). *Cancer Letters*, **131** (1): 55-64.

Lacourciere, G. M. and Armstrong, R. N. 1994. Microsomal and soluble epoxide hydrolases are members of the same family of C-X bond hydrolase enzymes. *Chemical Research in Toxicology*, **7** (2): 121-124.

Lai, P. B. S., Ross, J. A., Fearon, K. C. H., Anderson, J. D. and Carter, D. C. 1996. Cell cycle arrest and induction of apoptosis in pancreatic cancer cells exposed to eicosapentaenoic acid *in vitro*. *British Journal of Cancer*, **74**; 1375-1383.

Lands, W. E. M., Hamazaki, T., Yamazaki, K., Okuyama, H., Sakai, K., Goto, Y. and Hubbard, V. S. 1990. Changing dietary patterns. *The American Journal of Clinical Nutrition*, **51**: 991-993.

Larsson, S., Kumlin, M., Ingelman-Sundberg, M. and Wolk, A. 2004. Dietary long-chain n-3 fatty acids for the prevention of cancer: a review of potential mechanisms. *The American Journal of Clinical Nutrition*, **79**: 935-945.

Latham, P., Lund, E. K., Brown, J. C. and Johnson, I. T. 2001. Effects of cellular redox balance in induction of apoptosis by eicosapentaenoic acid in HT29 colorectal adenocarcinoma cells and rat colon *in vivo*. *Gut*, **49**: 97-105.

Lei, D., Wang, H., He, L., Zhang, J., Ni, B., Wang, X., Jin, H., Cahuzac, N., Mehrpour, M., Lu, Y. and Chen, Q. 2008. CD44 is of functional importance for colorectal cancer stem cells. *Clinical Cancer Research*, **14**: 6751-6760.

Leibovitz, A., Stinson, J. C., McCombs III, W. B., McCoy, C. E., Mazur, K. C. and Mabry, N. D. 1967. Classification of human colorectal adenocarcinoma cell lines. *Cancer Research*, **36** (12): 4562-4569.

Lewis, D. F. V., Loannides, C. and Parke, D. V. 1998. Cytochromes P450 and species differences in xenobiotic metabolism and activation of carcinogen. *Environmental Health Perspectives*, **106** (10): 633-641.

Ligo, M., Nakagawa, T., Ishikawa, C., Iwahori, Y., Asamoto, M., Yazawa, K., Araki, E. and Tsuda, H. 1997. Inhibitory effects of docosahexaenoic acid on colon carcinoma 26 metastasis to the lung. *British Journal of Cancer*, **75** (5): 650-655.

Lipinski, C. A., Lombardo, F., Dominy, B. W. and Feeney, P. J. 2001. Experimental and computational approaches to estimate solubility and permeability in drug discovery and development settings. *Advanced Drug Delivery Reviews*, **46:** 3-26.

Liska, D. J. 1998. The detoxification enzyme systems. *Alternative Medicine Review*, **3** (3): 187-198.

Liu, H., Chen, C., Yang, H., Pan, Y. and Zhang, X. 2011. Cancer stem cell subsets and their relationships. *Journal of Translational Medicine*, **9**: 50-59.

Loeb, K. R. and Loeb, L. A. 2000. Significance of multiple mutations in cancer. *Carcinogenesis*, **21** (3): 379-385.

Lu, I., Hasio, A., Hu, M., Yang, F. and Su, H. 2010. Docosahexaenoic acid induces proteasome-dependent degradation of estrogen receptor α and inhibits the downstream signalling target in MCF-7 breast cancer cells. *Journal of Nutritional Biochemistry*, **21**: 512-517.

Lu, W., Ogasawara, M. A. And Huang, P. 2007. Models of reactive oxygen species in cancer. *Drug Discovery Today Disease Models*, **4**(2): 67-73.

Mandal, C. C., Ghosh-Choudhury, T., Yoneda, T., Ghosh-Choudhury, G. and Ghosh-Choudhury, N. 2010. Fish oil prevents breast cancer cell metastasis to bone. *Biochemical and Biophysical Research Communications*, **402**: 602-607.

Martins De Lima, T., Gorjão, R., Hatanaka, E., Cury-Boaventura, M. F., Portioli Silva, E. P., Procopio, J. and Curi, R. 2007. Mechanisms by which fatty acids regulate leucocyte function. *Clinical Science*, **113**: 65-77.

Matsuura, N., Miyamae, Y., Yamane, K., Nagao, Y., Hamada, Y., Kawaguchi, N., Katsuki, T., Hirata, K., Sumi, S. and Ishikawa, H. 2006. Aged garlic extract inhibits angiogenesis and proliferation of colorectal carcinoma cells. *The Journal of Nutrition*, **136:** 842S-846S.

Milner, J. A. 2004. Molecular targets for bioactive food components. *The Journal of Nutrition*, **134**: 2492S-2498S.

Mori, S., Chang, J. T., Andrechek, E. R., Matsumura, N., Baba, T., Yao, G., Kim, J. W., Gatza, M., Murphy, S. and Nevins, J. R. 2009. An anchorage-independent cell growth signature identifies tumors with metastatic potential. *Oncogene*, **28** (31): 2796-2805.

Multani, A. S., Ozen, M., Narayan, S., Kumar, V., Chandra, J., mcConkey, D. J., Newman, R. A. and Pathak, S. 2000. Caspase-dependent apoptosis induced by telomere cleavage and TRF2 loss. *Neoplasia*, **2**: 339-345.

Nebert, D. W. and Dieter, M. Z. 2000. The evolution of drug metabolism. *Pharmacology*, **61**: 124-135.

Nebert, D. W. and Russell, D. W. 2002. Clinical importance of the cytochromes P450. *The Lancet*, **360**: 1155-1162.

Nelson, D. L. and Cox, M. M. 2005. Lehninger: Principles of Biochemistry, 4th Ed. Sara Tenney, United States of America, 1119pp.

Nelson, D. R., Kamataki, T., Waxman, D. J., Guengerich, F. P., Estabrook, R. W., Feyereisen, R., Gonzalez, F. J., Coon, M., J., Gunsalus, I. C., Gotoh, O., Okuda, K. and Nebert, D. W. 1993. The P450 Superfamily: Update on new sequences, gene mapping, accession numbers, early trivial names, and nomenclature. *DNA and Cell Biology*, **12** (1): 1-51.

Node, K., Huo, Y., Ruan, X., Yang, B., Spiecker, M., Ley, K., Zeldin, D. and Liao, J. 1999. Anti-inflammatory properties of cytochrome P450 epoxygenase-derived eicosanoids. *Science*, **285**: 1276-1279.

Nussler, A. K., Wang, A., Neuhaus, P., Fischer, J., Yuan, J., Liu, L., Zeilinger, K., Gerlach, J., Arnold, P. J. and Albrecht, W. 2001. The suitability of hepatocyte culture models to study various aspects of drug metabolism. *Alternatives to Animal Experimentation*, **18** (2): 91-101.

Obermeier, H., Hrboticky, N. and Sellmayer, A. 1995. Differential effects of polyunsaturated fatty acids on cell growth and differentiation of premonocytic U937 cells. *Biochimica et Biophysica Acta,* **1266**: 179-185.

Ouhit, A., Abd Elmageed, Z. Y., Abdraboh, M. E., Lioe, T. F. and Raj, M. H. 2007. *In vivo* evidence for the role of CD44s in promoting breast cancer metastasis to the liver. *The American Journal of Pathology*, **171**: 2033-2039.

Pawlosky, R. J., Hibbeln, J. R., Lin, Y., Goodson, S., Riggs, P., Sebring, N., Brown, G. L. and Salem Jr, N. 2003. Effects of beef- and fish-based diets on the kinetics of n-3 fatty acid metabolism in human subjects. *The American Journal of Clinical Nutrition*, **77**: 565-572.

Pearce, R. E., McIntyre, C. J., Madan, A., Sanzgiri, U., Draper, A. J., Bullock, P. L., Cook, D. C., Burton, L. A., Latham, J., Nevins, C. and Parkinson, A. 1996. Effects of freezing, thawing, and storing human liver microsomes on cytochrome P450 activity. *Archives of Biochemistry and Biophysics*, **331** (2): 145-169.

Pelicano, H., Carney, D. and Huang, P. 2004. ROS stress in cancer cells and therapeutic implications. *Drug Resistance Updates,* **7**: 97-110.

Powel, P. K., Wolf, I. and Lasker, J. M. 1996. Identification of CYP4A11 as the major lauric acid ω-hydroxylase in human liver microsomes. *Archives of Biochemistry and Biophysics*, **335** (1): 219-226.

Qiang, L., Yang, Y., Ma., Y., Chen, F., Zhang, L., Liu, W., Qi, Q., Lu, N., Tao, L., Wang, X., You, Q. and Guo, Q. 2009. Isolation and characterization of cancer stem like cells in human glioblastoma cell lines. *Cancer Letters*, **279** (1): 13-21.

Risio, M., Candelaresi, G. and Rossini, F. P. 1993. Bromodeoxyuridine uptake and proliferating cell nuclear antigen expression throughout the colorectal tumor sequence. *Cancer Epidemiology, Biomarkers and Prevention*, **2**: 363-367.

Rose, D. P. and Connolly, J. M. 1999. Omega-3 fatty acids as cancer chemopreventive agents. *Pharmacology and Therapeutics*, **83**: 217-244.

Rydberg, P., Gloriam, D. E., Zaretzki, J., Breneman, C. and Oslen, L. 2010. SMARTCyp: A 2D method for prediction of cytochrome p450-mediated drug metabolism. *ACS Medicinal Chemistry Letters*, **1**: 96-100.

Sachs, R. K. and Brenner, D. J. 2005. Solid tumor risks after high doses of ionizing radiation. *Proceedings of the National Academy of Sciences of the United States on America*, **102** (37): 13040-13045.

Sack, U., Walther, W., Scudiero, D., Selby, M., Kobelt, D., Lemm, M., Fichtner, I., Schlag, P. M., Shoemaker, R. H. And Stein, U. 2011. Novel effect of antihelminthic niclosamide on S100A4-mediated metastatic progression in colon cancer. *Journal of the National Cancer Institute*, **103**: 1018-1036.

Sade, A., Tuncay, S., Cimen, I., Secercan, F. and Banerjee, S. 2012. Celecoxib reduces fluidity and decreases metastatic potential of colon cancer cell lines irrespective of COX-2 expression. *Bioscience Reports*, **32**: 35-44.

Sandler, R. S., Baron, J. A., Tosteson, T. D., Mandel, J. S. and Haile, R. W. 2000. Rectal mucosal proliferation and risk of colorectal adenomas: Results from a randomized controlled trial. *Cancer Epidemiology, Biomarkers and Prevention*, **9**: 653-656.

Scarth, J. P., Spencer, H. A., Hudson, S. C., Teale, P., Gray, B. P. and Hillyer, L. L. 2010. The application of *in vitro* technologies to study the metabolism of the androgenic/anabolic steroid stanozolol in the equine. *Steriods*, **75**: 57-69.

Schley, P. D., Jijon, H. B., Robinson, L. E. and Field, C. J. 2005. Mechanisms of omega-3 fatty acid-induced growth inhibition in MDA-MB-231 human breast cancer cells. *Breast Cancer Research and Treatment*, **92**: 187-195.

Schloss, I., Kidd, M. S., Tichelaar, H. Y., Young, G. O. and O'Keefe, S. J. 1997. Dietary factors associated with a low risk of colon cancer in coloured west coast fishermen. *South African Medical Journal*, **87** (2): 152-158.

Schmitz, G. and Ecker, J. 2008. The opposing effects of n-3 and n-6 fatty acids. *Progress in Lipid Research*, **47**:147-155.

Schonberg, S.A., Lundemo, A. G., Fladvad, T., Holmgren, K., Bremseth, H., Nilsen, A., Gederaas, O., Tvedt, K. E., Egeberg, K. W. and Krokan, H. E. 2006. Closely related colon cancer cell lines display different sensitivity to polyunsaturated fatty acids, accumulate different lipid classes and downregulate sterol regulatory element-binding protein 1. *The Journal of the Federation of American Societies for Experimental Biology*, **273**: 2749-2765.

Serhan, C., Gotlinger, K., Hong, S. and Arita, M. 2004. Resolvins, docosatrienes, and neuroprotectins, novel omega-3-derived mediators, and their asprin-triggered endogenous epimers: an overview of their protective roles in catabasis. *Prostaglandins and other Lipid Mediators*, **73**: 155-172.

Simon, H., Haj-Yehia, A. and Levi-Schaffer, F. 2000. Role of reactive oxygen species (ROS) in apoptosis induction. *Apoptosis*, **5**: 415-418.

Steeg, P. S. 2003. Metastasis suppressors alter the signal transduction of cancer cells. *Nature Reviews Cancer*, **3**: 55-63.

Subauste, M. C., Kupriyanova, T. A., Conn, E. M., Ardi, V. C., Quigley, J. P. and Deryuina, E. I. 2009. Evaluation of metastatic and angiogenic potentials of human colon carcinoma cells in chick embryo model systems. *Clinical and Experimental Metastasis*, **26** (8): 1033-1047.

Terpstra, O. T., van Blankenstein, M., Dees, J. and Eilers, G. A. 1987. Abnormal pattern of cell proliferation in the entire colonic mucosa of patients with colon adenoma or cancer. *Gastroenterology*, **92** (3): 704-708.

The 2004 National Cancer Registry report. Downloaded from www.cansa.org.za on 3 January 2013.

Van Poppel, G. and van den Berg, H. 1997. Vitamins and cancer. *Cancer Letters*, **114**: 195-202.

Van Rollins, M., Baker, R. C., Sprecher, H. W. and Murphy, R. 1984. Oxidation of docosahexaenoic acid by rat liver microsomes. *The Journal of Biological Chemistry*, **259** (9): 5776-5783.

Volpato, M., Coletta, L., Loadman, P. M. and Hull, M. A. 2012. 224 The relationship between the anti-cancer activity of the omega-3 polyunsaturated fatty acid eicosapentaenoic acid (EPA) and colorectal cancer cell migration. *European Journal of Cancer*, **48**: 68.

Wang, C., Xie, J., Guo, J., Manning, H. C., Gore, J. C. and Guo, N. 2012. Evaluation of CD44 and CD133 as cancer stem cell markers for colorectal cancer. *Oncology Reports*, 28 (4): 1301-1308.

Wang, X., Penalva, L. O., Yuan, H., Linnoila, R. I., Lu, J., Okano, H. and Glazer, R. I. 2010. Musashi1 regulates breast tumor cell proliferation and is a prognostic indicator of poor survival. *Molecular Cancer*, **9**: 221-233.

Waskell, L., Koblin, D. and Canova-Davis, E. 1982. The lipid composition of human liver microsomes. *Lipids*, **17** (4): 317-320.

Weber, G. F., Bronson, R. T., Ilagan, J., Cantor, H., Schmits, R. and Mak, T. W. 2002. Absence of the CD44 gene prevents sarcoma metastasis. *Cancer Research*, **62**: 2281-2286.

W.H.O. 2008. GLOBOCAN 2008 fast stats. International Agency for Research on Cancer, 1-8.

Wicha, M. S., Liu, S. and Dontu, G. 2006. Cancer stem cells: An old idea-A paradigm shift. *Cancer Research*, **66** (4): 1883-1890.

Wilkening, S., Stahl, F. and Bader, A. 2003. Comparison of primary human hepatocytes and hepatoma cell line HEPG2 with regard to their biotransformation properties. *Drug Metabolism and Disposition*, **31**: 1035-1042.

Wrighton, S. A., Ring, B. J. and VandenBranden, M. 1995. The use of *in vitro* metabolism techniques in the planning and interpretation of drug safety studies. *Toxicologic Pathology*, **23** (2): 199-208.

Wu, J., Chen, C., Chang, W., Chung, K., Liu, Y., Lu, F. And Chen, C. 2010. Anti-cancer effects of protein extracts from *Calcatia lilacina*, *Pleurotus ostreatus* and *Volvariella colvacea*. *Evidence-Based Complementary and Alternative Medicine*, **2011**: 1-10.

Wu, M., Tsai, Y., Hua, K., Chang, K., Kuo, M. and Lin, M. 2012. Eicosapentaenoic acid and docosahexaenoic acid inhibit macrophage-induced gastric cancer cell migration by attenuating the expression of matrix metalloproteinase 10. *Journal of Nutritional Biochemistry*, **23**: 1434-1439.

Xie, J., Du, G., McEntee, E., Aung, H. H., He, H., Mehendale, S. R., Wang, C. and Yuan, C. 2011. Effects of triterpenoid glycosides from fresh ginseng berry on SW480 human colorectal cancer cell line. *Cancer Research and Treatment*, **43** (1): 49-55.

Xu, X., Zhang, X. A. and Wang, D. W. 2011. The roles of CYP450 epoxygenases and metabolites, epoxyeicosatrienoic acids, in cardiovascular and malignant diseases. *Advanced Drug Delivery Reviews*, **63** (8): 597-609.

Yamazaki, H. and Shimada, T. 1997. Progesterone and testosterone hydroxylation by cytochromes P450 2C19, 2C9, and 3A4 in human liver microsomes. *Archives of Biochemistry and Biophysics*, **346** (1): 161-169.

Yang, T., Fang, S., Zhang, H., Xu, L., Zhang, Z., Yuan, K., Xue, C., Yu, H., Zhang, S., Li, Y., Shi, H. and Zhang, Y. 2012. N-3 PUFAs have antiproliferative and apoptotic effects on human colorectal cancer stem-like cells *in vitro*. *Journal of Nutritional Biochemistry*. In print. http://dx.doi.org/10.1016/j.jnutbio.2012.03.023

Yao, H., Chang, Y., Lan, S., Chen, C., Hsu, J. and Yeh, T. 2006. The inhibitory effect of polyunsaturated fatty acids on human CYP enzymes. *Life Sciences,* **79**: 2432-2440.

Zhang, G., Ma, L., Xie, Y., Miao, X. and Jin, C. 2012. Esophageal cancer tumorspheres involve cancer stem-like populations with elevated aldehyde dehydrogenase enzymatic activity. *Molecular Medicine Reports*, **6** (3): 519-524.

Zhang, N., Yin, Y., Xu, S. and Chen, W. 2008. 5-Fluorouracil: Mechanisms of resistance and reversal strategies. *Molecules*, **13**: 1551-1569.